MYCOSPHERE 16(1): 169–244 (2025) www.mycosphere.org ISSN 2077 7019
Doi 10.5943/mycosphere/16/1/3

ARTICLE

Morpho-molecular characterization and pathogenicity of fungi associated with sweet cherry (*Prunus avium*) trunk diseases in China

Zhang W[1±], Chen P[1±], Zhou Y[1,2,3], Manawasinghe IS[4], Ji S[1], Li X[1], Al-Otibi F[5], Hyde KD[2,3,4,5], Abeywickrama PD[1*], and Yan J[1*]

[1] *Beijing Key Laboratory of Environment Friendly Management on Fruit Diseases and Pests in North China; Institute of Plant Protection, Beijing Academy of Agriculture and Forestry Sciences, Beijing 100097, P.R. China*
[2] *Center of Excellence in Fungal Research, Mae Fah Luang University, Chiang Rai 57100, Thailand*
[3] *School of Science, Mae Fah Luang University, Chiang Rai 57100, Thailand*
[4] *Innovative Institute for Plant Health, Zhongkai University of Agriculture and Engineering, Guangzhou 510225, Guangdong, P.R. China*
[5] *Department of Botany and Microbiology, College of Science, King Saud University, P.O. Box 22452, Riyadh 11495, Saudi Arabia*

Citation – Zhang W, Chen P, Zhou Y, Manawasinghe IS, Ji S, Li X, Al-Otibi F, Hyde KD, Abeywickrama PD, Yan J 2025 – Morpho-molecular characterization and pathogenicity of fungi associated with sweet cherry (*Prunus avium*) trunk diseases in China. Mycosphere 16(1), 169–244, Doi 10.5943/mycosphere/16/1/3

Abstract

The production of sweet cherries makes a substantial economic contribution to many nations. However, little is known about the microfungi associated with sweet cherries globally, although fungal pathogens significantly affect tree health and production. Samples exhibiting trunk disease symptoms were collected from six provinces in China and 193 fungal isolates were obtained. Based on morpho-molecular approaches, these ascomycetous taxa were classified into 26 species in ten genera, nine families in *Dothideomycetes*, *Leotiomycetes* and *Sordariomycetes*. Among them, nine novel host records and two new geographical reports are identified. Pathogenicity assays revealed *Colletotrichum godetiae*, *Co. fioriniae*, *Fusarium annulatum*, *F. verticillioides*, *F. compactum*, *F. citri*, *Fusarium* sp., *Neocosmospora solani* and *Ne. metavorans* were causing symptoms on one-year old detached sweet cherry shoots. *Fusarium planum*, *F. sulawesiense* and *F. lateritium* did not develop any symptoms during the pathogenicity assay. *Botryosphaeria dothidea*, *Cladosporium anthropophilum*, *Cl. cladosporioides*, *Cl. perangustum*, *Cl. ramotenellum*, *Cl. sphaerospermum*, *Cl. tenuissimum*, *Nothophoma pruni*, *No. quercina*, *Alternaria alternata*, *Monilinia fructicola*, *Cytospora leucostoma*, *Clonostachys farinose*, *Fusarium planum*, *F. sulawesiense* and *F. lateritium* species were associated with trunk disease symptoms. In addition, we provide updated backbone trees for *Alternaria*, *Botryosphaeria*, *Cladosporium*, *Clonostachys*, *Colletotrichum*, *Cytospora*, *Fusarium*, *Monilinia*, *Neocosmospora* and *Nothophoma*. These findings revealed the high diversity of microfungi associated with cherry trunk diseases and this study is the first comprehensive study on the pathogenic micro-fungi associated with sweet cherry trunk diseases in China. Future studies are required to understand the pathogenicity mechanisms and disease epidemiology of isolated species and their impact on cherry production in China.

Keywords – Fungal taxonomy – *Fusarium oxysporum* species complex – Koch's postulates – *Monilinia* – Trunk diseases

Submitted: 15 July 2024; **Accepted**: 03 January 2025; **Published:** 05 March 2025
***Corresponding Author:** Pranami D. Abeywickrama – e-mail – pranamiabeywickrama@yahoo.com,
Jiye Yan – e-mail – jiyeyan@vip.163.com
[±] Authors contributed equally to this work.
Accepted by: Thilini Chethana Kandawatte

Table of Content

Phylum ***Ascomycota*** Caval. Sm.
Subphylum ***Pezizomycotina*** O. E. Erikss. & K. Winka
Class ***Dothideomycetes*** O. E. Erikss. & Winka
Botryosphaeriales C. L. Schoch, Crous & Shoemaker
Botryosphaeriaceae Theiss. & Syd.
1. ***Botryosphaeria dothidea*** (Moug.) Ces. & De Not.- (Associated with branch die-back): New collection

Cladosporiales Abdollahz. & Crous
Cladosporiaceae Chalm. & R.G. Archibald
2. ***Cladosporium anthropophilum*** Sand.-Den., Gené & Wiederh.- (Associated with branch die-back, leafspots, shot hole and leaf necrosis): New collection
3. ***Cladosporium cladosporioides*** (Fresen.) G.A. de Vries- (Associated with branch die-back, and diseased leaves and fruits): New collection
4. ***Cladosporium perangustum*** Bensch, Crous & U. Braun- (Associated with branch die-back): New host record
5. ***Cladosporium ramotenellum*** K. Schub., Zalar, Crous & U. Braun- (Associated with branch die-back and leafspots): New collection
6. ***Cladosporium sphaerospermum*** Penz.- (Associated with branch die-back): New host record
7. ***Cladosporium tenuissimum*** Cooke- (Associated with branch die-back): New collection

Pleosporomycetidae C.L. Schoch, Spatafora, Crous & Shoemaker
Pleosporales Luttr. ex M.E. Barr
Didymellaceae Gruyter, Aveskamp & Verkley
8. ***Nothophoma pruni*** Chethana, J.Y. Yan, X.H. Li & K.D. Hyde- (Associated with branch die-back): New collection
9. ***Nothophoma quercina*** (Syd. & P. Syd.) Qian Chen & L. Cai- (Associated with branch die-back): New collection

Pleosporaceae Nitschke
10. ***Alternaria alternata*** (Fr.) Keissl.- (Associated with branch die-back and diseased fruits): New collection

Leotiomycetes O.E. Erikss. & Winka
Helotiales Nannf.
Sclerotiniaceae Whetzel
11. ***Monilinia fructicola*** (G. Winter) Honey- (Associated with dead branches): New collection

Sordariomycetes O.E. Erikss. & Winka
Diaporthomycetidae Senan., Maharachch. & K.D. Hyde
Diaporthales Nannf.
Cytosporaceae Fr.
12. ***Cytospora leucostoma*** (Pers.) Sacc.- (Associated with branch die-back): New geographical record

Hypocreomycetidae O.E. Erikss. & Winka
Glomerellales Chadef. ex Réblová, W. Gams & Seifert
Glomerellaceae Locq. ex Seifert & W. Gams

13. ***Colletotrichum fioriniae*** (Marcelino & Gouli) Pennycook- (Pathogenic): New host record
14. ***Colletotrichum godetiae*** Neerg.- (Pathogenic): New collection

Hypocreales Lindau
Bionectriaceae Samuels & Rossman
15. ***Clonostachys farinosa*** (Henn.) Rossman- (Associated with diseased leaves): New host record

Nectriaceae Tul. & C. Tul.
16. ***Fusarium planum*** S.L. Han, M.M. Wang & L. Cai- (Associated with branch die-back): New host record
17. ***Fusarium annulatum*** Bugnic. - (Pathogenic): New host record
18. ***Fusarium verticillioides*** (Sacc.) Nirenberg- (Pathogenic): New geographical record
19. ***Fusarium citri*** M.M. Wang, Qian Chen & L. Cai- (Pathogenic): New collection
20. ***Fusarium compactum*** (Wollenw.) Raillo- (Pathogenic): New collection
21. ***Fusarium sulawesiense*** Maryani, Sand.-Den., L. Lombard, Kema & Crous- (Associated with diseased twigs): New host record
22. ***Fusarium lateritium*** Nees- (Associated with diseased twigs): New collection
23. ***Fusarium*** sp. – (Pathogenic): New collection
24. ***Neocosmospora falciformis*** (Carrión) L. Lombard & Crous- (Pathogenic): New host record
25. ***Neocosmospora metavorans*** (Al-Hatmi, S.A. Ahmed & de Hoog) Sand.-Den. & Crous- (Pathogenic): New host record
26. ***Neocosmospora solani*** (Mart.) L. Lombard & Crous- (Pathogenic): New host record

INTRODUCTION

Prunus avium L. (sweet cherry) is an important stone fruit in *Rosaceae* (Blando & Oomah 2019). Sweet cherry has become one of the most appreciated fruits by consumers due to its attractive appearance, and taste (Wani et al. 2014, Blando & Oomah 2019, Chen et al. 2023). They are mostly cultivated in temperate regions (Srivastava et al. 2019) and originated from Europe and Asia (Blando & Oomah 2019). Sweet cherry has been cultivated in over 50 countries worldwide with an estimated production of 5.81 million tons in 2021 and 900 thousand hectares under cultivation (FAO 2023). China is one of the major cherry producers in the world and the area of sweet cherry cultivation has increased over the years (Chen et al. 2023). There are two main cherry-growing areas in China; Bohai Bay region and along the Longhai railway line area (Zhang et al. 2017, Chen et al. 2023).

Cherry trees are susceptible to many diseases caused by fungi, bacteria, viruses and insects (Chethana et al. 2019, Chen et al. 2023, Zhou et al. 2023a). Among these, fungal diseases including fruit rots, leafspots, gummosis, branch dieback, and canker frequently occur in almost all cherry-growing countries. Cherry leaf spot pathogens in Chinese cherry orchards have been extensively studied in recent years (Chethana et al. 2019, Zhou et al. 2022, 2023a). Chethana et al. (2019) isolated and identified *Alternaria prunicola*, *A. alternata*, *A. pseudoeichhorniae*, *Colletotrichum aenigma*, *C. pseudotheobromicola*, *Epicoccum pseudokeratinophilum*, *Nothophoma pruni*, *N. quercina* and *Stagonosporopsis citrulli* as leafspot causing pathogens. Zhou et al. (2023a) identified 13 *Colletotrichum* species (*C. aenigma*, *C. gloeosporioides*, *C. fructicola*, *C. siamense*, *C. temperatum*, *C. conoides*, *C. hebeiense*, *C. sojae*, *C. plurivorum*, *C. karsti*, *C. truncatum*, *C. incanum* and *C. dematium*) causing cherry leaf spots in China (Zhou et al. 2022). In addition, Zhou et al. (2022) reported seven *Fusarium* species (*F. citri*, *F. curvatum*, *F. ipomoeae*, *F. luffae*, *F. lateritium*, *F. compactum*, and *F. nygamai*) associated with cherry leafspot disease in China. Even though there are a considerable number of studies on fungi causing cherry leaf spot disease in China, little is known about the fungal species associated with cherry trunk diseases. Therefore, it is crucial to study the trunk diseases of cherries, as they have significant impacts on the life span of cherry orchards and the fruit production industry.

Trunk disease is a broad term that is used to describe various abnormalities of the woody parts of perennials, including vines and fruit trees (Cloete et al. 2011, Chen et al. 2023, Zhou et al. 2023b). There is evidence of the high incidence of fungal trunk diseases (FTD) in many economically important crops, especially fruit trees, nuts and olives (Guarnaccia et al. 2022). Therefore, studies on FTD have become a major concern among farming communities, stakeholders and researchers (Guarnaccia et al. 2022). *Phaeoacremonium* species have been reported to be associated with necrotic wood of *Prunus* trees (Damm et al. 2008, Soltaninejad et al. 2017) and *Botryosphaeriaceae* species are also well-known trunk and shoot dieback pathogens on stone fruits (Soltaninejad et al. 2017, Manawasinghe et al. 2016). In South Africa, *Cryptovalsa*, *Eutypa* and *Eutypella* species have been identified as pathogens associated with *Prunus* trunk disease (Moyo et al. 2018). Recently, Chen et al. (2023) reported *Diaporthe hongkongensis* causing sweet cherry branch dieback disease and, further, they have confirmed the host association of *D. eres* with sweet cherries in China. Even though China is one of the largest cherry producers in the world, there is no comprehensive study on cherry trunk pathogens in China. Therefore, the objectives of this present study were to (i) identify fungal species associated with sweet cherries based on morpho-molecular approaches and (ii) test and evaluate the pathogenicity of isolated ascomycetous fungi on *Prunus avium*. For all identified taxa, their phylogeny, descriptions and colored illustrations are provided.

MATERIALS AND METHODS

Disease symptoms, sampling and fungal isolation

Field surveys on sweet cherry trunk diseases were conducted during 2020–2022. Disease samples with typical symptoms of branch dieback, canker, twig blight and gummosis (Fig. 1) were collected from cherry orchards in Beijing municipality and Guizhou, Hebei, Liaoning, Shandong and Zhejiang provinces. The cherry trees were carefully observed and the number of disease samples collected would depend on the incidence of trunk diseases in the orchard and the province. Plant parts that exhibited the symptoms were carefully removed from the trees and taken to the laboratory for further assessment. For the isolation of fungi, tissue isolation was followed as described in Senanayake et al. (2020). Either, potato dextrose agar (PDA; 200g potatoes, 20g dextrose, 20g agar/L), malt extract agar (MEA; 30g malt extract, 5g mycological peptone, 15g agar per L) and/ or oat meal agar (OMA; 1L oatmeal extract, 15-20g agar) was used to culture the fungal species. Plates were incubated at 25–28 °C. The axenic cultures were obtained via either single-hyphal tip isolation and/or single-spore isolation (Senanayake et al. 2020). All the fungal cultures were deposited in the culture collection of the Beijing Academy of Agriculture and Forestry Sciences (JZB). Herbarium materials (as dry cultures) were deposited in the Fungarium at the Beijing Academy of Agriculture and Forestry Sciences (JZBH).

DNA extraction, PCR amplification and sequencing

Total genomic DNA was extracted from 5–7 days old pure cultures using the TIANcombi DNA Lyse & Det PCR Kit (Tiangen Biotech Co., Ltd, Beijing, China) following the manufacturer's protocols. In total, 7 gene regions were amplified and sequenced (Table 1). Polymerase chain reaction (PCR) mixture for all gene regions was as follows: 1 µL genomic DNA, 45 µl of Golden Star T6 Super PCR mix (1.1×) (Tsingke Biotechnology Co., Ltd., Beijing, China), 2 µl of 10 µM each forward and reverse primer in a total volume of 50 µL. Respective primer sequences are given in Table 1. The PCR was performed in a C1000 TouchTM thermal cycler (Bio-Rad Laboratories Inc., USA) and the results were observed after 1.5% agarose gel electrophoresis under ultraviolet light using GelDocXR+ (Bio-Rad Laboratories Inc., USA). All the PCR products were sequenced by Sinogenomax Co., Ltd, Beijing, China. The sequence quality was evaluated by examining the chromatograms using BioEdit v.7.0.9.0 (Hall 1999). Forward and reverse sequences were combined using Contig Express (v.9.1.0). All the sequences generated in this study were deposited in GenBank and respective GenBank numbers are given in Table 2.

Figure 1 – Field symptoms of Cherry trunk diseases. a, b, d Cherry plants showing branch die-back symptoms. c Died cheery tree. e–g Cross section of Cherry branches showing canker and necrosis symptoms. h–j Gummosis.

Table 1 Gene regions, respective primers and references used in the study.

Gene region*	Primer pairs	Sequence (5'-3')	References
ITS	ITS1	TCCGTAGGTGAACCTGCGG	White et al. (1990)
	ITS4	TCCTCCGCTTATTGATATGC	
LSU	LROR	GTACCCGCTGAACTTAAGC	Rehner & Samuels (1994), Vilgalys & Hester (1990)
	LR5	ATCCTGAGGGAAACTTC	
	LR7	TACTACCACCAAGATCT	
tef1-α	EF1-688F	CGGTCACTTGATCTACAAGTGC	Alves et al. (2008), Carbone & Kohn (1999), O'Donnell et al. (1998)
	EF1-1251R	CCTCGAACTCACCAGTACCG	
	EF1-728F	CATCGAGAAGTTCGAGAAGG	
	EF1-986R	TACTTGAAGGAACCCTTACC	
	EF1	ATGGGTAAGGARGACAAGAC	
	EF2	GGARGTACCAGTSATCATG	
ß-tubulin	T1	AACATGCGTGAGATTGTAAGT	O'Donnell & Cigelnik (1997), Glass & Donaldson (1995), Woudenberg et al. (2009)
	Bt2a	GGTAACCAAATCGGTGCTGCTTTC	
	Bt2b	ACCCTCAGTGTAGTGACCCTTGGC	
	TUB2Fd	GTBCACCTYCARACCGGYCARTG	
	TUB4Rd	CCRGAYTGRCCRAARACRAAGTTGTC	
RPB2	RPB2-5F2	GGGGWGAYCAGAAGAAGGC	Sung et al. (2007), Liu et al. (1999)
	fRPB2-7cR	CCCATRGCTTGTYYRCCCAT	
GAPDH	gpd1	CAACGGCTTCGGTCGCATTG	Berbee et al. (1999), Templeton et al. (1992)
	gpd2	GCCAAGCAGTTGGTTGTGC	
	GDF	GCCGTCAACGACCCCTTCATTGA	
	GDR	GGGTGGAGTCGTACTTGAGCATGT	
actin	ACT-512F	ATGTGCAAGGCCGGTTTCGC	Carbone & Kohn (1999)
	ACT-783R	TACGAGTCCTTCTGGCCCAT	

* ITS: internal transcribed spacer regions, LSU: Large subunit ribosomal RNA, tef1-α: translation elongation factor 1-alpha, RPB2: RNA polymerase largest subunit II, GAPDH: glyceraldehyde-3-phosphate dehydrogenase.

Phylogenetic analysis

The initial identification of species was done by searching against the sequences in the NCBI BLASTn search engine (https://blast.ncbi.nlm.nih.gov/Blast.cgi), and relevant sequences were downloaded from NCBI following recent taxonomic treatments. Using MAFFT v. 7 (http://mafft.cbrc.jp/alignment/server) downloaded sequences were aligned with the sequences generated in this study. Sequence alignments were trimmed using trimAl software and manual trimming was done where necessary (Capella-Gutiérrez et al. 2009). Combined and single gene files were prepared and analyzed based on each genus/family as given in the most recent publications. In the present study, phylogenetic analyses are based on maximum likelihood (ML) and Bayesian inferences (BI).

The evolutionary models for gene regions were selected using MrModeltest v. 2.3 (Nylander 2004). Both ML and BI analyses were carried out in the CIPRES Science Gateway portal (www.phylo.org, Miller et al. 2010). Maximum likelihood analyses were accomplished using RAxML-HPC2 on XSEDE v. 8.2.8. The GTR+I+G evolution model was used with 1000 non-parametric bootstrapping iterations. Bayesian Inference analyses were performed using MrBayes v. 3.2.7 (Ronquist et al. 2012). The best model of evolution was determined by MrModeltest v. 2.4 (Nylander 2004) for each gene. The Markov Chain Monte Carlo sampling (BMCMC) analysis was conducted with four simultaneous Markov chains. The MCMC heated chain was set with a 05 "temperature" value and run for 1,000,000 generations. Trees were sampled at every 100th generation. From the 10,000 trees obtained, the first 2,000 representing the burn-in phase were discarded. To calculate posterior probabilities, the remaining 8,000 trees were used.

Morphological characterization

For each fungal species, colony morphology and conidial characters were recorded. After 5–7 days of growth on PDA, or MEA/OMA at 25 °C – 28 °C, colony color was noted by following Rayner's color chart (Rayner 1970). Axio Imager Z2 photographic microscope (Carl Zeiss Microscopy, Oberkochen, Germany) was used to capture digital images of morphological characters. ZEN PRO 2012 (Carl Zeiss Microscopy, Oberkochen, Germany) was used to take measurements. Conidial length and width were measured for 40 conidia for each isolate, and the means were calculated. Conidial shape and color were also recorded.

Pathogenicity assay

To determine if the isolated fungal species in this study are capable of causing damage to the *Prunus avium* in laboratory conditions, pathogenicity tests were conducted by following the guidelines mentioned in Bhunjun et al. (2021a). Experiments were started by inoculating selected fungal strains on one-year-old healthy detached shoots of *Prunus avium* cv. 'Tieton'. Healthy shoots were collected from Tongzhou Experimental Station for Cherries, Beijing Academy of Forestry and Pomology Sciences, Beijing, China. Shoot surfaces were sterilized by washing in 75% ethanol for 1 min, then using 10% sodium hypochlorite for 1 min, and followed by washing shoots with distilled water three times. The experiment was conducted using 15 shoots per isolate (including nine shoots for control), inoculated by the wounded inoculation method. These experiments were repeated once. The wound inoculations were performed in the middle of each shoot. The outer layer of the bark was injured with a cork borer (diam. 5 mm). Agar plugs containing the mycelium of each fungal isolate were used to inoculate the wound sites of each of the shoots. The agar plugs without any mycelium were used as the control. All inoculated shoots were placed in a plastic container with soil and incubated in a moist chamber at 25 °C with an 80% relative humidity until symptoms appeared. Lesion lengths were recorded seven or ten days after the inoculation. Koch's postulates were confirmed by re-isolating the inoculated fungus. The re-isolated fungus was identified based on cultural, and morphological characteristics and by sequencing of the ITS region.

RESULTS

The present paper aims to survey and identify the fungal trunk diseases of *Prunus avium*, with a particular focus on the Chinese situation of their causal organisms. Based on the morphology and multi-loci phylogeny, here we have provided detailed accounts for 26 fungal species which are distributed in nine families in Ascomycota.

Prevalence of fungal species in Chinese cherry orchards

In total, 193 fungal isolates that belong to 26 fungal species were identified from sweet cherry trunk diseases in Beijing municipality and Guizhou, Hebei, Liaoning, Shandong and Zhejiang provinces of China.

These species comprised *Botryosphaeria dothidea* (19 isolates), *Cladosporium anthropophilum* (8 isolates), *Cl. cladosporioides* (9 isolates), *Cl. perangustum* (2 isolates), *Cl. ramotenellum* (8 isolates), *Cl. sphaerospermum* (2 isolates), *Cl. tenuissimum* (7 isolates), *Nothophoma pruni* (14 isolates), *No. quercina* (11 isolates), *Alternaria alternata* (27 isolates), *Monilinia fructicola* (7 isolates), *Cytospora leucostoma* (5 isolates), *Colletotrichum fioriniae* (9 isolates), *Co. godetiae* (13 isolates), *Clonostachys farinosa* (2 isolates), *Fusarium planum* (2 isolates), *F. annulatum* (11 isolates), *F. verticillioides* (3 isolates), *F. citri* (3 isolates), *F. compactum* (1 isolate), *F. sulawesiense* (3 isolates), *F. lateritium* (13 isolates), *Fusarium* sp. (4 isolates), *Neocosmospora falciformis* (2 isolates), *Ne. metavorans* (4 isolates), *Ne. solani* (4 isolates). Of these 26 species, *Alternaria alternata* (15%) was most commonly isolated, followed by *Botryosphaeria dothidea* (11%), *Nothophoma pruni* (8%) and *Colletotrichum godetiae* (7%). The most isolates were obtained from Beijing and it is most probably because of the more intensive sampling carried out there.

Table 2 Strains/isolates obtained in this study and their GenBank accession numbers.

Species	Culture no.	GenBank Accession no.						
		ITS	tef1-α	ß-tubulin	actin	RPB2	GAPDH	LSU
Alternaria alternata	JZB3180080	ON013969	ON152818	–	–	OM965644	OP422980	–
	JZB3180081	ON013970	ON152819	–	–	OM965645	OP422981	–
	JZB3180082	ON013971	ON152820	–	–	OM965646	OP422982	–
	JZB3180083	ON013972	ON152821	–	–	OM965647	OP422983	–
	JZB3180085	ON013974	ON152823	–	–	OM965649	OP422985	–
	JZB3180088	ON013977	ON152826	–	–	OM965652	OP422988	–
	JZB3180089	ON013978	ON152827	–	–	OM965653	OP422989	–
	JZB3180090	ON013979	ON152828	–	–	OM965654	OP422990	–
	JZB3180091	ON013980	ON152829	–	–	OM965655	OP422991	–
	JZB3180092	ON013981	ON152830	–	–	OM965656	OP422992	–
	JZB3180093	ON013982	ON152831	–	–	OM965657	OP422993	–
	JZB3180099	ON013988	ON152837	–	–	OM965663	OP422999	–
	JZB3180100	ON013989	ON152838	–	–	OM965664	OP423000	–
	JZB3180101	ON013990	ON152839	–	–	OM965665	OP423001	–
	JZB3180107	ON013996	ON152845	–	–	OM965671	OP423007	–
	JZB3180108	ON013997	ON152846	–	–	OM965672	OP423008	–
	JZB3180110	ON013999	ON152848	–	–	OM965674	OP423010	–
	JZB3180112	ON014001	ON152850	–	–	OM965676	OP423012	–
	JZB3180113	ON014002	ON152851	–	–	OM965677	OP423013	–
	JZB3180114	ON014003	ON152852	–	–	OM965678	OP423014	–
	JZB3180115	ON014004	ON152853	–	–	OM965679	OP423015	–
	JZB3180116	ON014005	ON152854	–	–	OM965680	OP423016	–
	JZB3180118	ON014007	ON152856	–	–	OM965682	OP423018	–
	JZB3180119	ON014008	ON152857	–	–	OM965683	OP423019	–
	JZB3180122	ON014011	ON152860	–	–	OM965686	OP423022	–
	JZB3180123	ON014012	ON152861	–	–	OM965687	OP423023	–
	JZB3180126	ON014015	ON152864	–	–	OM965690	OP423026	–
Botryosphaeria dothidea	JZB310221	OP363875	OP381599	OP381615	–	–	–	OP379543
	JZB310222	OP363876	OP381600	OP381616	–	–	–	OP379544
	JZB310223	OP363877	OP381601	OP381617	–	–	–	OP379545
	JZB310224	OP363878	OP381602	OP381618	–	–	–	OP379546
	JZB310225	OP363879	OP381603	OP381619	–	–	–	OP379547
	JZB310226	OP363880	OP381604	OP381620	–	–	–	OP379548
	JZB310227	OP363881	OP381605	OP381621	–	–	–	OP379549

Table 2 Continued.

Species	Culture no.	GenBank Accession no.						
		ITS	tef1-α	ß-tubulin	actin	RPB2	GAPDH	LSU
	JZB310228	OP363882	OP381606	OP381622	–	–	–	OP379550
	JZB310229	OP363883	OP381607	OP381623	–	–	–	OP379551
	JZB310230	OP363884	OP381608	OP381624	–	–	–	OP379552
	JZB310231	OP363885	OP381609	OP381625	–	–	–	OP379553
	JZB310232	OP363886	OP381610	OP381626	–	–	–	OP379554
	JZB310233	OP363887	OP381611	OP381627	–	–	–	OP379555
	JZB310234	OP363888	OP381612	OP381628	–	–	–	OP379556
	JZB310235	OP363889	OP381613	OP381629	–	–	–	OP379557
	JZB310236	OP363890	OP381614	OP381630	–	–	–	OP379558
	JZB310237	OP363891	–	OP381631	–	–	–	OP379559
	JZB310238	OP363892	–	OP381632	–	–	–	OP379560
	JZB310239	OP363893	–	OP381633	–	–	–	OP379561
Cladosporium tenuissimum	JZB390019	OM883836	OM920416	–	OM906948	–	–	–
	JZB390020	OM883837	OM920417	–	OM906949	–	–	–
	JZB390021	OM883838	OM920418	–	OM906950	–	–	–
	JZB390022	OM883839	OM920419	–	OM906951	–	–	–
	JZB390023	OM883840	OM920420	–	OM906952	–	–	–
	JZB390024	OM883841	OM920421	–	OM906953	–	–	–
	JZB390025	OM883842	OM920422	–	OM906954	–	–	–
Cl. anthropophilum	JZB390026	OM900039	OM920423	–	OM953782	–	–	–
	JZB390027	OM900040	OM920424	–	OM953783	–	–	–
	JZB390028	OM900041	OM920425	–	OM953784	–	–	–
	JZB390029	OM900042	OM920426	–	OM953785	–	–	–
	JZB390030	OM900043	OM920427	–	OM953786	–	–	–
	JZB390031	OM900044	OM920428	–	OM953787	–	–	–
	JZB390032	OM900045	OM920429	–	OM953788	–	–	–
	JZB390033	OM900046	OM920430	–	OM953789	–	–	–
Cl. cladosporioides	JZB390040	OR936276	OR980953	–	OR964111	–	–	–
	JZB390041	OR936277	OR980954	–	OR964112	–	–	–
	JZB390042	OR936278	OR980955	–	OR964113	–	–	–
	JZB390043	OR936279	OR980956	–	OR964114	–	–	–
	JZB390044	–	OR980957	–	OR964115	–	–	–
	JZB390045	OR936280	OR980958	–	OR964116	–	–	–
	JZB390046	OR936281	OR980959	–	OR964117	–	–	–

Table 2 Continued.

Species	Culture no.	GenBank Accession no.						
		ITS	tef1-α	ß-tubulin	actin	RPB2	GAPDH	LSU
	JZB390047	OR936282	OR980960	–	OR964118	–	–	–
	JZB390048	OR936283	OR980961	–	OR964119	–	–	–
Cl. ramotenellum	JZB390061	OR936284	OR980962	–	OR964120	–	–	–
	JZB390062	OR936285	OR980963	–	OR964121	–	–	–
	JZB390063	OR936286	OR980964	–	OR964122	–	–	–
	JZB390064	OR936287	OR980965	–	OR964123	–	–	–
	JZB390065	OR936288	OR980966	–	OR964124	–	–	–
	JZB390066	OR936289	OR980967	–	OR964125	–	–	–
	JZB390067	OR936290	OR980968	–	OR964126	–	–	–
	JZB390068	OR936291	OR980969	–	OR964127	–	–	–
Cl. perangustum	JZB390056	OR958627	OR980970	–	OR964128	–	–	–
	JZB390057	OR958628	OR980971	–	OR964129	–	–	–
Cl. sphaerospermum	JZB390059	OR958629	OR980972	–	OR964130	–	–	–
	JZB390060	OR958630	OR980973	–	OR964131	–	–	–
Clonostachys farinosa	JZB3530055	PQ459775	PQ469037	PQ469039	–	–	–	PQ459781
	JZB3530056	PQ459781	PQ469038	PQ469040	–	–	–	PQ459782
Colletotrichum godetiae	JZB330329	OP389167	–	OP561410	–	–	OP422958	–
	JZB330330	OP389168	–	OP561411	–	–	OP422959	–
	JZB330331	OP389169	–	OP561412	–	–	OP422960	–
	JZB330332	OP389170	–	OP561413	–	–	OP422961	–
	JZB330333	OP389171	–	OP561414	–	–	OP422962	–
	JZB330334	OP389172	–	OP561415	–	–	OP422963	–
	JZB330335	OP389173	–	OP561416	–	–	OP422964	–
	JZB330336	OP389174	–	OP561417	–	–	OP422965	–
	JZB330337	OP389175	–	OP561418	–	–	OP422966	–
	JZB330338	OP389176	–	OP561419	–	–	OP422967	–
	JZB330339	OP389177	–	OP561420	–	–	OP422968	–
	JZB330340	OP389178	–	OP561421	–	–	OP422969	–
	JZB330341	OP389179	–	OP561422	–	–	OP422970	–
Colletotrichum fioriniae	JZB330342	OP389180	–	OP561423	–	–	OP422971	–
	JZB330343	OP389181	–	OP561424	–	–	OP422972	–
	JZB330344	OP389182	–	OP561425	–	–	OP422973	–

Table 2 Continued.

Species	Culture no.	GenBank Accession no.						
		ITS	tef1-α	ß-tubulin	actin	RPB2	GAPDH	LSU
	JZB330345	OP389183	–	OP561426	–	–	OP422974	–
	JZB330346	OP389184	–	OP561427	–	–	OP422975	–
	JZB330347	OP389185	–	OP561428	–	–	OP422976	–
	JZB330348	OP389186	–	OP561429	–	–	OP422977	–
	JZB330349	OP389187	–	OP561430	–	–	OP422978	–
	JZB330350	OP389188	–	OP561431	–	–	OP422979	–
Cytospora leucostoma	JZB3670001	OQ828651	–	PP101838	PP068466	–	–	OQ828682
	JZB3670002	OQ828652	PP101834	PP101839	PP068467	–	–	OQ828683
	JZB3670003	OQ828653	PP101835	PP101840	PP068468	–	–	OQ828684
	JZB3670004	OQ828654	PP101836	PP101841	PP068469	–	–	OQ828685
	JZB3670005	OQ828655	PP101837	PP101842	PP068470	–	–	OQ828686
Fusarium fujikuroi species complex								
F. annulatum	JZB3110234	ON798833	OP245126	–	–	ON868387	–	–
	JZB3110235	ON798834	OP245127	–	–	ON868388	–	–
	JZB3110236	ON798835	OP245128	–	–	ON868389	–	–
	JZB3110237	ON798836	OP245129	–	–	ON868390	–	–
	JZB3110238	ON798837	OP245130	–	–	ON868391	–	–
	JZB3110239	ON798838	OP245131	–	–	ON868392	–	–
	JZB3110240	ON798839	OP245132	–	–	ON868393	–	–
	JZB3110241	ON798840	OP245133	–	–	ON868394	–	–
	JZB3110231	ON798830	OP245123	–	–	ON868384	–	–
	JZB3110232	ON798831	OP245124	–	–	ON868385	–	–
	JZB3110233	ON798832	OP245125	–	–	ON868386	–	–
F. planum	JZB3110229	ON798828	OP245121	–	–	ON868382	–	–
	JZB3110230	ON798829	OP245122	–	–	ON868383	–	–
F. verticillioides	JZB3110226	ON798825	OP245118	–	–	ON868379	–	–
	JZB3110227	ON798826	OP245119	–	–	ON868380	–	–
	JZB3110228	ON798827	OP245120	–	–	ON868381	–	–
Fusarium incarnatum-equiseti species complex								
F. citri	JZB3110253	ON798852	OP245142	–	–	ON868406	–	–
	JZB3110254	ON798853	OP245143	–	–	ON868407	–	–
	JZB3110255	ON798854	OP245144	–	–	ON868408	–	–
F. compactum	JZB3110252	ON798851	–	–	–	ON868405	–	–
F. sulawense	JZB3110256	ON798855	OP245145	–	–	ON868409	–	–

Table 2 Continued.

Species	Culture no.	GenBank Accession no.						
		ITS	tef1-α	ß-tubulin	actin	RPB2	GAPDH	LSU
	JZB3110257	ON798856	OP245146	–	–	ON868410	–	–
	JZB3110258	ON798857	OP245147	–	–	ON868411	–	–
Fusarium lateritium species complex								
F. lateritium	JZB3110343(SDZG34-C-S1)	–	PQ475740	–	–	PQ475753	–	–
	JZB3110344(SDZG34-C-S2)	–	PQ475741	–	–	PQ475754	–	–
	JZB3110345(SYZG-10-B-S1)	PQ461338	PQ475742	–	–	PQ475755	–	–
	JZB3110346(SYZG-10-B-S2)	PQ461339	PQ475743	–	–	PQ475756	–	–
	JZB3110347(SYZG-10-B-S3)	PQ461340	PQ475744	–	–	PQ475757	–	–
	JZB3110348(SYZG-10-B-S4)	PQ461341	PQ475745	–	–	PQ475758	–	–
	JZB3110350(SYZG23-A-S3)	PQ461343	PQ475746	–	–	PQ475759	–	–
	JZB3110351(SYZG26-A-S1)	PQ461344	PQ475747	–	–	PQ475760	–	–
	JZB3110352(SYZG26-A-S2)	PQ461345	PQ475748	–	–	PQ475761	–	–
	JZB3110354(SYYP5-A-S1)	PQ461347	PQ475749	–	–	PQ475762	–	–
	JZB3110357(SYYP5-B-S1)	PQ461350	PQ475750	–	–	PQ475763	–	–
	JZB3110358(SYYP5-B-S2)	PQ461351	PQ475751	–	–	PQ475764	–	–
	JZB3110359(SYYP5-B-S3)	PQ461352	PQ475752	–	–	PQ475765	–	–
Fusarium oxysporum species complex								
Fusarium sp.	JZB3110360(ZZG2-B-S2)	PQ469915	PQ475770	–	–	PQ475766	–	–
	JZB3110361(ZZG2-B-S3)	PQ469916	PQ475771	–	–	PQ475767	–	–
	JZB3110362(TZZG43-A-S1)	PQ469917	PQ475772	–	–	PQ475768	–	–
	JZB3110363(TZZG43-A-S2)	PQ469918	PQ475773	–	–	PQ475769	–	–
Monilinia fructicola	JZB3690001	PP101295	PP110487	–	–	–	–	–
	JZB3690002	PP101296	PP110488	–	–	–	–	–
	JZB3690003	PP101297	PP110489	–	–	–	–	–
	JZB3690004	PP101298	PP110490	–	–	–	–	–
	JZB3690005	PP101299	PP110491	–	–	–	–	–
	JZB3690006	PP101300	PP110492	–	–	–	–	–
	JZB3690007	PP101301	PP110493	–	–	–	–	–

Table 2 Continued.

Species	Culture no.	GenBank Accession no.						
		ITS	tef1-α	ß-tubulin	actin	RPB2	GAPDH	LSU
Neocosmospora falciformis	JZB3110250	ON798849	–	–	–	ON868403	–	–
	JZB3110251	ON798850	–	–	–	ON868404	–	–
Ne. metavorans	JZB3110242	ON798841	OP245134	–	–	ON868395	–	–
	JZB3110243	ON798842	OP245135	–	–	ON868396	–	–
	JZB3110244	ON798843	OP245136	–	–	ON868397	–	–
	JZB3110247	ON798846	OP245139	–	–	ON868400	–	–
Ne. solani	JZB3110245	ON798844	OP245137	–	–	ON868398	–	–
	JZB3110246	ON798845	OP245138	–	–	ON868399	–	–
	JZB3110248	ON798847	OP245140	–	–	ON868401	–	–
	JZB3110249	ON798848	OP245141	–	–	ON868402	–	–
Nothophoma pruni	JZB380087	ON316849	–	ON350994	–	ON350972	–	ON318981
	JZB380088	ON316850	–	ON350995	–	ON350973	–	ON318982
	JZB380089	ON316851	–	ON350996	–	ON350974	–	ON318983
	JZB380090	ON316852	–	ON350997	–	ON350975	–	ON318984
	JZB380091	ON316853	–	ON350998	–	ON350976	–	ON318985
	JZB380092	ON316854	–	ON350999	–	ON350977	–	ON318986
	JZB380093	ON316855	–	ON351000	–	ON350978	–	ON318987
	JZB380094	ON316856	–	ON351001	–	ON350979	–	ON318988
	JZB380095	ON316857	–	ON351002	–	ON350980	–	ON318989
	JZB380096	ON316858	–	ON351003	–	ON350981	–	ON318990
	JZB380097	ON316859	–	–	–	ON350982	–	ON318991
	JZB380098	ON316860	–	ON351004	–	ON350983	–	ON318992
	JZB380099	ON316861	–	ON351005	–	ON350984	–	ON318993
	JZB380100	ON316862	–	ON351006	–	ON350985	–	ON318994
No. quercina	JZB380101	ON316863	–	ON351007	–	ON350986	–	ON318995
	JZB380102	ON316864	–	ON351008	–	ON350987	–	ON318996
	JZB380103	ON316865	–	ON351009	–	ON350988	–	ON318997
	JZB380104	ON316866	–	ON351010	–	ON350989	–	ON318998
	JZB380105	ON316867	–	ON351011	–	ON350990	–	ON318999
	JZB380106	ON316868	–	ON351012	–	ON350991	–	ON319000
	JZB380107	ON316869	–	ON351013	–	ON350992	–	ON319001
	JZB380108	ON316870	–	ON351014	–	ON350993	–	ON319002

*****ITS: internal transcribed spacer regions, LSU: Large subunit ribosomal RNA, tef1-α: translation elongation factor 1-alpha, ß-tubulin: Beta tubulin, RPB2: RNA polymerase largest subunit II, GAPDH: glyceraldehyde-3-phosphate dehydrogenase. JZB: Culture collection of Beijing Academy of Agriculture and Forestry Sciences.

Taxonomy

Fungal classes, orders, families and genera were treated according to Wijayawardene et al. (2020, 2022a) and Hyde et al (2024).

Dothideomycetes O.E. Erikss. & Winka

We follow the latest taxonomic treatments and updated accounts of Dothideomycetes as in Hongsanan et al. (2020a, b) and Wijayawardene et al. (2020, 2022a).

Botryosphaeriaceae Theiss. & Syd. [as 'Botryosphaeriacae']

Botryosphaeriaceae is the largest family in *Botryosphaeriales* and currently, it consists of 32 genera (Wu et al. 2021). Species in *Botryosphaeriaceae* are distributed worldwide and occur on a wide range of plants (Crous et al. 2006, Slippers & Wingfield 2007, Phillips et al. 2013, 2019, Yan et al. 2013, Zhang et al. 2016, Hongsanan et al. 2020a, Batista et al. 2021, Manawasinghe et al. 2022, Jayawardena et al. 2022, Wijayawardene et al. 2022b, Wang et al. 2024). For the taxonomic treatment of this family, we follow Phillips et al. (2013) and Zhang et al. (2021).

Botryosphaeria Ces. & De Not.

Botryosphaeria dothidea, is the type species of *Botryosphaeria* (Phillips et al. 2013). Initially, *Botryosphaeria* was identified as a saprobe from a dead woody plant in 1863 and has repeatedly now been identified as pathogens and endophytes (Slippers & Wingfield 2007). These species are common pathogens, saprobes and endophytes of a wide range of nursery and economically important plant hosts (Guarnaccia et al. 2022, Jayawardena et al. 2022, Wijayawardene et al. 2022b, Senanayake et al. 2023, Wang et al. 2024). For the updated taxonomic treatment of this genus, we follow Zhang et al. (2021). In the present study, we obtained 19 *Botryosphaeria* isolates. Based on the multigene phylogenetic analysis, all 19 isolates clustered together with the clade *Botryosphaeria dothidea*. The phylogenetic tree and species description with illustrations are given below (Fig. 2).

Botryosphaeria dothidea (Moug.) Ces. & De Not., Comm. Soc. crittog. Ital. 1(fasc. 4): 212 (1863) Fig. 3

Index Fungorum number: IF183247

Associated with *Prunus avium* branches with die-back symptoms. Sexual morph: not observed. Asexual morph: *Conidiomata* pycnidial, produced on the culture. *Conidiophores* are hyaline, smooth and thin walled, cylindrical, often reduced to conidiogenous cells. *Conidiogenous cells* phialidic or cylindrical, hyaline, 15–36 µm long, 2–5 µm wide at the base, 1.5–3 (–5) µm wide at the tip. *Conidia* aseptate, hyaline, narrowly fusiform, or irregularly fusiform, base subtruncate to bluntly rounded 18–26 × 5–7 µm (av. 23 ± 2 × 6 ± 1 µm, n = 50), L/W = 4.

Cultural characteristics – Colonies on PDA reaching 73 mm after three days at 25 ºC. Initial colony white, becoming grey to black from above, and black in reverse after seven days. Mycelium mat moderately dense, with smooth margin.

Material examined – China, Beijing, from the *Prunus avium* branch with die-back symptoms, April 2022, P. Chen, (dried cultures JZBH310221–JZBH310227, JZBH310233–JZBH310238) living cultures, JZB310221–JZB310227, JZB310233–JZB310238; Guizhou Province, from the *Prunus avium* branch with die-back symptoms, April 2022, P. Chen, (dried cultures JZBH310228–JZBH310230) living cultures, JZB310228–JZB310230; Shandong Province, from the *Prunus avium* branch with die-back symptoms, April 2022, P. Chen, (dried cultures JZBH310231, JZBH310232, JZBH310239) living cultures, JZB310231, JZB310232, JZB310239.

Notes – *Botryosphaeria dothidea* is a common latent fungal pathogen, that mainly causes cankers and die-back in many woody hosts (Marsberg et al. 2017). This species has been reported worldwide and shows a cosmopolitan distribution (Phillips et al. 2013). This species has already been identified on sweet cherries in China as causing gummosis in Yuci City, Shanxi Province (Zhang et al. 2019) and leaf spot disease in Beijing, Shandong and Liaoning Provinces (Zhou et al. 2021).

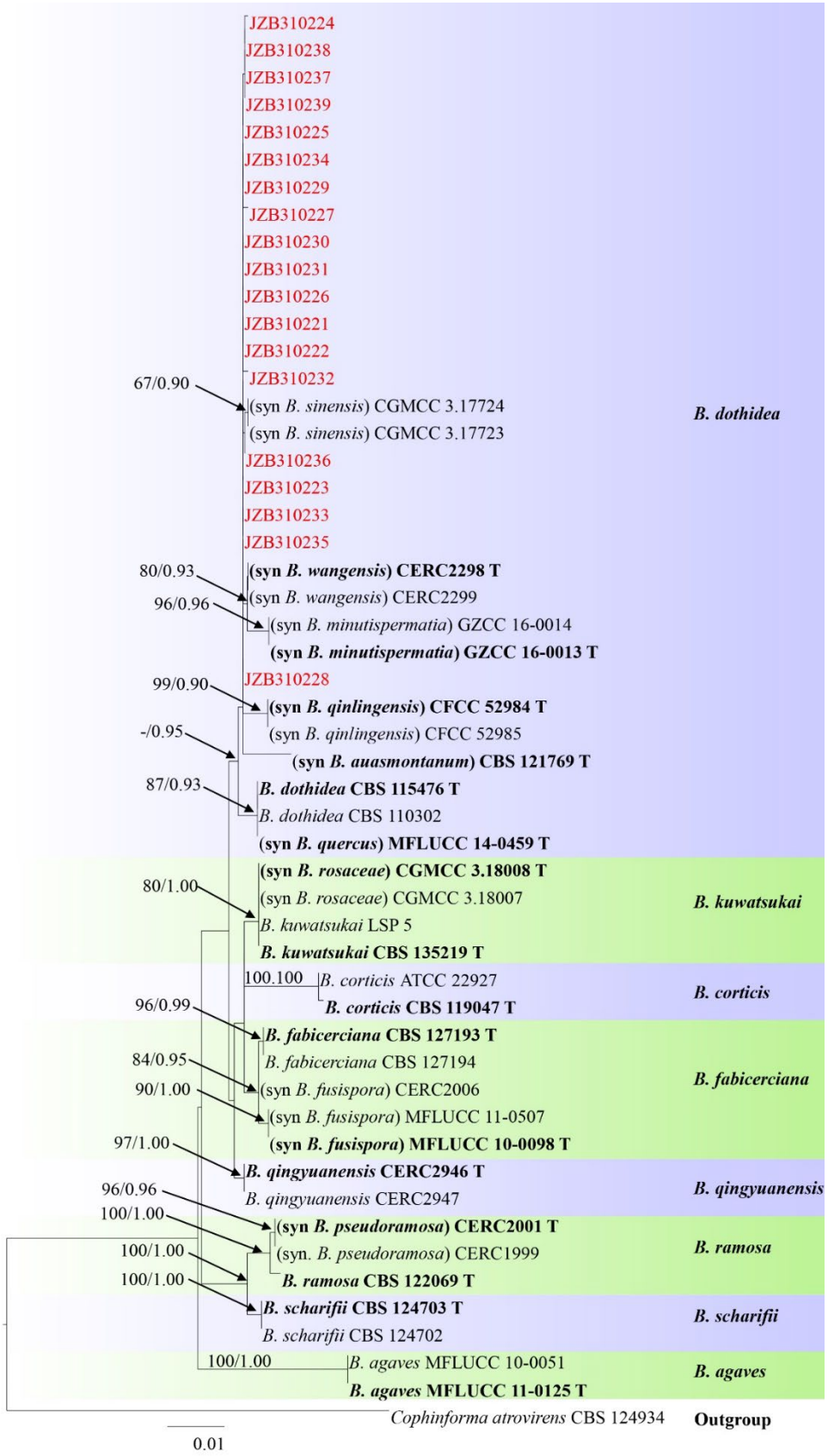

Figure 2 – Phylogenetic tree generated by maximum likelihood analysis of combined ITS, tef1-α and ß-tubulin sequence data of *Botryosphaeria* species. The tree is rooted with *Cophinforma atrovirens* (CBS 124934). Maximum likelihood values (BT) ≥ 60% and Bayesian posterior probabilities values (PP) ≥ 0.90 are shown respectively near the nodes. The scale bar indicates 0.01 changes. The ex-type strains are bold, marked with "T" in the end and isolates from the current study

are in red. The maximum likelihood alignment matrix had 207 distinct alignment patterns with 14.73% of undetermined characters or gaps. Estimated base frequencies were as follows: A = 0.210389, C = 0.311956, G = 0.255512, T = 0.222143. substitution rates AC = 0.616726, AG = 2.603279, AT = 0.932524, CG = 0.631950, CT = 4.367045, GT = 1.000000; gamma distribution shape parameter α= 0.901636.

We have obtained 19 fungal isolates from symptomatic die-back branches collected from Beijing, Guizhou and Shandong Provinces. Phylogenetically, all these isolates were clade with other reference strains of *B. dothidea* with high statistical support (Fig. 2). Morphologically, isolates obtained in this study are similar to the characters of ex-epitype of *B. dothidia* (CBS115476) as given in the Phillips et al. (2013). When comparing the morphology with the ex-epitype strain (CBS115476), our isolates showed larger conidiogenous cells and smaller conidia. These are probably because of host and environmental variations. We did not observe any spermatophores, spermatogenous cells or spermatia in our isolated strains. Hence, based on both morpho-molecular data, here we report the *B. dothidea* associated with sweet cherry branches with die-back disease in China. However, the pathogenicity of our *B. dothidea* strains needs to be confirmed with further studies.

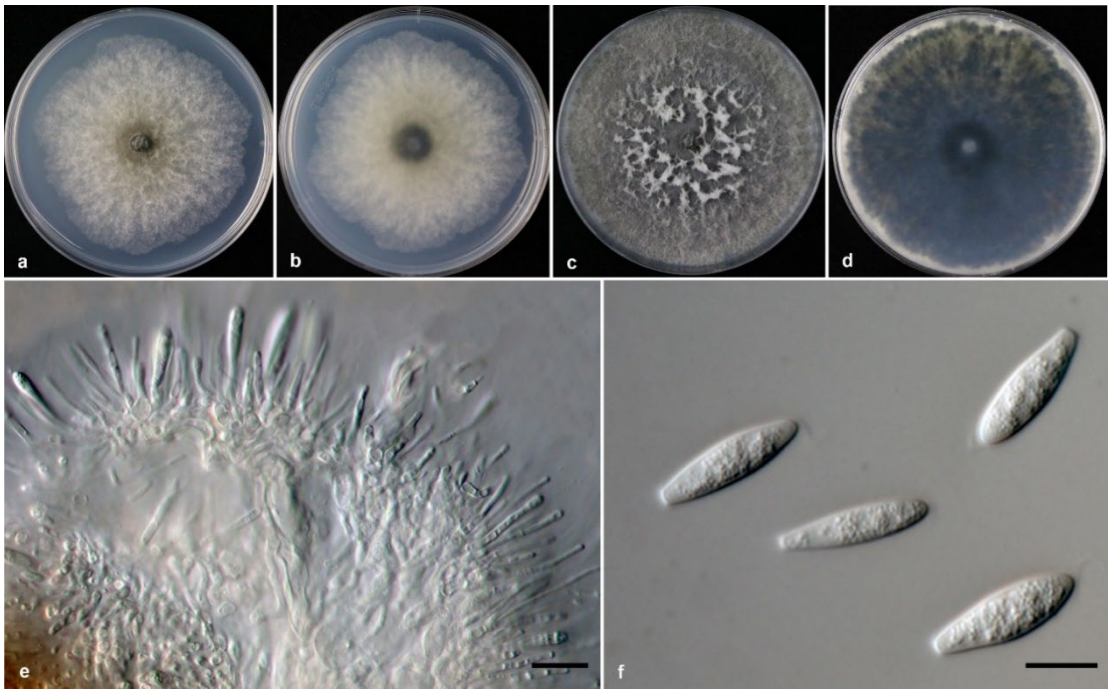

Figure 3 – *Botryosphaeria dothidea* (JZB310221). a–d Upper and reverse view of a colony grown on PDA at 25 °C dark. a, b After 3 days. c, d After 7 days. e Developing conidia attached to the conidiophores. f Conidia. Scale bars: e = 20 μm, f = 10 μm.

Cladosporiales Abdollahz. & Crous

Based on multigene phylogenetic analysis, Abdollahzadeh et al. (2020) elevated *Cladosporiaceae* to *Cladosporiales*.

Cladosporiaceae Chalm. & R.G. Archibald

Cladosporiaceae species are mostly saprobic and endophytic. There are few species reported as fungicolous, lichenicolous, or plant pathogens. For taxonomic treatments of this family, we follow Abdollahzadeh et al. (2020).

Cladosporium Link

Cladosporium was established by Link (1816) and it is considered one of the largest and most heterogeneous genera of dematiaceous hyphomycetes (Bensch et al. 2012, Jayawardena et al. 2018).

Species in *Cladosporium* are characterized by a unique coronate structure of conidiogenous loci and conidial hila, and central convex dome surrounded by a raised periclinal rim (Bensch et al. 2012, Jayawardena et al. 2018). There are more than 800 epithets given in Index Fungorum (2025). They are the most common air-borne microorganisms (Abdollahzadeh et al. 2020, Wang et al. 2022) and many species belonging to *Cladosporium* are reported as endophytes, pathogens, and hyperparasites of other fungi. For the taxonomic treatment of this genus, we follow Abdollahzadeh et al. (2020) and Wang et al. (2022).

Cladosporium anthropophilum Sand.-Den. et al., Persoonia 36: 290. 2016 Fig. 5a–d

Index Fungorum number: IF815334

Associated with *Prunus avium* branches with die-back symptoms, leaf spots and leaves with shot-hole and necrosis symptoms. Sexual morph: not observed. Asexual morph: *Hyphomycetous*. *Mycelium* immersed. *Hyphae* branched or unbranched, septate, subhyaline to pale olivaceous. *Conidiophores* macro and semi-macronematous, branched, 29–266 µm long. *Conidiogenous cells* terminal and intercalary, cylindrical or sub-cylindrical, 17–35 × 3–4 µm. *Ramoconidia* cylindrical, 19–37 × 4–4.5 µm, 0 (–1)-septate, pale olivaceous, smooth, thickened and darkened. *Secondary ramoconidia* ellipsoid to subcylindrical, 12–16.5 × 3–4 µm, subhyaline or pale olivaceous, smooth. *Intercalary conidia* limoniform to ellipsoid, 3.5–7 × 2.5–3 µm, aseptate. *Conidia* forming short, branched chains, terminal conidia ovoid to ellipsoidal, 3.5–5 × 2–3 µm.

Cultural characteristics – Colonies on PDA reaching 60–65 mm after 14 d at 25 ℃ in dark, upper surface grey olivaceous, olivaceous or greenish olivaceous, reverse olivaceous black, velvety or powdery, margin white, regular, flat, sometimes showing cottony to floccose white to grey cushions.

Material examined – China, Beijing, from the *Prunus avium* branch with die-back symptoms, April 2021, S. X. Ji, (dried culture JZBH390026) living culture, JZB390026; Beijing, from the leafspots of *Prunus avium*, April 2021, S. X. Ji, (dried culture JZBH390027) living culture, JZB390027; Liaoning Province, from the *Prunus avium* branch with die-back symptoms, April 2021, S. X. Ji, (dried cultures JZBH390028, JZBH390029) living cultures, JZB390028, JZB390029; Liaoning Province, from the leafspots of *Prunus avium*, April 2021, S. X. Ji, (dried cultures JZBH390030, JZBH390031) living cultures, JZB390030, JZB390031; Guizhou Province, from the *Prunus avium* leaves with shot-hole and necrosis symptoms, April 2021, S. X. Ji, (dried cultures JZBH390032, JZBH390033) living cultures, JZB390032, JZB390033.

Notes – *Cladosporium anthropophilum* was initially described from human clinical samples from the USA and this species is considered the second most dominant species identified in a set of clinical isolates from the USA after *C. halotolerans* (Sandoval-Denis et al. 2015, 2016). Later this species was isolated from different host plants as pathogens, endophytes and also saprobes (Bensch et al. 2018, Lee et al. 2019, Tibpromma et al. 2019, Cho et al. 2023). Even though *C. anthropophilum* morphologically similar to *C. cladosporioides*, phylogenetically they are distinct (Sandoval-Denis et al. 2015). Here we obtained eight fungal isolates from diseased *Prunus avium* branches with die-back symptoms and leaves with shot-holes, necrosis and spots. Based on multi-locus phylogenetic data they were classified with ex-type strain (CBS 140685) and other reference strains of *Cladosporium anthropophilum* with high statistical support (Fig. 4). When comparing the morphology of our isolates of *C. anthropophilum* with the ex-type of *C. anthropophilum* (CBS 140685), our isolates produce smaller conidiophores (29–266 µm long vs up to 550 µm), conidiogenous cells (17–35 × 3–4 µm vs 15–54 × 3–5 µm), ramoconidia (19–37 × 4–4.5 µm vs 20–42 × 2–5 µm), secondary ramoconidia (12–16.5 × 3–4 µm vs 7–28 × 2–5 µm), intercalary conidia (3.5–7 × 2.5–3 µm vs 4.5–11 × 2–3 µm) and terminal conidia (3.5–5 × 2–3 µm vs 3.5–9 × 2–3 µm). Therefore, based on morpho-molecular data, we identified our isolates as *C. anthropophilum.* The exact life style (either pathogenic, saprobic or secondary invaders) of our *C. anthropophilum* strains needs to be confirmed with further studies.

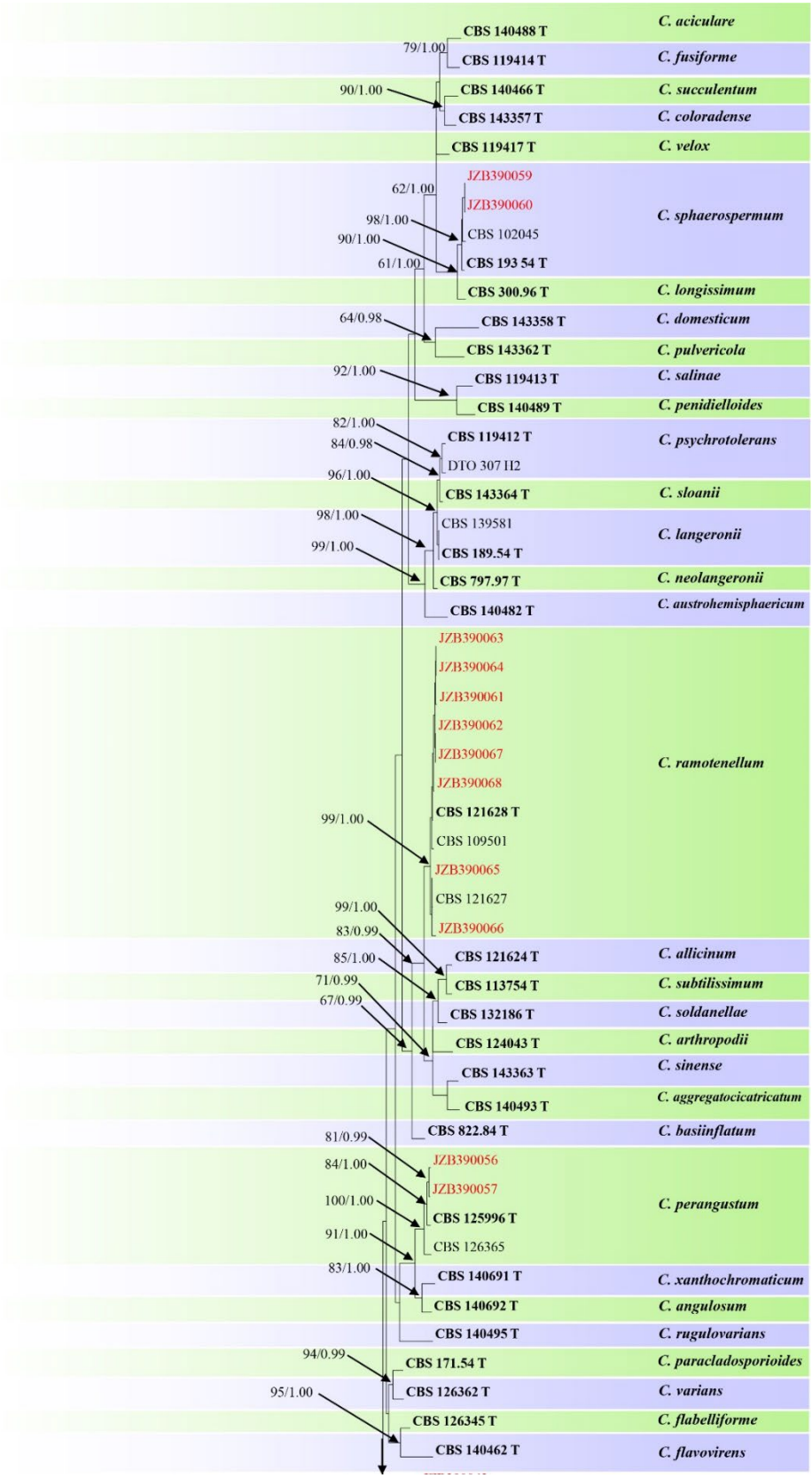

Figure 4 – Phylogenetic tree generated by maximum likelihood analysis of combined ITS, tef1-α and actin sequence data of species belonging to *Cladosporium*. The tree was rooted with *Cercospora beticola* (CBS 116456). RAxML bootstrap support values (BT) ≥ 60% and Bayesian posterior probabilities (PP) ≥ 0.90 are shown respectively near the nodes. The scale bar indicates 0.3 changes. The ex-type strains are marked in bold and the isolate numbers from the current study are in red. The maximum likelihood alignment matrix had 579 distinct alignment patterns with 22.21% of

undetermined characters or gaps. Estimated base frequencies were as follows: A = 0.223364, C = 0.301529, G = 0.239292, T =0.235815. substitution rates AC = 1.580186, AG = 3.241721, AT = 1.708694, CG = 0.878278, CT = 4.468190, GT = 1.000000; gamma distribution shape parameter α= 0.785574.

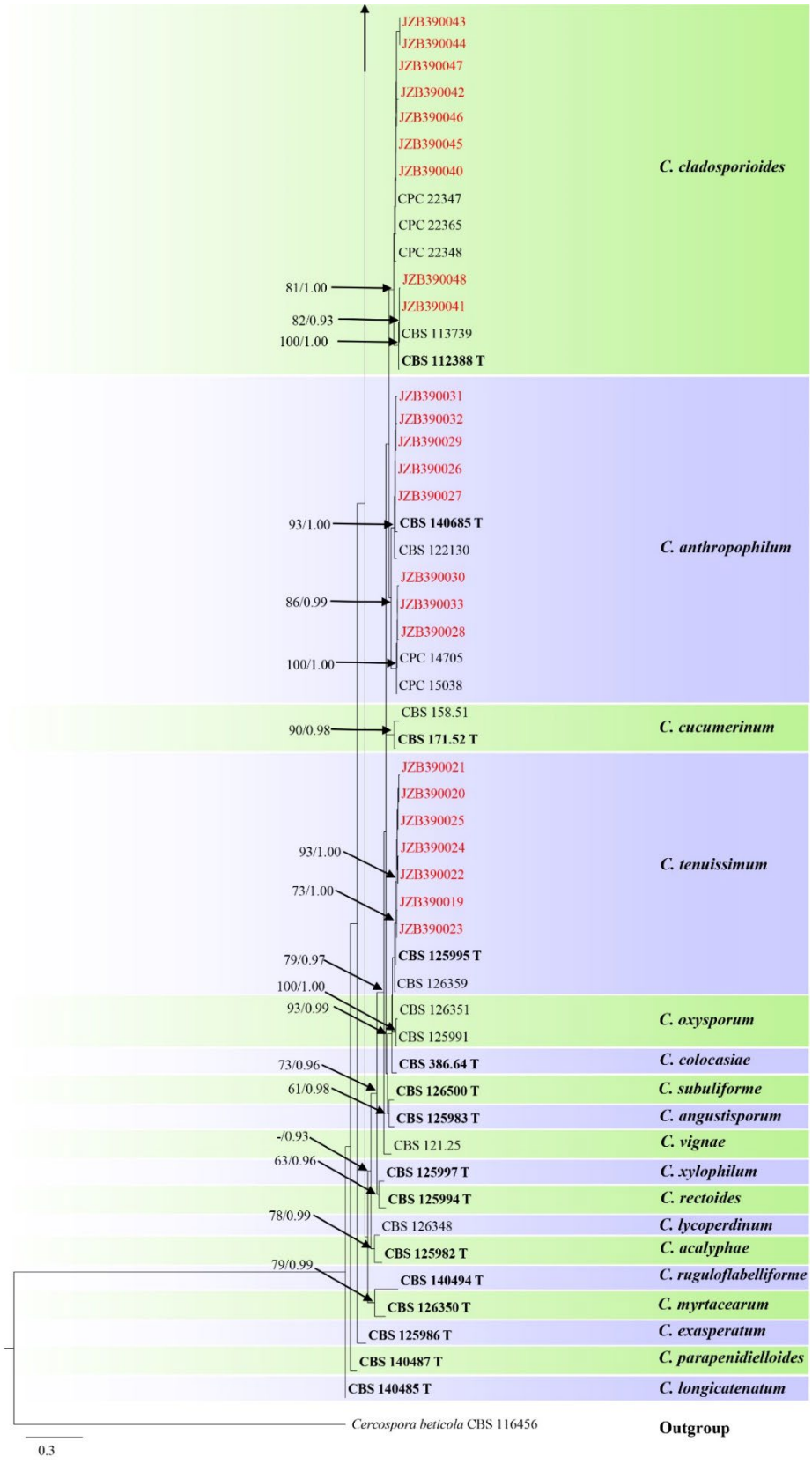

Figure 4 – Continued.

Cladosporium cladosporioides (Fresen.) G.A. de Vries, Contrib. Knowledge of the Genus Cladosporium Link ex Fries: 57 (1952) Fig. 5e–i

Index Fungorum number: IF815334

Associated with *Prunus avium* branches with die-back symptoms, diseased leaves and fruits. Sexual morph: not observed. Asexual morph: *Hyphomycetous*. *Mycelium* mainly immersed, sparse hyphae, unbranched or sparingly branched, septate. *Conidiophores* macro-, semi-macro- or micronematous, arising terminally from ascending hyphae, strait to somewhat flexuouse, cylindrical to cylindrical-oblong, (31–) 40–255(–452) × 3–5 μm, branched or unbranched. *Conidiogenous cells* integrated, terminal, cylindrical-oblong, 22.3–67.7 × 2.6–4.8 μm (av. ± SD: 42.4 ± 12.8 × 4 ± 0.5 μm, n = 20). *Conidia* numerous, in long branched chains, branching in all directions; small terminal conidia obovoid or subglobose, 3.4–5.7 × 2.5–3.8 μm (av. ± SD: 4.4 ± 0.5 × 2.9 ± 0.3 μm, n = 30), aseptate. *Intercalary conidia* limoniform, ellipsoid-ovoid, fusiform or subcylindrical, aseptate, 5.2–7×2.5–3.3 μm (av. ± SD: 6 ± 0.4 × 2.9 ± 0.2 μm, n = 30).

Cultural characteristics – Colonies on PDA reaching 30 mm after 7 d at 25 ℃ in dark, upper surface grey olivaceous to dull green or greenish-olivaceous, reverse olivaceous-black, velvety or powdery, margin white, regular, flat.

Material examined – China, Beijing, from the *Prunus avium* branch with die-back symptoms, July 2022, S. X. Ji & P. Chen, (dried cultures JZBH390040, JZBH390042–JZBH390046) living cultures, JZB390040, JZB390042–JZB390046; Liaoning Province, from the *Prunus avium* branch with die-back symptoms, July 2022, S. X. Ji & W. Zhang (dried culture JZBH390047) living culture, JZB390047; Beijing, from the diseased fruit of *Prunus avium,* July 2022, S. X. Ji & P. Chen, (dried culture JZBH390041) living culture, JZB390041; Beijing, from a leaf of *Prunus avium,* July 2022, S. X. Ji & P. Chen, (dried culture JZBH390048) living culture, JZB390048.

Notes – *Cladosporium cladosporioides* is one of the most commonly isolated species of *Cladosporium* and this species has been reported mainly as a common saprotroph and also causes secondary infection on decaying plant parts (Bensch et al. 2010). Also, this species has been isolated from air, soil, textiles and several other substrates (Bensch et al. 2010). Nine *Cladosporium* strains were recovered in this study, and phylogenetically they were classified with reference isolates of *Cladosporium cladosporioides* with good statistical support (Fig. 4). When compare the morphology of our isolates with the ex-type of *C. cladosporioides* (CBS 112388), our isolates produce larger conidiophores ((31–) 40–255(–452) × 3–5 μm vs 9–150 × (1–)1.5–2.5(–3) in CBS 112388), conidiogenous cells (22.3–67.7 μm vs (7–)16–38 μm long) and approximately similar size of conidia (3.4–5.7 × 2.5–3.8 μm vs 3–6(–7) × (1.5–)2–2.5(–3) μm). Therefore, based on morpho-molecular data, we identified our isolates as *C. cladosporioides*. However, we could not confirm whether our strains were pathogens or caused secondary infections on sweet cherry shoots.

Cladosporium perangustum Bensch et al., Stud. Mycol. 67: 65. 2010 Fig. 6a–d

Index Fungorum number: IF517085

Associated with *Prunus avium* branches with die-back symptoms. Sexual morph: not observed. Asexual morph: *Hyphomycetous*. *Mycelium* immersed and superficial and hyphae loosely branched, septate, subhyaline to pale-olivaceous or pale-olivaceous-brown. *Conidiophores* solitary, macro-, semi-macro- or micronematous, arising terminally and laterally from hyphae, erect, straight or slightly flexuous, filiform to narrowly cylindrical-oblong and subhyaline, pale olivaceous or pale olivaceous brown. *Conidiogenous cells* terminal or intercalary. *Ramoconidia* cylindrical-oblong, 0−1 septate, sometimes slightly dark, 8–36 × 2.5–4 μm (av. ± SD: 16.1 ± 7.2 × 3.2 ± 0.4 μm). *Secondary ramoconidia* narrowly ellipsoid to cylindrical-oblong, pale olivaceous brown, smooth. *Conidia* numerous, in branched chains, branching in all directions, small terminal conidia globose-subglobose or ovoid to obovoid, (–2.7)3–6 × 2–3 μm (av. ± SD: 3.8 ± 0.7 × 2.7 ± 0.2 μm).

Cultural characteristics – Colonies on PDA reaching 50 mm diam. after 14 d at 25 ℃ in dark. Upper surface grey olivaceous to olivaceous, olivaceous grey, sometimes with patches of smoke-grey or pale greenish-grey. Reverse olivaceous grey, iron-grey olivaceous-black, velvety, fluffy, floccose or powdery, margins glabrous to feathery, whitish.

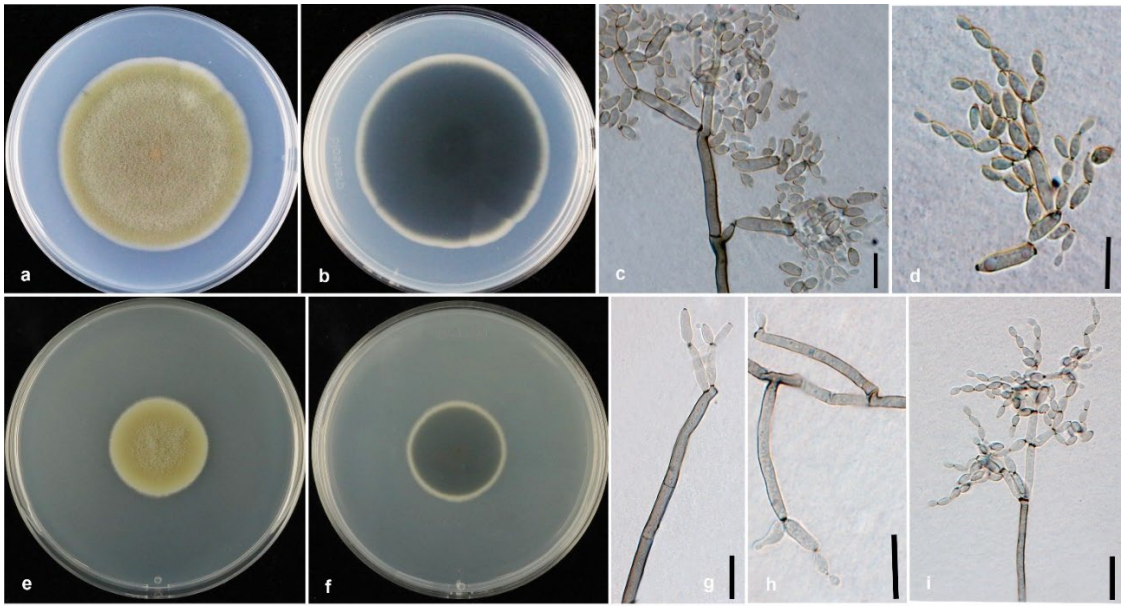

Figure 5 – a–d *Cladosporium anthropophilum* (JZB390029). a, b Upper and reverse view of colony grown on PDA at 25 °C dark after 14 days. c, d Branching conidiophore, secondary ramoconidia and conidial chains on PDA. e–i *Cladosporium cladosporioides* (JZB390040). e, f Upper and reverse view of colony grown on PDA at 25 °C dark after seven days. g–i Branching conidiophore, secondary ramoconidia and conidial chains on PDA. Scale bars: c, d = 10 µm, g–i = 20 µm.

Material examined – China, Liaoning Province, from the *Prunus avium* branch with die-back symptoms, April 2020, S. X. Ji, (dried cultures JZBH390056, JZBH390057) living cultures, JZB390056, JZB390057.

Notes – *Cladosporium perangustum* has been reported from different substrates including plant materials and food (Bensch et al. 2010). This species has been later reported to cause leaf spots on a few plant hosts. *Cladosporium perangustum* was identified as causing grape flyspeck disease on the Shine-Muscat table grapes in South Korea (Hassan et al. 2021) and causing leaf spots on *Syagrus oleracea* (bitter coconut) in Brazil (Oliveira et al. 2014). In China, this species has been recorded as causing leaf spots on Chinese bayberry (*Myrica rubra*) (Lu et al. 2015). Based on multi-loci phylogenetic data two *Cladosporium* isolates were clade with reference strains of *C. perangustum* with high statistical support (Fig. 4). These two isolates share similar morphological characters with ex-type of *C. perangustum* (CBS 125996) with minor size differences. So far, this species has not report on *Prunus avium* worldwide, therefore here, we report the novel host association of *C. perangustum* on sweet cherries from China.

Cladosporium ramotenellum K. Schub. et al., Stud. Mycol. 58: 137. 2007 Fig. 6e–i

Index Fungorum number: IF504577

Associated with *Prunus avium* branches with die-back symptoms and leafspots. Sexual morph: not observed. Asexual morph: *Hyphomycetous*. *Mycelium* unbranched or sparingly branched, smooth. *Conidiophores* solitary, macro- and micronematous, erect, straight or slightly flexuous, cylindrical, subhyaline to pale olivaceous or brown, smooth or minutely verruculose, 24–106 × 3–5 µm (av. ± SD: 61.5 ± 20.9 × 3.9 ± 0.4 µm, n = 15). *Conidiogenous cells* integrated, terminal or intercalary, cylindrical, 25–43 × 4–5 µm (av. ± SD: 34.6 ± 7.9 × 3.9 ± 0.4 µm, n = 5). *Ramoconidia* cylindrical-oblong, subhyaline to pale olivaceous, smooth, 13–34 × 4–5 (av. ± SD: 23.1 ± 6.9 × 4.6 ± 0.4 µm, n = 10). *Secondary ramoconidia* ellipsoid or subcylindrical to cylindrical-oblong, subhyaline to pale olivaceous, 5–23 × 3–5 µm (av. ± SD: 10.9±4.7 × 4.4 ± 0.5 µm, n = 33). *Intercalary conidia* subcylindrical to limoniform, or ellipsoid, 4–7 × 3–4 µm (av. ± SD: 5.4 ± 0.5 × 3.3 ± 0.2 µm, n = 50), 0–septate, subhyaline. *Conidia* numerous, in branched chains, small terminal conidia

numerous, globose, subglobose or ovoid, aseptate, 3–7.5 × 2–4 µm (av. ± SD: 4.3 ± 0.6 × 3.1 ± 0.3 µm, n = 46).

Cultural characteristics – Colonies on PDA reaching 61 mm diam. after 14 days at 25 °C in dark. Upper surface grey-greenish to olivaceous and reverse olivaceous-black. Margin entire edge, hyaline, aerial mycelium absent, growth flat. No prominent exudates.

Material examined – China, Beijing, from the *Prunus avium* branch with die-back symptoms, March 2021, S. X. Ji & W. Zhang, (dried cultures JZBH390061–JZBH390065, JZBH390067), living cultures JZB390061–JZB390065, JZB390067. Beijing, from leafspots of *Prunus avium*, March 2021, S. X. Ji & W. Zhang, (dried culture JZBH390066), living culture JZB390066. Liaoning Province, from the *Prunus avium* branch with die-back symptoms, March 2021, S. X. Ji & W. Zhang, (dried culture JZBH390068), living culture JZB390068.

Notes – *Cladosporium ramotenellum* initially recovered from hypersaline water in saltern in Slovenia (Zalar et al. 2007). Later, this species was found to be a quite common saprobic species, being widely distributed and occurring on various substrates (Bensch et al. 2015). As a plant pathogen, this species has been reported to cause sooty spots on easy peeler mandarins in Peru and postharvest sooty spots and decay on clementines in the United States (Murciano et al. 2021, Hu 2023). We have recovered eight isolates of *Cladosporium* and based on multi-loci phylogenetic data, all our isolates clade together with the ex-type isolate (CBS 121628) and other reference strains of *C. ramotenellum* with 99 BT/1.00 PP statistical support (Fig. 4). Morphologically, our isolates share similar characters as the ex-type isolate of *C. ramotenellum* with minor size differences.

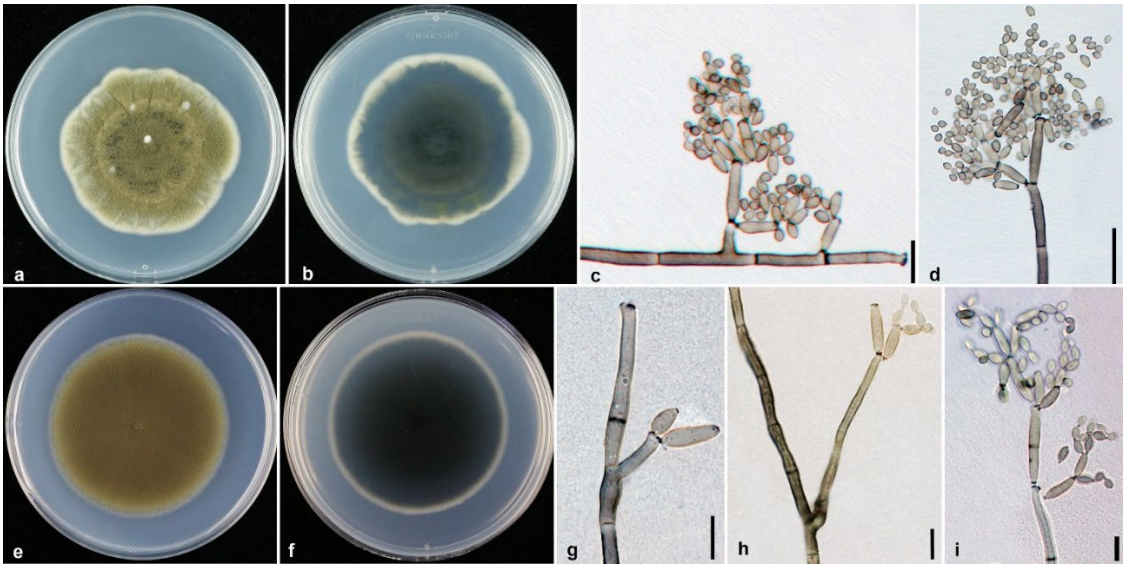

Figure 6 – a-d *Cladosporium perangustum* (JZB390057). a Upper view. b Reverse view of the colony in PDA after 14 d at 25 °C in the dark. c, d Conidiophores and conidial chains. Scale bars: c, d = 20 µm. e-i *Cladosporium ramotenellum* (JZB390064). e Upper view. f Reverse view of the colony in PDA after 14 d at 25 °C in the dark. g–i Conidiophores and conidial chains. Scale bars: g–i = 10 µm.

Cladosporium sphaerospermum Penz., in Saccardo, Michelia 2(no. 8): 473 (1882) Fig.7a–d

Index Fungorum number: IF119529

Associated with *Prunus avium* branches with die-back symptoms. Sexual morph: not observed. Asexual morph: *Hyphomycetous*. *Mycelium* superficial, hyphae branched, septate, pale olivaceous green, smooth. *Conidiophores* micro- and macronematous, arising terminally and laterally from hyphae, erect or ascending, straight to slightly flexuous. *Conidiogenous cells* integrated, terminal, sometimes intercalary, cylindrical, 9–35 × 3–4 µm (av. ± SD: 17 ± 6.1 × 3.4 ± 0.3 µm, n = 40). *Conidia* catenate, in branched chains, branching in all directions, straight, small terminal conidia

globose to subglobose, sometimes ovoid, aseptate. *Ramoconidia* often formed, cylindrical, slightly thickened and somewhat darkened, 4–19 × 3–4 μm (av. ± SD: 9.3 ± 3.7 × 3.3 ± 0.3 μm, n = 45).

Cultural characteristics – Colonies on PDA reaching 50 mm diam. after 14 d at 25 °C in the dark. Upper surface greenish-olivaceous, reverse iron-grey or greyish-blue, olivaceous-black. Margins white, regular, narrow, growth flat. No prominent exudates formed.

Material examined – China, Beijing, from the *Prunus avium* branch with die-back symptoms, March 2021, S. X. Ji & W. Zhang, (dried cultures JZBH390059, JZBH390060), living cultures JZB390059, JZB390060.

Notes – *Cladosporium sphaerospermum* is a dematiaceous saprobic species that is commonly found in diverse environments including indoor and outdoor air, soil, decaying vegetation, paint, silicone and textiles (Bensch et al. 2018). Initially, this species was described from decaying *Citrus* leaves and branches in Italy (Bensch et al. 2018). We recovered two isolates of *Cladosporium* from Beijing and based on multi-loci phylogenetic data our isolates clade together with ex-neo type strain (CBS 193.54) and reference strain (CBS 102045) of *C. sphaerospermum* with high statistical report. Morphologically, our isolates share similar characteristics as ex-neotype of *C. sphaerospermum* with minor size differences (Bensch et al. 2018). So far, this species has not been reported from *Prunus avium* worldwide, therefore in this study, we report the novel host association of *C. sphaerospermum* on *Prunus avium* in China.

Cladosporium tenuissimum Cooke, Grevillea 6(no. 40): 140 (1878) Fig. 7e–j

Index Fungorum number: IF145672

Associated with *Prunus avium* branches with die-back symptoms. Sexual morph: not observed. Asexual morph: *Hyphomycetous*. *Mycelium* immersed and superficial, hyphae branched, septate. *Conidiophores* solitary, macro- and micronematous, arising terminally and laterally from hyphae, cylindrical-oblong to almost filiform. *Conidiogenous cells* (4.5–) 6.5–45 μm long, with 1−3 conidiogenous loci at the apex. *Ramoconidia* cylindrical with a broadly truncate base, 10.7–42.6 × 2.8–4 μm (n = 5). *Secondary ramoconidia* ellipsoid or subcylindrical, 8.6–20.9 × 3.3–5.3 μm (av. 12.7 × 4.2 μm, n = 20) 0–1-septa, with 2–3 distal conidial hilum. *Conidia* catenate, formed in branched chains, small terminal conidia subglobose, ovoid to obovoid or somewhat limoniform, 3–5.2 × 2.4–3.3 μm (av. 4.1 × 2.7 μm, n = 50), aseptate. *Intercalary conidia* limoniform, ovoid or ellipsoid 3.9–6.6 × 2.3–3.5 μm (av. 4.9–2.9 μm, n = 50), 0(–1)-septa, pale olivaceous brown.

Cultural characteristics – Colonies on PDA reaching 65–69.5 mm after 14 d at 25 °C in the dark. Upper surface greenish-olivaceous or grey-olivaceous, reverse iron-grey or greyish-blue, olivaceous black. Margins white, regular, narrow.

Material examined – China, Beijing, from the *Prunus avium* branch with die-back symptoms, March 2021, S. X. Ji & W. Zhang, (dried cultures JZBH390024, JZBH390055), living cultures JZB390024, JZB390025. Zhejiang Province, from the *Prunus avium* branch with die-back symptoms, May 2021, S. X. Ji & W. Zhang, (dried cultures JZBH390019–JZBH390023), living cultures JZB390019–JZB390023.

Notes – *Cladosporium tenuissimum* is a common saprobe and it has been identified from different substrates including air, soil, water and different plant parts (Bensch et al. 2018). *Cladosporium tenuissimum* caused leaf spot on Panicle Hydrangea (Li et al. 2021), Peanut (*Arachis hypogaea*) (Geng et al. 2022), pumpkins (*Cucurbita maxima*), melon (*Cucumis melon*) (Gomes et al. 2023) and fruit brown spot on dekopon (*Citrus reticulata*) (Xiao et al. 2023). We recovered seven *Cladosporium* isolates from two provinces in China, and based on the analysis of combined sequence data, they cluster with *Cladosporium tenuissimum* reference strain (CBS 126359) and type strain (CBS 125995) with high statistical support (93% BT and 1.0 PP) (Fig. 4). Morphologically, our isolates share similar characters as type strain of *C. tenuissimum* with minor morphological differences.

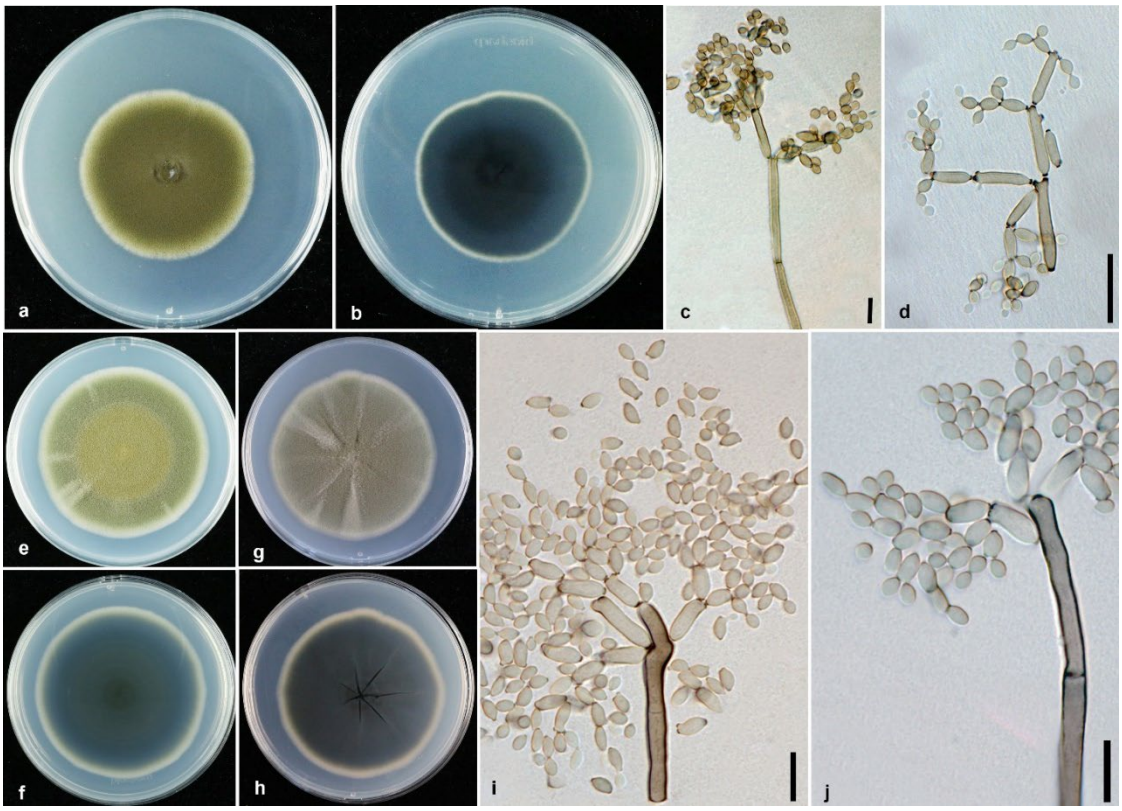

Figure 7 – a–d *Cladosporium sphaerospermum* (JZB390060). a Upper view. b Reverse view of the colony in PDA after 14 d at 25 °C in the dark. c, d Conidiophores and conidial chains. e–j *Cladosporium tenuissimum* (JZB390019). e–h Upper and reverse view of the colony in PDA after 14 d at 25 °C in the dark. i, j Conidiophores and conidial chains. Scale bars: c, i, j = 10 µm, d = 20 µm.

Pleosporomycetidae C.L. Schoch, Spatafora, Crous & Shoemaker
Pleosporales Luttr. ex M.E. Barr

We follow the latest treatments and updated accounts of *Pleosporales* in Hongsanan et al. (2020b), Wijayawardene et al. (2022a) and Pem et al. (2024).

Didymellaceae Gruyter, Aveskamp & Verkley

Didymellaceae is one of the most species-rich families in the Ascomycota and species in *Didymellaceae* inhabit a wide range of ecosystems (Chen et al. 2017). This family was established in 2009 to accommodate three genera and several phoma-like genera (Chen et al. 2015). Recently, Pem et al. (2024) have accepted 47 genera to the *Didymellaceae*.

Nothophoma Qian Chen & L. Cai

Nothophoma was established by Chen et al. (2015), with the type species *Nothophoma infossa*. These species have been reported as plant pathogens, on various hosts (Chethana et al. 2019). In addition, they have also been reported from clinical samples of humans in the respiratory secretion and bronchial wash sample (Valenzuela-Lopez et al. 2018). In this study, 22 *Nothophoma* isolates were obtained from diseased twigs of *Prunus avium*. Based on the multigene gene phylogenetic analysis of ITS, LSU, ß-tubulin and RPB2 sequence data these strains were further identified into two *Nothophoma* species; named *N. pruni* and *N. quercina*. Illustrations and descriptions are provided below.

Nothophoma pruni Chethana, J.Y. Yan, X.H. Li & K.D. Hyde (2019) Fig. 9a–d

Index Fungorum number: IF828518

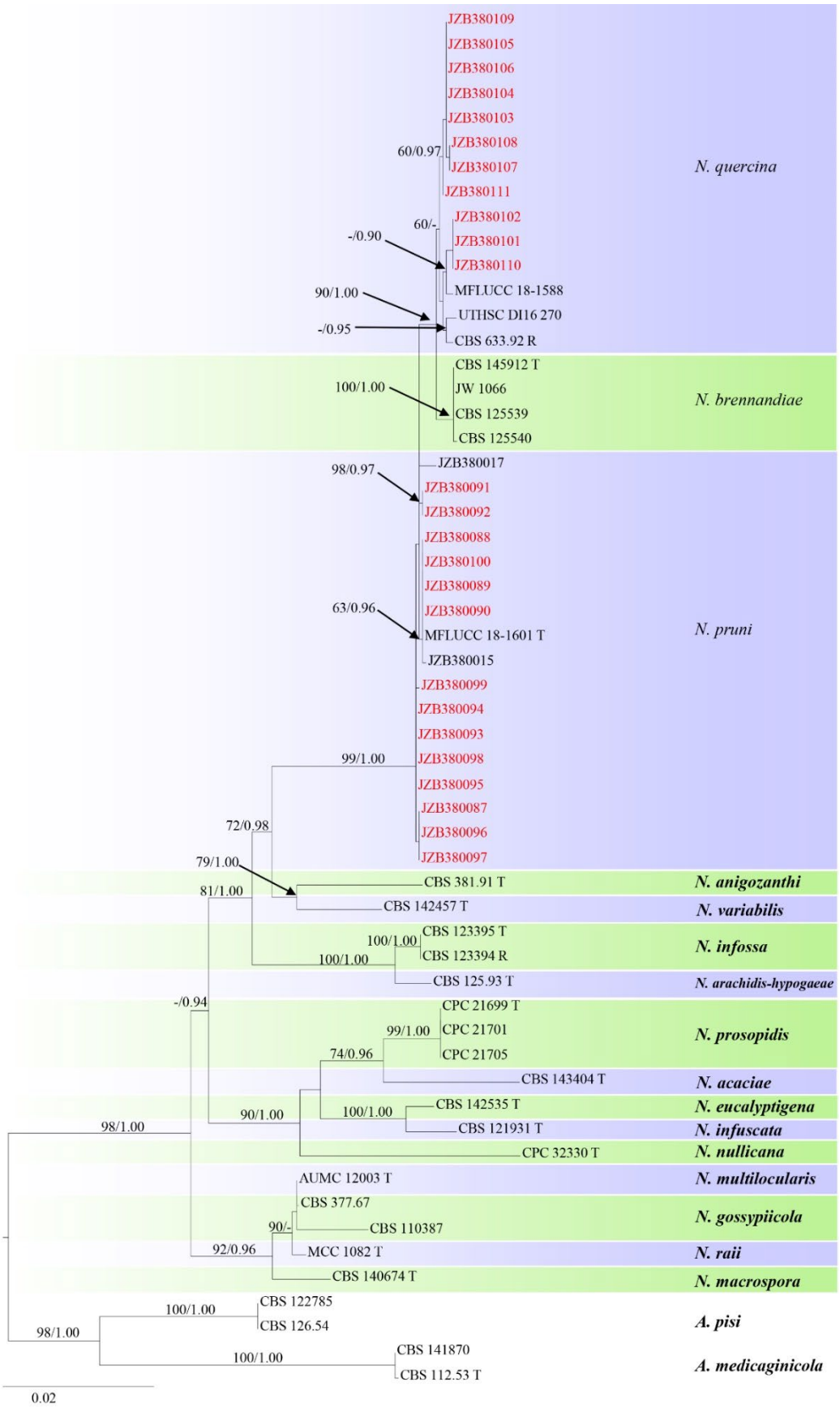

Figure 8 – Phylogenetic tree generated by maximum likelihood analysis of combined ITS, LSU, ß-tubulin and RPB2 sequence data of species belonging to *Nothophoma*. The tree was rooted with *Ascochyta pisi* (CBS 122785, CBS 126.54) and *A. medicaginicola* (CBS 141870, CBS 112.53). RAxML bootstrap support values ≥ 60% (BT) and Bayesian posterior probabilities ≥ 0.90 (PP) are

shown respectively near the nodes. The scale bar indicates 0.02 changes. The ex-type strains are bold and isolates from the current study are in red. The maximum Likelihood alignment matrix had 353 distinct alignment patterns, with 8.17% of undetermined characters or gaps, estimated base frequencies were as follows; A = 0.237990, C = 0.243063, G = 0.280542, T = 0.238405; substitution rates AC = 1.736338, AG = 5.999085, AT =1.580204, CG = 0.527705, CT = 17.070812, GT = 1.000000; gamma distribution shape parameter α = 0.956462.

Associated with *Prunus avium* branches with die-back symptoms. Sexual morph: not observed. Asexual morph: *Pycnidia* on the PDA, solitary, scattered, globose to irregular shaped, black. *Pycnidial wall* multi-layered *Conidiophores* hyaline. *Conidiogenous cells* phialidic, hyaline, simple, doliiform to ampulliform, variable in size. *Conidia* obovoid to oblong or variable in size and shape, hyaline to pale brown, smooth-walled, aseptate, guttulate, 4.8–8.8×2.9–5 μm (av. ± SD: 6.3 ± 0.9×3.7 ± 0.5 μm, n = 40).

Cultural characteristics – Colonies on PDA reach 65–68 mm diam. after 14 d at 25 °C in the dark. Upper surface greenish olivaceous to grey olivaceous near the centre, with a dull white margin and reverse olivaceous to greyish sepia streaks and white in the margin. Margin regular, aerial mycelium.

Material examined – China, Beijing, from the *Prunus avium* branch with die-back symptoms, April 2021, S. X. Ji & W. Zhang, (dried cultures JZBH380087–JZBH380092), living cultures JZB380087–JZB380092. Shandong Province, from the *Prunus avium* branch with die-back symptoms, May 2021, S. X. Ji & W. Zhang, (dried cultures JZBH380093–JZBH380100), living cultures JZB380093–JZB380100.

Notes – *Nothophoma pruni* was initially identified from the leaf spots of *Prunus avium* which were collected from Beijing, China (Chethana et al. 2019). In this study, we isolated 14 strains of *Nothophoma* from two locations in China, including Beijing. Based on multi-loci phylogenetic analysis, these strains were clade with reference strains of *N. pruni* with high statistical support (Fig. 8). Our isolates also share similar morphological characteristics as in ex-type of *Nothophoma pruni* (MFLUCC 18–1601) with minor size differences, however, we observed the conidia of our isolates were pale brown (Chethana et al. 2019). In this study, we report the new collection of *N. pruni* from Chinese cherry orchards.

Nothophoma quercina (Syd. & P. Syd.) Qian Chen & L. Cai (2015) Fig. 9e–g

Index Fungorum number: IF814086

Associated with *Prunus avium* branches with die-back symptoms. Sexual morph: not observed. Asexual morph: *Pycnidia* forming on PDA, solitary or aggregated, black. *Pycnidial wall* multi-layered. *Conidiophores* hyaline. *Conidiogenous cells* phialidic, hyaline, simple, variable in size. *Conidia* brown, subglobose or circular, smooth-walled, unicellular 4.3–6.3 × 3.3–5.2 μm (av. ± SD: 5.2 ± 0.5 × 3.9 ± 0.4 μm, n = 40).

Cultural characteristics – Colonies on PDA reaching 58 mm after 7 d at 25 °C in the dark. Upper surface olivaceous grey to mouse grey, and reverse dark olivaceous grey to dark ochreous in the centre and white at the margin. Margin regular, aerial mycelium felty.

Material examined – China, Shandong Province, from the *Prunus avium* branch with die-back symptoms, May 2021, S. X. Ji & W. Zhang, (dried cultures JZBH380101–JZBH380110), living cultures JZB380101–JZB380110. Beijing, from the *Prunus avium* branch with die-back symptoms, August 2021, S. X. Ji & W. Zhang, (dried cultures JZBH380111), living culture JZB380111.

Notes – *Nothophoma quercina* has been reported as saprobe and as well as a pathogen from many plant hosts, including *Erysiphe alphitoides*, *Quercus* sp., *Ulmus* sp. and *Ziziphus jujuba*, *Chaenomeles sinensis*, *Malus micromalus*, *Phellodendron amurense*, *Pistacia vera* and *Prunus avium*. Chethana et al. (2019), first reported the novel host association of *N. quercina* with *Prunus avium* in Beijing, China. We recovered 11 isolates of *Nothophoma* from samples collected from Shandong and Beijing. Based on morpho-molecular data, we identified these isolates as *N. quercina*. Here, we report the new collection of *N. quercina* from Chinese cherry orchards.

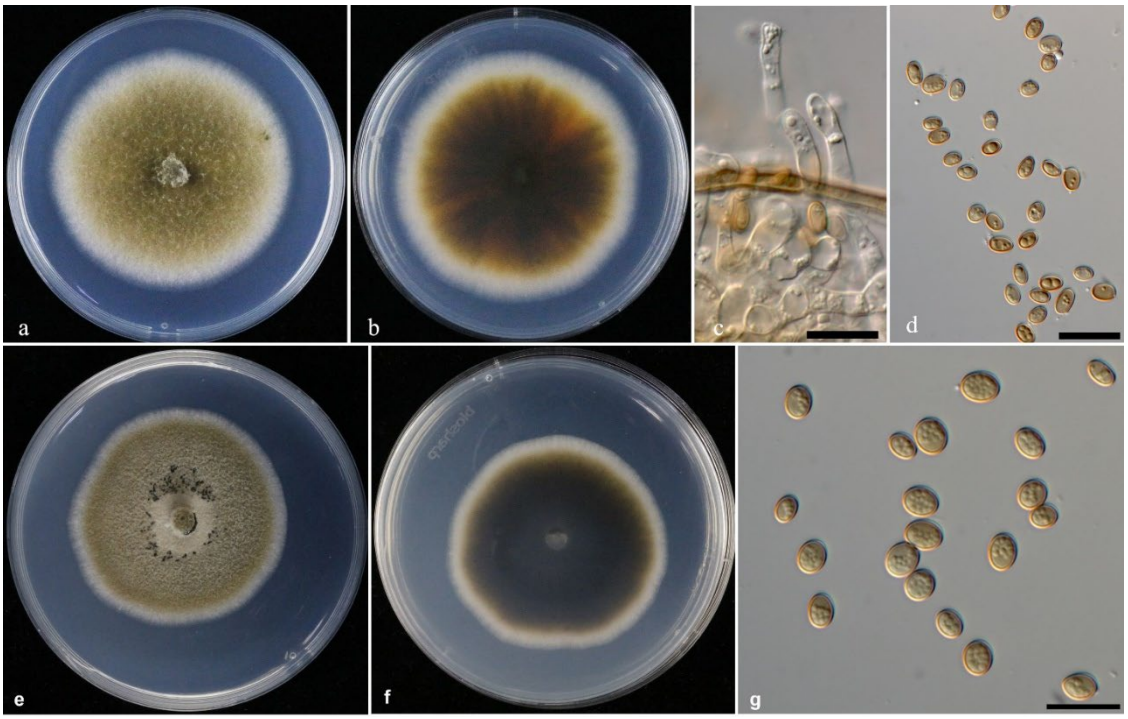

Figure 9 – a–d *Nothophoma pruni* (JZB380094). a Surface view. b Reverse view of the colony in PDA after 14 d at 25 °C in the dark. c Conidiogenous cells. d Conidia. e–g *Nothophoma quercina* (JZB380103). e Surface view. f Reverse view of the colony in PDA after 14 d at 25 °C in the dark. g Conidia. Scale bars: c, d, g = 10 μm.

Pleosporaceae Nitschke

Pleosporaceae is an important family in Dothideomycetes, and Pleosporalean species show a cosmopolitan distribution worldwide (Hongsanan et al. 2020a). Currently, 23 genera have been accepted in *Pleosporaceae* (Hongsanan et al. 2020a).

Alternaria Nees

Alternaria is a ubiquitous genus, and occupies diverse ecological niches and ranging from saprobes on a broad range of hosts and substrates (such as dead plants, paper, and food) to endophytes on a variety of asymptomatic plant tissues, as well as plant and animal (including human) pathogens globally (Thambugala et al. 2017, Jayawardena et al. 2018, 2019a, b, Hongsanan et al. 2020a, Li et al. 2023). *Alternaria* (*Pleosporaceae*, *Pleosporales*) was introduced by Nees (1816) and was typified with *Alternaria tenuis* (Li et al. 2023). Currently, *Alternaria* consists of 29 internal complexes/sections and comprises over 790 species epithets (Hongsanan et al. 2020a, Li et al. 2023). *Alternaria* species can produce a broad spectrum of secondary metabolites which have benefits for biotechnological applications. *Alternaria* species may also produce mycotoxins and phytotoxins (Jayawardena et al. 2019a, b, Li et al. 2023).

Alternaria alternata (Fr.) Keissl. (1912) Fig. 11

Index Fungorum number: IF119834

Associated with dead branches of *Prunus avium* with die-back symptoms and diseased fruits. Sexual morph: not observed. Asexual morph: *Hyphomycetous*. *Hyphae* superficial, hyaline to subhyaline, septate, branched, smooth to verruculose, *Conidiophores* erect, solitary, lateral or terminal, arising from superficial mycelium, 31–107 × 3–5 μm (av. = 61.3 × 4.2 μm, n = 30). *Conidiogenous cells* 6–28× 4–5 μm (av. = 12 × 4.3 μm, n = 20). *Conidia* pale to dark brown, 16–41 × 8–16 μm (av. 26.2 ×11.8 μm, n = 40), muriform, catenate, ovoid to chiefly obclavate or obpyriform, beakless or with short beak (2.5–12.8 × 2.6–4.8 μm, av. = 4.8×3.6 μm, n = 40).

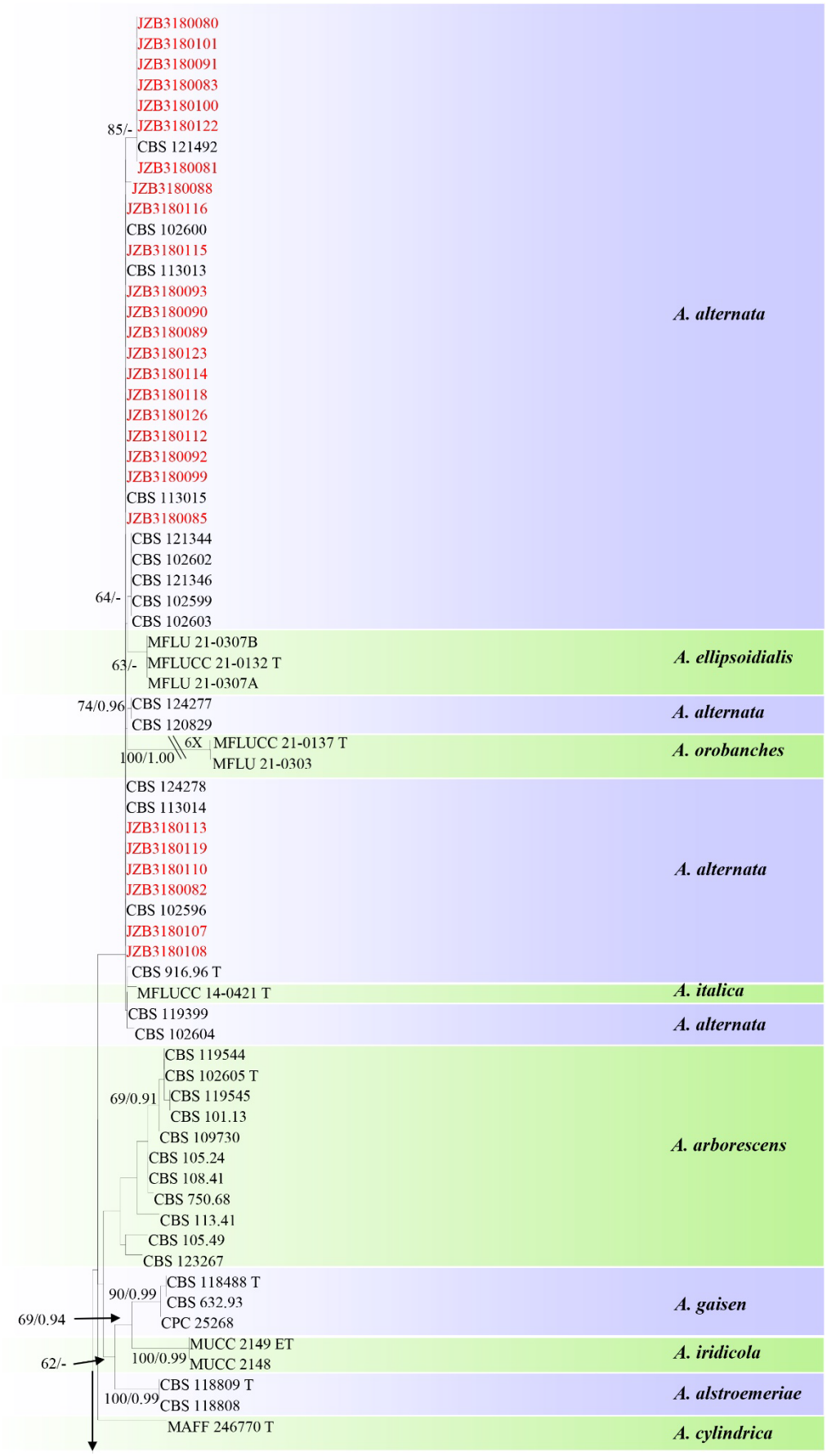

Figure 10 – Phylogenetic tree generated by maximum likelihood analysis of combined ITS, tef1-α, RPB2 and GAPDH sequence data of species belonging to *Alternaria* section *Alternaria*. The tree was rooted with *A. alternantherae* (CBS 124392). RAxML bootstrap support values ≥ 60% and (BT)

Bayesian posterior probabilities ≥ 0.90 (PP) are shown respectively near the nodes. The scale bar indicates 0.01 changes. The ex-type strains are marked in bold and the isolate numbers from the current study are in red. The maximum likelihood alignment matrix has 370 distinct alignment patterns with 8.34% of undetermined characters or gaps. Estimated base frequencies were as follows: A = 0.242637, C = 0.275609, G = 0.243538, T = 0.238216. substitution rates AC = 0.831627, AG = 2.318291, AT = 1.007507, CG = 0.651749, CT = 4.259901, GT = 1.000000; gamma distribution shape parameter α = 0.817461.

Cultural characteristics – Colonies growing on PDA reaching 59 mm in five days at 25 ℃. Upper surface dull white, and in the centre pale greenish olivaceous, reverse pale to dark olivaceous green, margin white. Circular, entire edged, flat, floccose to woolly. No prominent exudates formed.

Material examined – China, Beijing, from dead branches of *Prunus avium* with die-back symptoms, March 2021, S. X Ji & W. Zhang, (dried cultures JZBH3180080–JZBH3180083, JZBH3180088, JZBH3180089, JZBH3180110, JZBH3180112–JZBH3180116, JZBH3180119, JZBH3180122, JZBH3180123, JZBH3180126), living cultures JZB3180080–JZB3180083, JZB3180088, JZB3180089, JZB3180110, JZB3180112–JZB3180116, JZB3180119, JZB3180122, JZB3180123, JZB3180126. Beijing, from *Prunus avium* fruit, March 2021, S. X Ji & W. Zhang, (dried cultures JZBH3180085, JZBH3180107, JZBH3180108), living cultures JZB3180085, JZB3180107, JZB3180108. Liaoning Province, from dead branches of *Prunus avium* with die-back symptoms, March 2021, S. X Ji & W. Zhang, (dried cultures JZBH3180090–JZBH3180093, JZBH3180099–JZBH3180101, JZBH3180107, JZBH3180108), living cultures JZB3180090–JZB3180093, JZB3180099–JZB3180101, JZB3180107, JZB3180108. Shandong Province, from *Prunus avium* fruit, March 2021, S. X Ji & W. Zhang, (dried culture JZBH3180118), living culture JZB3180118.

Notes – *Alternaria alternata* is a common pathogen and a saprobe of many plant hosts. This species has been reported to cause leaf spot disease in Cherry in China and Greece (Chethana et al. 2019). In total, 41 isolates that were morphologically similar to *Alternaria* were recovered from the samples collected from four locations in China. Their DNA sequences (data not shown) are similar to each other and therefore we select 27 isolates for further analysis. Based on morphological and multi-locus sequence analysis, we identified these isolates as *Alternaria alternata* (Fig. 10). Here, we report *Alternaria alternata* associated with diseased samples of *Prunus avium* as a new collection from China.

Leotiomycetes O.E. Erikss. & Winka

Leotiomycetes were established by Eriksson & Winka (1997) to accommodate the inoperculate discomycetes. Species in this class are ecologically diverse and reported as endophytes, saprobes, pathogens, parasites, mycorrhizal fungi, root symbionts and wood-rotting fungi (Ekanayaka et al. 2019). We follow the latest treatments and updated accounts of *Leotiomycetes* in Ekanayaka et al. (2019).

Helotiales Nannf. ex Korf & Lizoň (= Cyttariales Luttr. ex Gamundí)

Helotiales was established by Nannfeldt (1932), to accommodate fungi with cupulate apothecia covered by long cylindrical hairs. Many authors have stated the polyphyletic nature within *Leotiomycetes*, and according to Ekanayaka et al. (2019), this order includes 25 families/family-level clades. Currently, 36 families have been classified into this order (Wijayawardene et al. 2022a).

Sclerotiniaceae Whetzel ex Whetzel

This family was previously classified into *Helotiales*; however, Ekanayaka et al. (2019) have accommodated this family into "*Sclerotiniales*". Species in this family are mostly saprobic or pathogenic. Many devastating plant pathogens including *Botrytis cinerea* have been classified in this family (Dean et al. 2012, Ekanayaka et al. 2019).

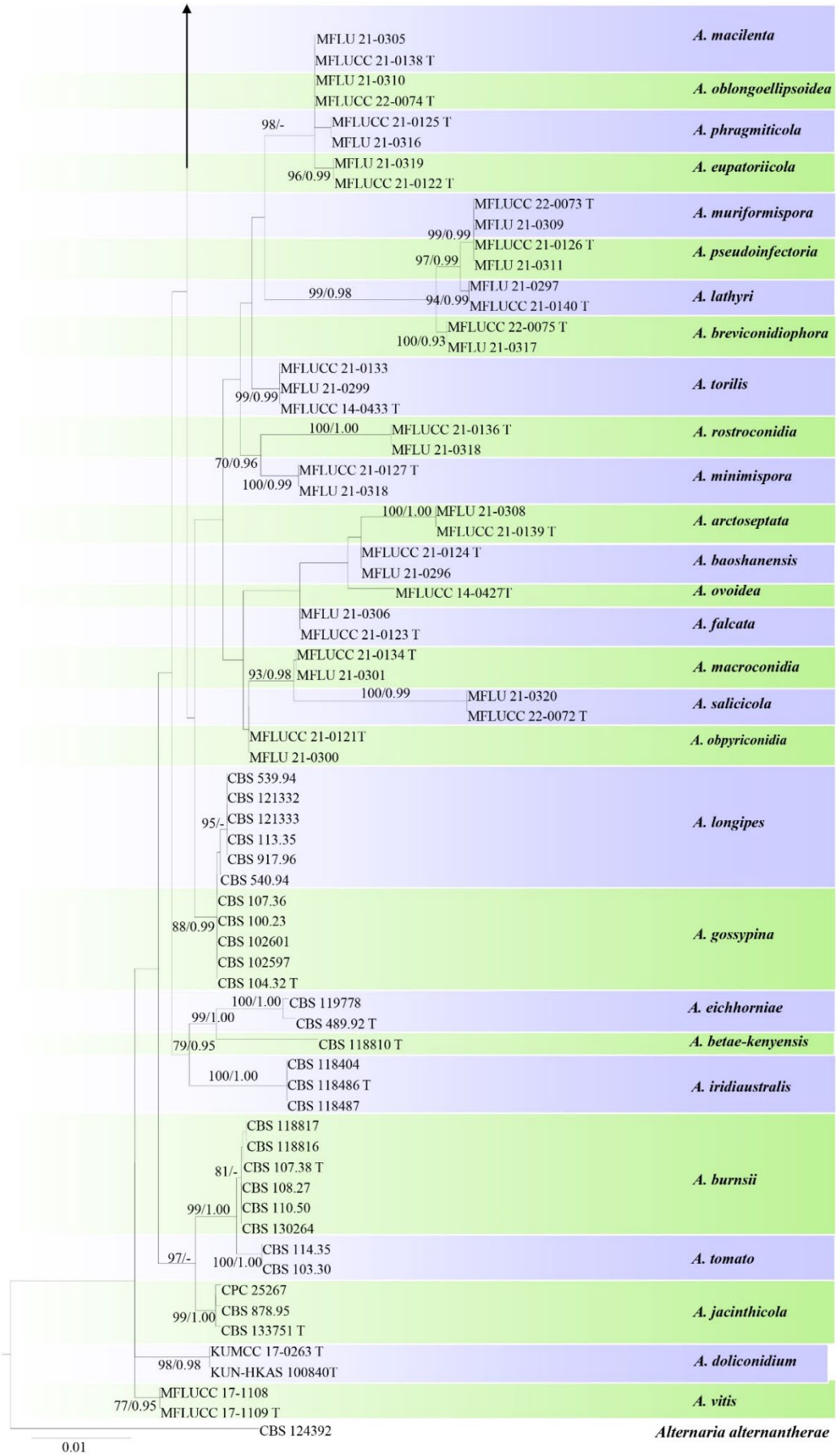

Figure 10 – Continued.

Figure 11 – *Alternaria alternata* (JZB3180112). a Upper view. b Reverse view of the colony in PDA after 5 d at 25 °C in the dark. c, d Conidiophores and conidiogenous cell. e Conidial chains. f–i Conidia. Scale bars: c–g = 20 µm, e = 20 µm, h, i = 10 µm.

Monilinia Honey

Monilinia is classified in *Sclerotiniaceae* and includes aggressive and economically significant plant pathogenic species that are found all over the world (Hrustić et al. 2012, Martini 2012, Marin-Felix et al. 2017, Vilanova et al. 2021). These species have been identified as one of the major global fruit production constraints. Three species of *Monilinia* (*M. fructicola*, *M. fructigena*, and *M. laxa*) are responsible for devastating brown rot and blossom blight on fruit trees, especially on stone fruits including almonds, apricots, cherries, nectarines and peaches (Marin-Felix et al. 2017, Abate et al. 2018, Iqbal et al. 2022). They can damage fruits both before and after harvest. Furthermore, in Central Europe and Asia, a few minor species (*M. mumecola*, *M. polystroma*, and *M. yunnanensis*) have also been documented to induce brown rot in stone fruits. Most *Monilinia* species have been classified as quarantine pathogens in several countries based on the European and Mediterranean Plant Protection Organization's (EPPO) classification system (Hrustić et al. 2012, Martini 2012, Marin-Felix et al. 2017, Abate et al. 2018, Iqbal et al. 2022, Baltazar et al. 2023, EPPO 2023).

Monilinia fructicola (G. Winter) Honey (1928) Fig. 13

Index Fungorum number: IF236989

Associated with dead twigs of *Prunus avium*. Sexual morph: not observed. Asexual morph: *Conidiophores* single or aggregated and forming sporodochia on the culture, hyaline to subhyaline, branched, thin walled, septate. *Conidia* oval, or lemon shaped, aseptate, hyaline to subhyaline, smooth- and thin-walled, formed in chains, 10.6–17.2 × 8–11.9 µm (av. ± SD, 13 ± 1.4 × 9.5 ± 0.9 µm, n = 50).

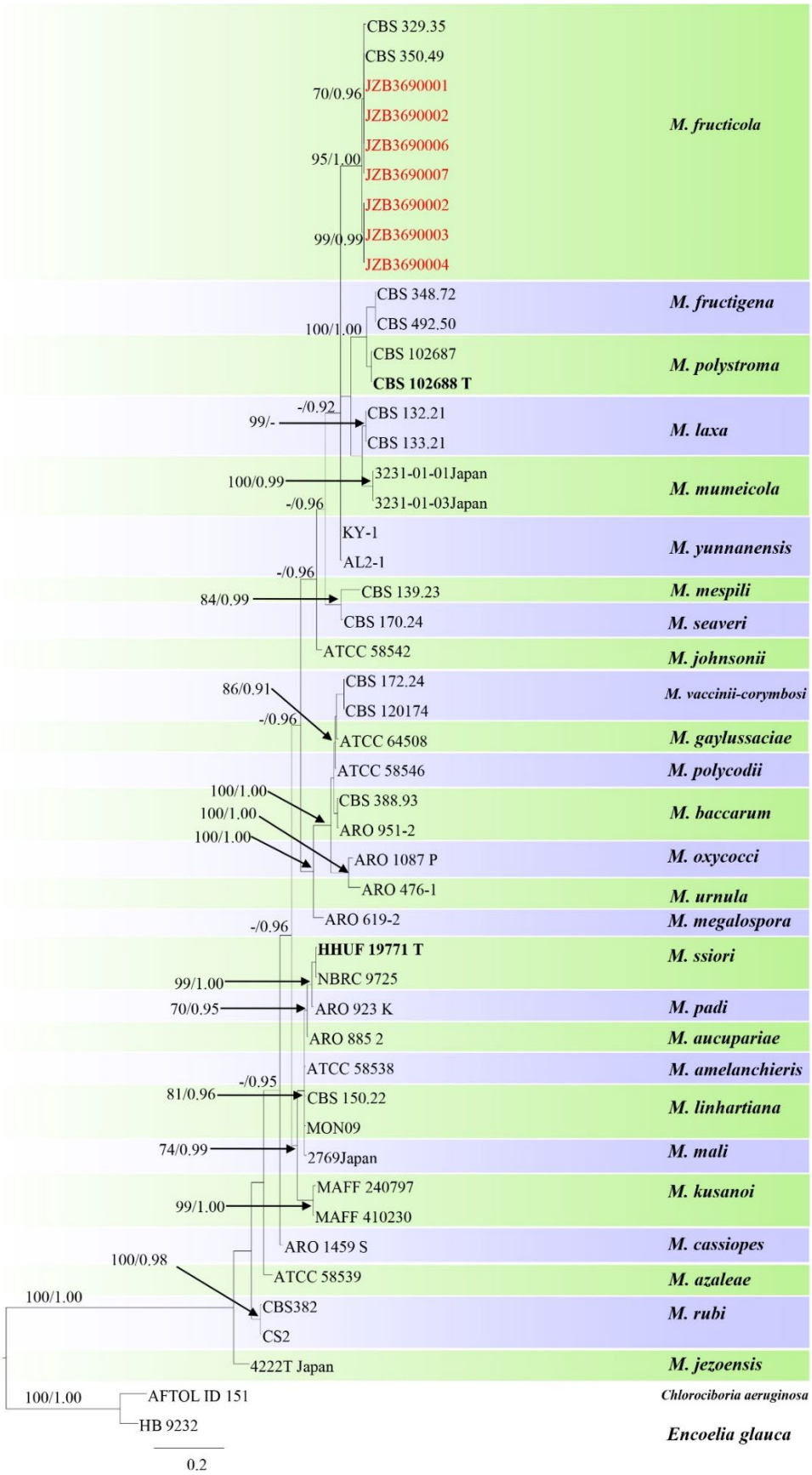

Figure 12 – Phylogenetic tree generated by maximum likelihood analysis of combined ITS and tef1-α sequence data of species belonging to *Monilinia*. The tree was rooted with *Encoelia glauca* (HB 9232) and *Chlorociboria aeruginosa* (AFTOL-ID 151). RAxML bootstrap support values ≥ 60% and (BT) Bayesian posterior probabilities ≥ 0.90 (PP) are shown respectively near the nodes. The scale

bar indicates 0.2 changes. The ex-type strains are marked in bold and the isolate numbers from the current study are in red. The maximum likelihood alignment matrix has 524 distinct alignment patterns with 40.13% of undetermined characters or gaps. Estimated base frequencies were as follows: A = 0.234656, C = 0.254136, G = 0.229684, T = 0.281525. substitution rates AC = 1.763587, AG = 4.099954, AT = 1.365434, CG = 1.098898, CT = 6.673663, GT = 1.000000; gamma distribution shape parameter α = 1.057761.

Cultural characteristics – Colonies on PDA reaching 73 mm after seven days at 25 ℃. Upper surface white to pale grey in the centre, and reverse off-white to olive-grey in the centre. Margin entire or lobed giving a rosette-like appearance.

Material examined – China, Shandong Province, from the dead twigs of *Prunus avium*, April 2022, P. Z. Chen, (dried cultures JZBH3690001–JZBH3690007), living cultures JZB3690001–JZB3690007.

Notes – We have identified seven isolates of *Monilinia* from dead branches of *Prunus avium*. Based on combined sequenced data analysis of ITS and tef1-α, all these isolates were clustered with reference strains of *M. fructicola* (CBS 329.35 and CBS 350.49) (Fig. 12). *Monilinia* is known as a brown rot-causing fungus for many plant hosts. So far, this species; *M. fructicola* has not been reported from sweet cherries in China. Therefore, here we report a new geographical record of *M. fructicola* associated with *Prunus avium* in China.

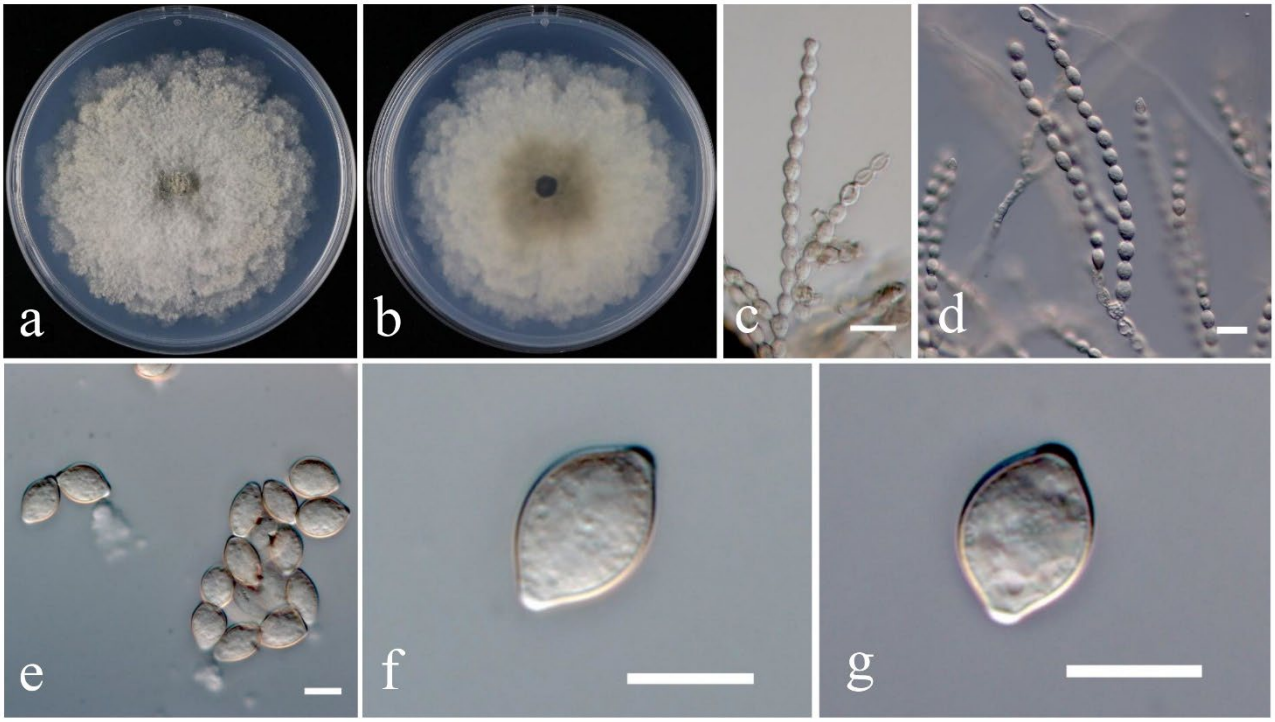

Figure 13 – *Monilinia fruticola* (JZBH3690001). a Upper view. b Reverse view of colony in PDA after 7 d at 25 °C in dark. c–d Conidial chains. e–g Conidia. Scale bars: c–d = 20 μm, e–g = 10 μm.

Sordariomycetes O.E. Erikss. & Winka
Diaporthomycetidae Senan., Maharachch. & K.D. Hyde

We follow the latest treatments and updated accounts of *Sordariomycetes* in Hyde et al. (2020b) and Wijayawardene et al. (2020, 2022a).

Diaporthales Nannf

Diaporthales was introduced by Nannfeldt (1932), to accommodate the eu-diaportheen and valseen taxa (Senanayake et al. 2018). Currently, 30 families have been accepted to this order (Hyde et al. 2020b).

Cytosporaceae Fr.

Cytosporaceae was established by Fries (1821) and currently six genera are listed (*Cryptascoma*, *Cytospora*, *Pachytrype*, *Paravalsa*, *Waydora*, and *Xenotypa*) (Hyde et al. 2020b).

Cytospora Ehrenb.

Cytospora was established to *Cytosporaceae* (*Diaporthales*) by Ehrenberg (1818) describing four species. This genus was typified by *C. chrysosperma* (Norphanphoun et al 2017, Hyde et al. 2018, Pan et al. 2021, Manawasinghe et al 2022). *Cytospora* is one of the most important genera that have a worldwide distribution and a wide host range (Norphanphoun et al 2017, Hyde et al. 2018, Pan et al. 2021, Manawasinghe et al 2022). Species in *Cytospora* are mainly pathogens, which cause cankers, and diebacks on branches and trunks in woody hosts (Norphanphoun et al 2017, Pan et al. 2021, Manawasinghe et al 2022). Initially, the identification of *Cytospora* species was mainly based on host associations, however, while single *Cytospora* species may occur on several unrelated hosts or within a single plant species identification may be more difficult (Norphanphoun et al 2017). Currently, 773 name records are listed in Index Fungorum (2025). Recent studies on *Cytospora* include Jayawardena et al. (2019b), Hyde et al. (2020a, b), Li et al. (2020), Senanayake et al. (2023) and Wijayawardene et al. (2022a). In the present study, five *Cytospora* isolates were obtained and based on morphology and molecular phylogeny; they were identified as *Cytospora leucostoma*.

Cytospora leucostoma (Pers.) Sacc., Michelia 2(no. 7): 264 (1881) Fig. 15

Index Fungorum number: IF213669

Associated with *Prunus avium* branch with die-back symptoms. Sexual morph: not observed. Asexual morph: *Coelomycetous*. *Conidiomata* formed on PDA after twenty days, pycnidial, globose to subglobose, without conceptacle, mouse-grey in centre with grey to off-white surface hyphae, 136–199(–306) × 118–192(–252) µm (n = 10). *Conidiophores* hyaline, smooth-walled, reduced to filamentous conidiogenous cells, that are wider at the base and taper towards apex. *Conidiogenous cells* enteroblastic, phialidic, sub-cylindrical, hyaline, 9.2–15.8(–17.9) × 1.6–3.2 µm (av. = 12.4 ×2 µm, n = 20). *Conidia* hyaline, allantoid, eguttulate, smooth, aseptate, thin-walled, 4.6–6.7 × 1.2–1.7 µm (av. = 5.9 ×1.4 µm, n = 40).

Cultural characteristics – Colonies on PDA reaching 59–66 mm diam. after 2 d at 25 °C (fast growth rate: 29 mm d^{-1}). Upper surface off-white to white, reverse off white to light yellow with age. Aerial mycelia is fluffy and moderately rich.

Material examined – China, Beijing, from the *Prunus avium* branch with die-back symptoms, August 2021, P. Chen (dried cultures JZBH3670001–JZBH3670005), living cultures JZB3670001–JZB3670005).

Notes – We have obtained five *Cytospora* isolates from the *Prunus avium* branch samples that showed die-back symptoms. Based on multi-gene phylogenetic analysis of concatenated ITS, LSU, actin, RPB2, and ß-tubulin sequence datasets, these *Cytospora* isolates are clustered with reference strains of *C. leucostoma* (CFCC 53141 and CFCC 53156) with high statistical support (96 BT/0.94 PP). According to Fan et al. (2020), *Cytospora leucostoma* is a common species that causes cankers on *Rosaceae* in China. Here, we report the new collection of *C. leucostoma* on *Prunus avium* in China.

Hypocreomycetidae O.E. Erikss. & Winka

Glomerellales Chadef. ex Réblová, W. Gams & Seifert

Currently, five families (*Australiascaceae*, *Glomerellaceae*, *Malaysiascaceae*, *Plectosphaerellaceae*, and *Reticulascaceae*) are accepted in *Glomerellales* (Wijayawardene et al. 2022a).

Glomerellaceae Locq. ex Seifert & W. Gams, Mycologia 98: 1083 (2007)

Glomerellaceae is monotypic with the single genus *Colletotrichum* (Hyde et al. 2020b). Species in *Glomerellaceae* are reported as parasitic, endophytic and saprobic on a wide range of plants (Hyde et al. 2020b).

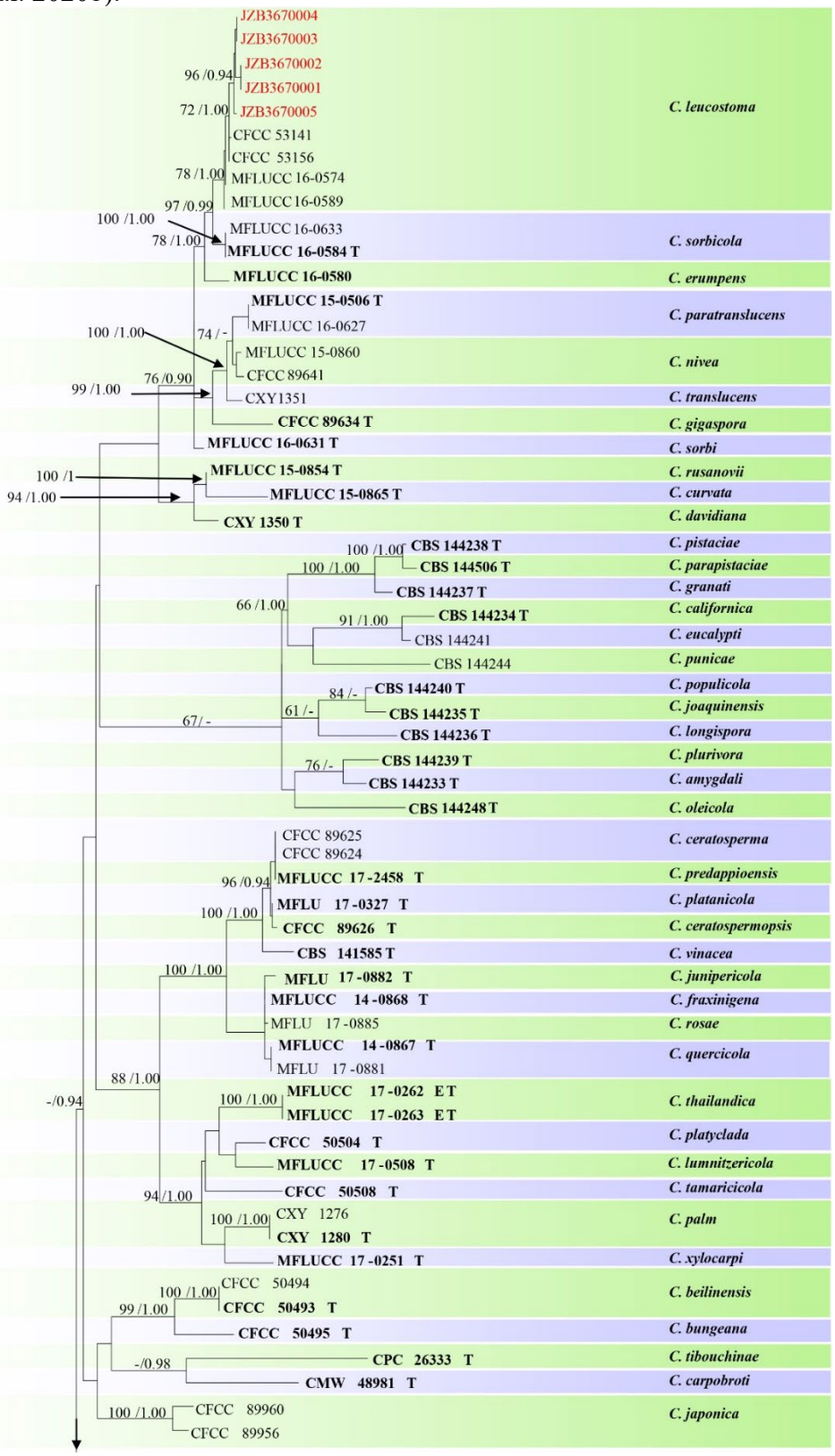

Figure 14 – Phylogenetic tree generated by maximum likelihood analysis of combined ITS, LSU, actin, tef1-α and ß-tubulin sequence data of species belonging to *Cytospora*. RAxML bootstrap

support values (BT) ≥ 60% or Bayesian posterior probabilities (PP) ≥ 0.90 are indicated respectively near the nodes. The scale bar indicates 0.05 changes. The type strains are marked with “T” or “ET” in the end and isolates from the current study are in blue. A total of 120 strains are included in the sequence analyses, which comprise 2285 characters with gaps. *Diaporthe vaccinii* (CBS 160.32) is used as the outgroup taxon. The best-scoring RAxML tree with a final likelihood value of -28498.873420 is presented. The matrix had 1248 distinct alignment patterns, with 35.19% of undetermined characters or gaps. Estimated base frequencies were as follows; A = 0.237214, C = 0.281302, G = 0.250586, T = 0.230898; substitution rates AC = 1.657599, AG = 3.656491, AT = 1.943791, CG = 1.219714, CT = 6.708080, GT = 1.000000; gamma distribution shape parameter α = 0.861693.

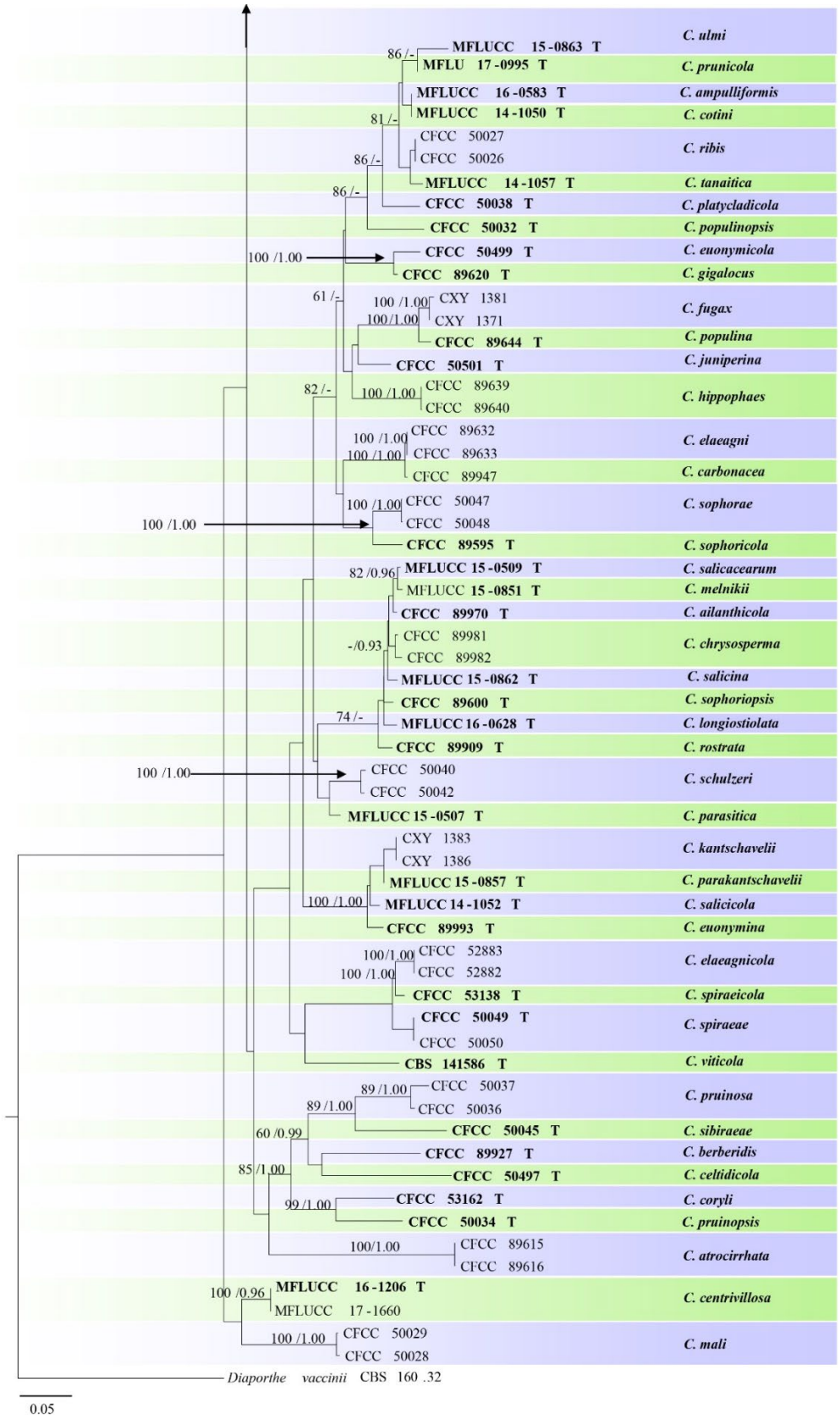

Figure 14 – Continued.

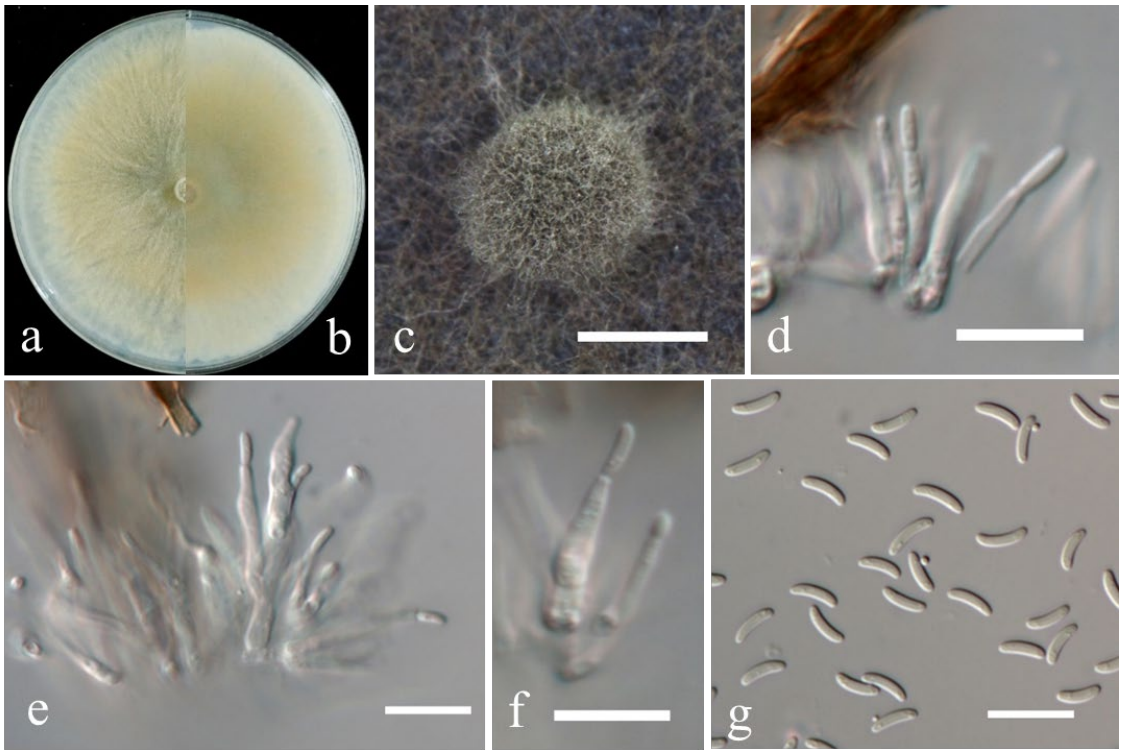

Figure 15 – *Cytospora leucostoma* (JZB3670005). a Upper view. b Reverse view of the colony in PDA after 7 d at 25 °C in the dark. c Pycnidia on PDA. d–f Conidia attached to the conidiophores. g Conidia. Scale bars: c = 100 μm, d–g = 10 μm.

Colletotrichum Corda, Deutschl. Fl., 3 Abt. (PilzeDeutschl.) 3(12): 41 (1831)

Colletotrichum was introduced by Corda (1831) with the type species *C. lineola* (Bhunjun et al. 2021b, Jayawardena et al. 2020, 2022). With time, based on minor morphological differences and different host associations many species have been introduced to the genus. However, lack of sexual morphs in this genus and overlapping morphological characteristics in asexual morphs, morphology-based species identification of *Colletotrichum* species has been difficult (Bhunjun et al. 2021b, Jayawardena et al. 2020, 2022). Therefore, since its introduction *Colletotrichum* was extensively revised by many researchers. Sutton (1980) revised the genus and accepted 20 species into the genus and later based on the evidence of morphological and cultural characteristics they increased it to 39 species (Sutton 1992). Hyde et al. (2009a, b) stated the necessary of incorporating molecular methods in the revision of *Colletotrichum* and later many studies have utilized the polyphasic approach to identify the *Colletotrichum* species (Cannon et al. 2012, Damm et al. 2012a, b, Jayawardena et al. 2016, 2020, 2022).

Colletotrichum species exhibited a broad range of lifestyles including endophytic, hemibiotrophic, latent or quiescent and necrotrophic. However, many species are reported as frequent plant pathogens on various economically important crops such as chilli, fruits, medicinal plants and ornamentals (Than et al. 2008, Huang et al. 2013, Chethana et al. 2019, Bhunjun et al. 2021b, Armand et al. 2023, Peng et al. 2023, Talhinhas & Baroncelli 2021, 2023, Zhang et al. 2023b, Zhang et al. 2023c). Previously, it was assumed that *Colletotrichum* species are host-specific and this resulted in the invalid introduction of a large number of taxa. However, this has not been well explored and further studies are needed to confirm it (Jayawardena et al. 2020). Talhinhas & Baroncelli (2023) provided an updated list for the hosts of *Colletotrichum* and they have mentioned that most *Colletotrichum* species occur on dicotyledonous plants (77%). Further, species in bambusicola, spaethianum, tibetense and graminicola/caudatum species complexes, are more commonly found in monocotyledonous plants (Talhinhas & Baroncelli 2023). Recently, Zhang et al. (2023b) researched the mechanisms behind the host range and preference of *Colletotrichum* species from ten species complexes and three singleton species. They observed that species from *C. acutatum*, *C. boninense*,

and *C. gloeosporioides* species complexes showed expanded gene families encoding CAZymes. This may be the most likely explanation of the authors of Zhang et al. (2023b) for the widespread and polyphagous nature of species in the above species complexes. They also stated the host preference of species in the *C. graminicola* species complex may be because of the fewer pectinase-encoding gene families in their genome (Zhang et al. 2023b).

Currently, *Colletotrichum* comprises 16 species complexes and 15 singleton species (Bhunjun et al. 2021b, Liu et al. 2023). In the present study, 22 *Colletotrichum* isolates were obtained from diseased cherry shoots, branches, fruits and leaf samples. These isolates were further identified into two species belonging to the *Colletotrichum acutatum* species complex.

Colletotrichum fioriniae (Marcelino & Gouli) Pennycook, Mycotaxon 132(1): 150 (2017) Fig. 17

Index Fungorum number: IF553097

Pathogenic on *Prunus avium*. Sexual morph: not observed. Asexual morph: *Conidiophores* hyaline to pale brown, smooth-walled, simple or septate and branched. *Conidiogenous* cells are hyaline to pale brown, cylindrical or ampulliform, 7.7–18.7 × 3.0–4.0 µm (n = 30). *Conidia* hyaline, smooth-walled, aseptate, cylindrical, both ends rounded, contents granular, 13.8–18.6 × 4.5–6.7 µm (mean ± SD = 16 ± 1.2 × 5.7 ± 0.6 µm, n = 40), L/W ratio = 2.8. *Appressoria* dark-brown, smooth-walled, mostly clavate, the edge entire to undulate, 7.1–19.3 × 4.0–7.8 µm (mean ± SD = 11.7 ± 2.9 × 5.3 ± 0.8, n = 30), L/W = 2.2.

Cultural characteristics – Colonies on PDA flat with entire margin, aerial mycelium sparse, cottony, surface grey; reverse dark red to pale orange with a white margin; colony diam. reaching 69–71 mm in 7 days.

Material examined – China, Guizhou Province, from the *Prunus avium* branch with die-back symptoms, April 2020, S. X. Ji (dried cultures JZBH330344 – JZBH330349), living cultures JZB330344 – JZB330349. Guizhou Province, from the *Prunus avium* leaves, April 2020, S. X. Ji (dried cultures JZBH330342, JZBH330343), living cultures JZB330342, JZB330343. Guizhou Province, from the *Prunus avium* fruit, April 2020, S. X. Ji (dried culture JZBH330350), living culture JZB330350.

Notes – Phylogenetic analysis of a combined ITS, GAPDH and ß-tubulin sequence dataset, placed nine *Colletotrichum* isolates in a clade with the *C. fioriniae* ex-holotype strain (CBS 128517) with 100% ML bootstrap and 1.0 Bayesian posterior probabilities (Fig. 16). All isolates of *Colletotrichum fioriniae* obtained from this study, shares similar colony morphology and spore characters with the description of type species of *C. fioriniae* (Damm et al. 2012b). *Colletotrichum fioriniae* caused leaf spots and fruit rots on several deciduous fruit trees including apple (*Malus domestica*), peach (*Prunus persica*), pear (*Pyrus pyrifolia*), kiwifruit (*Actinidia chinensis*) and also anthracnose on vegetables such as aubergine (*Solanum melongena*) and tomato (*Solanum lycopersicum*) (https://fungi.ars.usda.gov/). From this study, we report the first novel host association of *Colletotrichum fioriniae* on *Prunus avium* in China. Based on the pathogenicity test result, this species develops the symptoms on detached sweet cherry shoots.

Colletotrichum godetiae Neerg., Friesia 4(1-2): 72 (1950) Fig. 18

Index Fungorum number: IF440867

Pathogenic on *Prunus avium*. Sexual morph: not observed. Asexual morph: *Conidiophores* hyaline to pale brown, smooth-walled, simple or septate and branched. *Conidiogenous* cells are hyaline to pale brown, cylindrical, or ampulliform, 7.4–19.7 × 2.7–4.8 µm (n = 30). *Conidia* hyaline, smooth-walled, aseptate, cylindrical, both ends rounded, contents granular, 7.9–14.2 × 3.5–5.5 µm (mean ± SD = 11.4 ± 1.4 × 4.3 ± 0.4 µm, n = 40), L/W = 2.7. *Appressoria* 6.1–12.8 × 4.0–8.3 µm (mean ± SD = 9.9 ± 1.5 × 6.0 ± 1.1 µm, n = 30), L/W = 1.7.

Cultural characteristics – Colonies on PDA flat with entire margin, aerial mycelium abundant, cottony, surface grey with a white margin; reverse dark pale brown with a white margin; colony reaching 68–70 mm in 7 days.

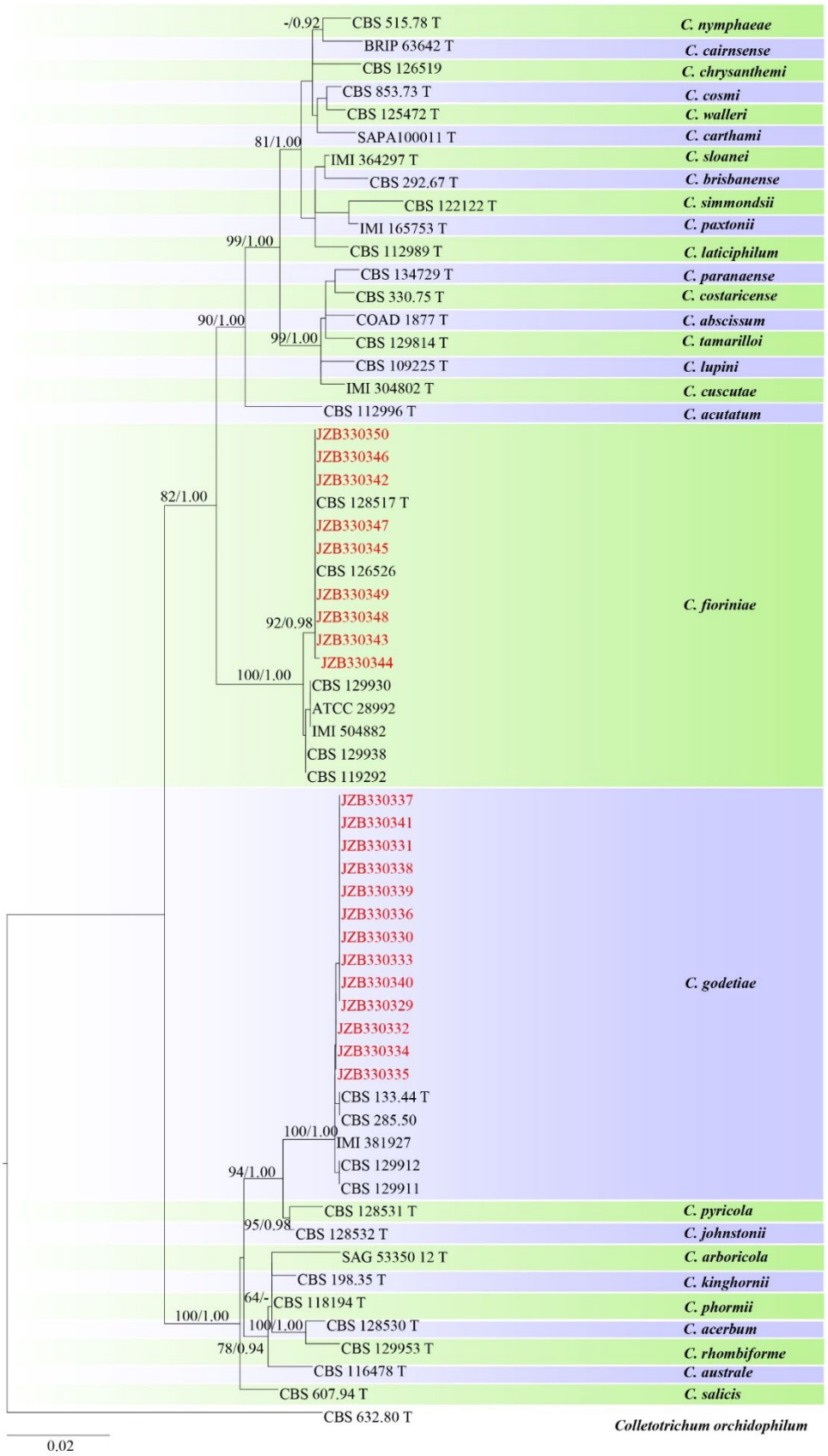

Figure 16 – Phylogenetic tree generated by maximum likelihood analysis of combined ITS, GAPDH and ß-tubulin sequence data of species belonging to *Colletotrichum acutatum* species complex. The tree was rooted with *Colletotrichum orchidophilum* (CBS 632.80, type strain). RAxML bootstrap support values (BT) ≥ 60% and Bayesian posterior probabilities (PP) ≥ 0.90 are shown respectively near the nodes. The scale bar indicates 0.02 changes. The ex-type strains are marked in bold and

isolates from the current study are in red. The maximum Likelihood alignment matrix had 247 distinct alignment patterns, with 3.99% of undetermined characters or gaps. Estimated base frequencies were as follows; A = 0.234535, C = 0.301209, G = 0.236492, T = 0.227764; substitution rates AC = 1.701911, AG = 5.315912, AT = 1.122256, CG = 0.609530, CT = 6.845513, GT = 1.000000; gamma distribution shape parameter α = 0.931680.

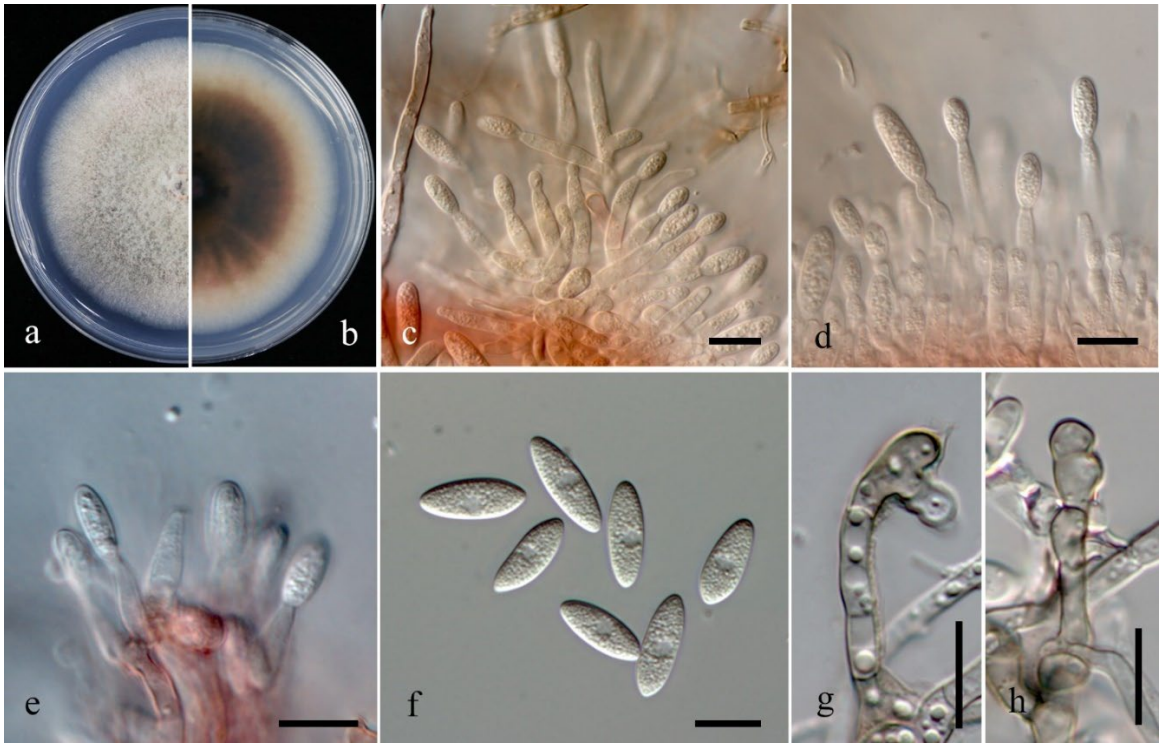

Figure 17 – *Colletotrichum fioriniae* (JZB330345). a, b Surface and reverse view of colony on PDA. c–e Immature and mature conidia are attached to the conidiophores. f Conidia. g, h Appressoria. Scale bars: c–h = 10 µm.

Material examined – China, Guizhou Province, from the *Prunus avium* branch with die-back symptoms, April 2020, S. X. Ji (dried cultures JZBH330337–JZBH330341), living cultures JZB330337–JZB330341. Guizhou Province, from the *Prunus avium* leaves, April 2020, S. X. Ji (dried cultures JZBH330329–JZBH330336), living cultures JZB330329–JZB330336.

Notes – Based on the combined ITS, GAPDH and ß-tubulin sequence analysis, 13 *Colletotrichum* isolates clustered with the *Colletotrichum godetiae* (ex-holotype strain CBS 133.44) with 100% ML and 1.0 BYPP) (Fig. 16). This species was first isolated from Clarkia seeds. However, *Colletotrichum godetiae* has since been reported from several plant hosts and it is known for causing anthracnose and leaf spots, fruit rot, die back and stem end rot (Peng et al. 2022). Based on the pathogenicity test result, we identified *Colletotrichum godetiae* causing branch die-back disease in *Prunus avium*. Peng et al. (2022) also reported *C. godetiae* causes anthracnose disease in Chinese sweet cherries (*Cerasus pseudocerasus*) and they have confirmed it by fulfilling Koch's postulates. Further, we report the new collection of *C. godetiae* on *Prunus avium.*

Hypocreales Lindau

We follow the latest treatments and updated accounts of *Sordariomycetes* as in Hyde et al. (2020b) and Wijayawardene et al. (2020, 2022a).

Bionectriaceae Samuels & Rossman

We follow the latest treatments and updated accounts of *Bionectriaceae* as in Perera et al. (2023). This family was established by Rossman et al. (1999) to *Hypocreales* and placed 26 genera

into the family at that time. However, with the extensive taxonomic and phylogenetic treatments, currently, *Bionectriaceae* consists of 41 genera (Perera et al. 2023).

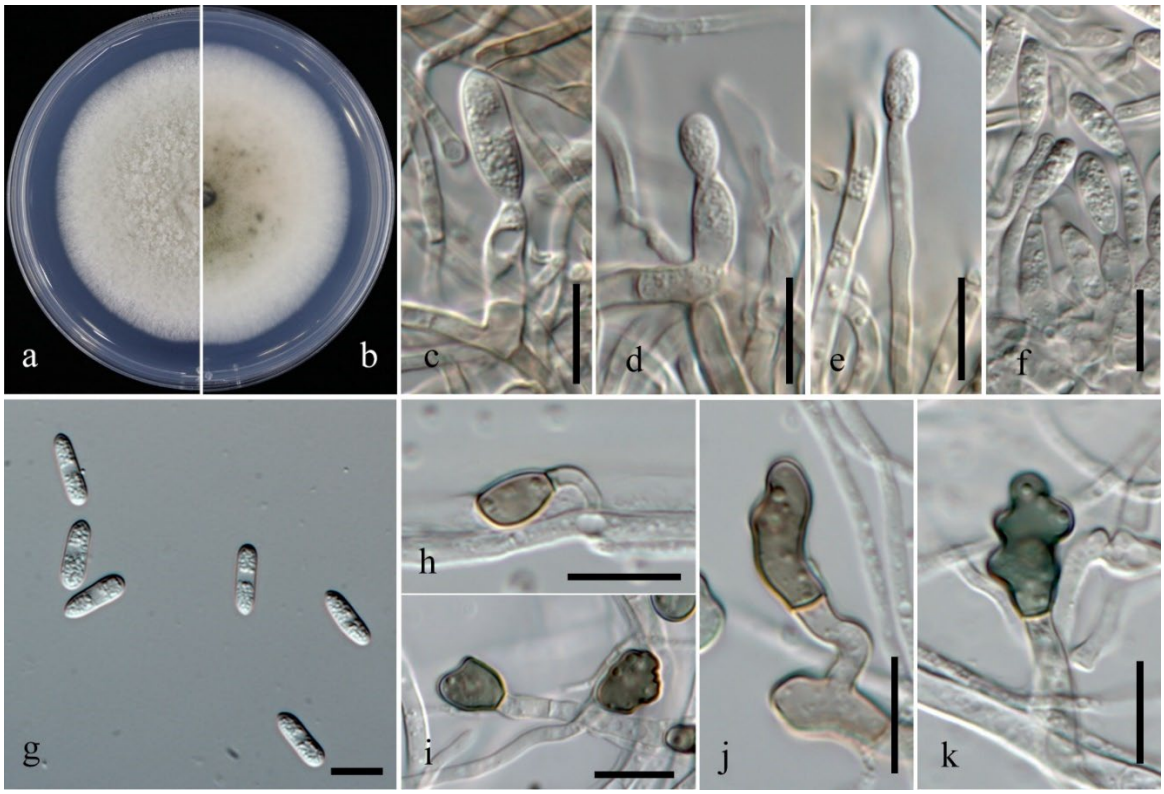

Figure 18 – *Colletotrichum godetiae* (JZB330337). a Upper view. b Reverse view of colony in PDA after 7 d at 25 °C in the dark. c–f Conidiogenous cells. g Conidia. h–k Appressoria. Scale bars: c–k = 10 μm.

Clonostachys Corda

Clonostachys is the type genus of *Bionectriaceae* and this genus was established by Corda (1839) (Abeywickrama et al. 2023, Dong et al. 2023, Perera et al. 2023). Many *Bionectria* species have been synonymized with *Clonostachys* and this genus was typified with the species *C. rosae* (Abeywickrama et al. 2023, Dong et al. 2023, Perera et al. 2023). Currently, there are 123 names listed in Species Fungorum (2025) under *Clonostachys*. *Clonostachys* species showed strong biological control abilities against various plant pathogenic fungi (Abeywickrama et al. 2023, Dong et al. 2023, Perera et al. 2023).

Clonostachys farinosa (Henn.) Rossman (2014) Fig. 20

Index Fungorum number: IF808883

Associated with diseased leaves of *Prunus avium*. Sexual morph: not observed. Asexual morph: *Conidiophores* monomorphic, verticillate, arising from the agar surface or the sparse aerial mycelium. *Stipe* 18.1–37.2 μm long, 2.2–3.8 μm wide (n = 7). Primary branches form independent side-branches, terminal branches and phialides divergent or adpressed, terminal phialides flask-shaped, or cylindrical but narrowing in the upper part. *Conidia* unicellular, oblong to ovoid, hyaline, smooth walled, 4.1–8.3×2.3–3.8 μm (av. ± SD: 6 ± 1×3 ± 0.4 μm, n = 40).

Cultural characteristics – Colonies on PDA reaching 42.5 mm after 7 days at 25 °C in the dark. Colony surface white, cottony mycelium and not pigmented. Reverse white to pale yellow.

Material examined – China, Liaoning Province, from diseased leaves of *Prunus avium*, April 2021, S. X. Ji & W. Zhang (dried cultures JZBH3530055, JZBH3530056), living cultures JZB3530055, JZB3530056.

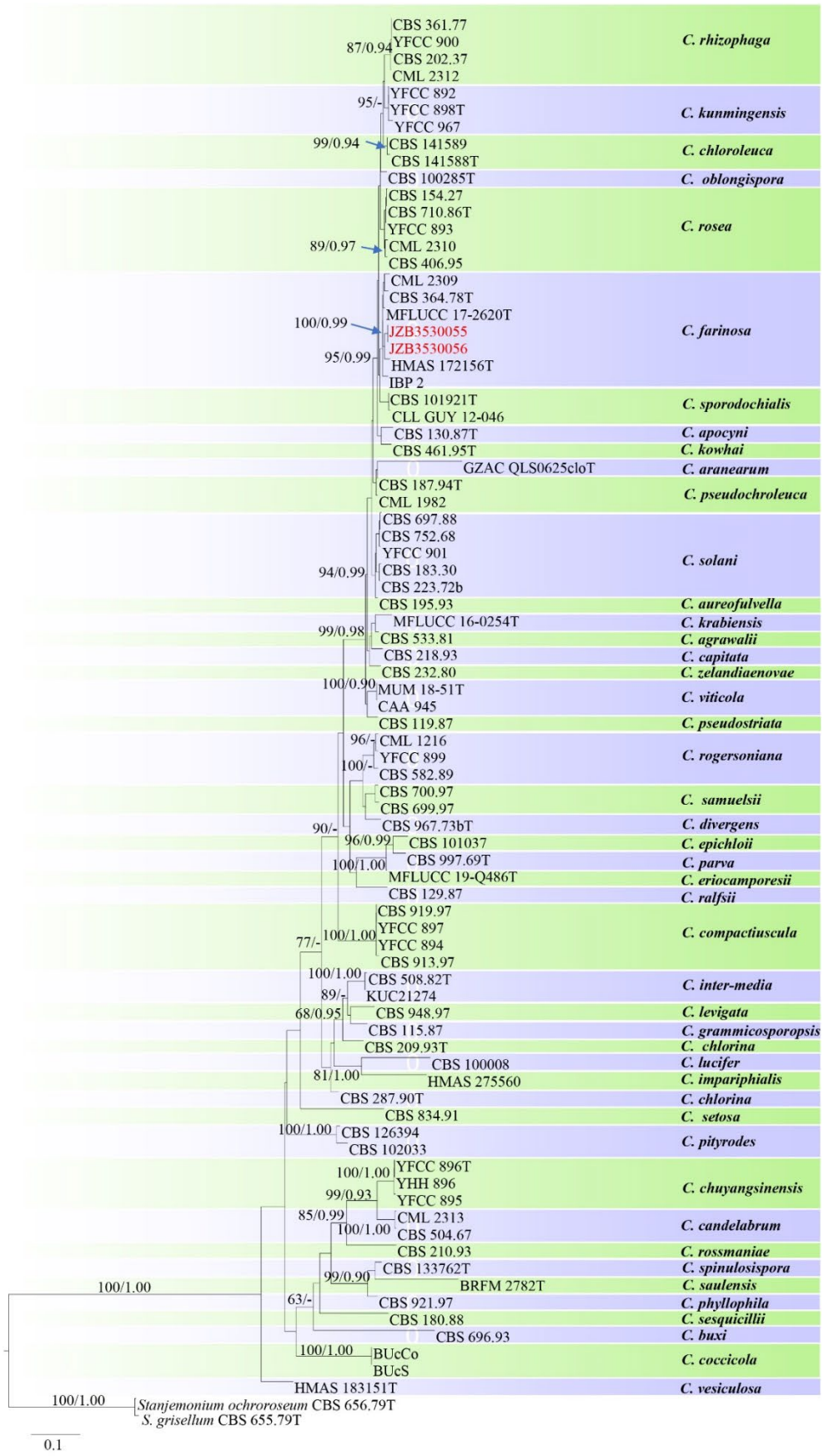

Figure 19 – Phylogenetic tree generated by maximum likelihood analysis of ITS sequence data of species belonging to *Clonostachys*. The tree was rooted with *Stanjemonium ochroroseum* (CBS 656.79, type strain) and *S. grisellum* (CBS 655.79, type strain). RAxML bootstrap support values (BT) ≥ 65% and Bayesian posterior probabilities (PP) ≥ 0.90 are shown respectively near the nodes.

The scale bar indicates 0.1 changes. The ex-type strains are marked in 'T' and isolates from the current study are in red. The maximum Likelihood alignment matrix had 304 distinct alignment patterns, with 13.71% of undetermined characters or gaps. Estimated base frequencies were as follows; A = 0. 234638, C = 0. 273519, G = 0. 253710, T = 0. 238133; substitution rates AC = 2.005889, AG = 3.211499, AT = 2.013671, CG = 0.795574, CT = 5.589118, GT = 1.000000; gamma distribution shape parameter α = 0.546549.

Notes – We recovered two isolates that morphologically resemble *Clonostachys* and phylogenetically were in a clade with reference strains of *C. farinosa* with high statistical support (Fig. 19). Recently, based on multi-loci sequence data several *Clonostachys* species (*C. byssicola*, *C. eriocamporesiana*, *C. indica*, *C. wenpingii*, *C. granuligera*, *C. squamuligera*, *C. spinulosa*) have been synonymized under *Clonostachys farinosa* (Zhao et al. 2023). So far, *C. farinosa* has not been reported from *Prunus avium* worldwide. Therefore, here we report the novel host association of *Clonostachys farinosa* on *Prunus avium* from China.

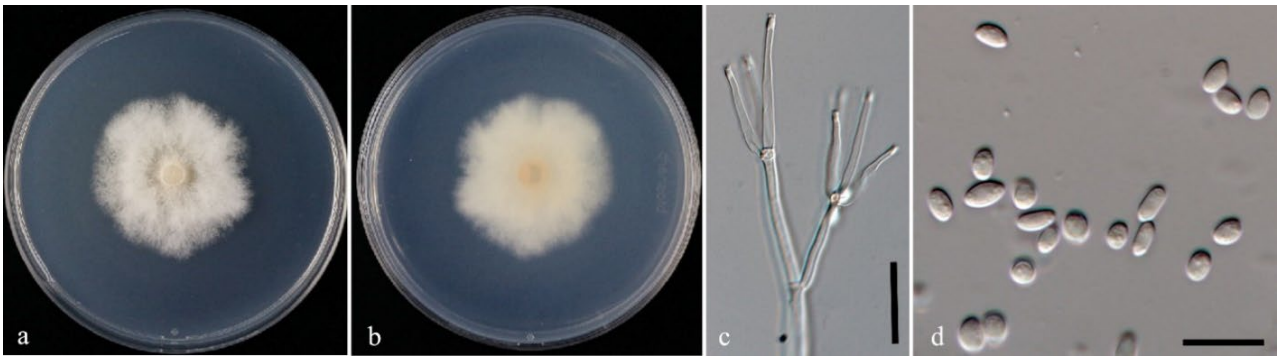

Figure 20 – *Clonostachys farinose* (JZB3530055). a Upper view. b Reverse view of colony in PDA after 7 d at 25 °C in the dark. c Conidiophores. d Conidia. Scale bars: c, d = 10 μm.

Nectriaceae Tul. & C. Tul. [as 'Nectriei']

Nectriaceae was established by Tulasne & Tulasne (1865) and it has undergone extensive taxonomic treatments since. *Nectriaceae* species are characterised by having different colour of uniloculate ascomata which are white, yellow, orange-red or purple (Lombard et al. 2015). Currently, 77 genera have been accepted to this family (Perera et al. 2023). These genera include more than 900 species and most of them are soil-borne saprobes or weak to virulent, facultative or obligate plant pathogens (Lombard et al. 2015, Abeywickrama et al. 2021, 2023, Perera et al. 2023). Some have been reported as facultatively fungicolous or insecticolous species (Lombard et al. 2015).

Fusarium Link

Fusarium was described by Link (1809) as *Fusisporium,* based on the species *F. roseum*. Later, Wollenweber & Reinking (1935) mentioned two other existing *Fusarium* species; *F. sambucinum* and *F. graminearum* and now *Fusarium sambucinum* is accepted as the type species. *Fusarium* is a ubiquitous and cosmopolitan fungal group. These species can be soilborne, airborne, or found in plant debris, and identified from any plant part. *Fusarium* species are reported to cause destructive damage to plants, animals, human health and food security (Moretti 2009, Dean et al. 2012, Jayawardena et al. 2019b, Torbati et al. 2019, Ebrahim et al. 2020, Crous et al. 2021, 2022, Hyde et al. 2023, Song et al. 2023, Zhang et al. 2023a). The head blight of wheat and Fusarium wilt of bananas are considered to be the most important diseases caused by *Fusarium*. These diseases not only cause significant production losses but also have a significant impact on communities that rely on these crops globally. Further, *Fusarium* species are recognized as one of the important pathogenic genera that produce mycotoxins and secondary metabolites (Jayawardena et al. 2019b, Crous et al. 2021, 2022, Mapook et al. 2022, Abeywickrama et al. 2023).

We utilized both morphological and phylogenetic evidence to identify the *Fusarium* species and in the present study, seven isolates belonging to three *Fusarium* species in *Fusarium incarnatum-equiseti* species complex, 16 isolates representing three species in the *Fusarium fujikuroi* species complex, 13 isolates belonging to one species in *Fusarium lateritium* species complex and four isolates belonging to one species in *Fusarium oxysporum* species complex were identified.

Fusarium planum S.L. Han, M.M. Wang & L. Cai (2023) Fig. 22

Index Fungorum number: IF474882

Associated with *Prunus avium* branch with die-back symptoms. Sexual morph: not observed. Asexual morph: *Microconidia* on aerial conidiophores hyaline, ellipsoidal to subcylindrical, smooth and thin-walled, 4.8–11.7 × 2.0–3.4 μm (av. 8.7 × 2.7 μm, n = 40). *Aerial phialide* 11.3–16.6 × 2.6–3.4 μm (n = 2). *Sporodochia* formed on carnation leaves irregular, orange-yellow. *Sporodochial conidiophores* verticillately or laterally branched, bearing terminal, single monophialides or terminal whorls with up to three monophialides; Sporodochial phialides subulate to lageniform, 13.2–18.6 × 2.8–5.1 μm (av. 15.7 × 3.8 μm, n = 10). *Conidia* on sporodochia falcate, apical cell conical with rounded to papillate apex, basal cell slightly papillate to foot-shaped, (1–) 2–5-septate, hyaline, thin- and smooth-walled; *1-septate conidia*: 23.4–45.7 × 3.0–5.1 μm (av. 34.5×4.2 μm, n = 7); *2-septate conidia*: 28.2–44.6 × 4.1–4.6 μm (av. 35.7×4.4 μm, n = 3); *3-septate conidia*: 28.5–52.7 × 2.7–3.9 μm (av. 39.5× 3.2 μm, n = 40). *4-septate conidia*: 43.3–59.8 ×4.2–5.4 μm (av. 50.4×4.9 μm, n = 21); 5-septate conidia: 50.8–63.9 × 4.7–5.6 μm (av. 56.4×5.1 μm, n = 12). *Chlamydospores* not observed.

Cultural characteristics – Colonies on PDA reaching 50–52 mm diam. in 4 d at 25 °C (growth rate: 11 mm/d). Floccose to fluffy, white, reverse apricot or pale orange. Aerial mycelium is abundant.

Material examined – China, Beijing, from the *Prunus avium* branch with die-back symptoms, March 2021, P. Chen (dried cultures JZBH3110229, JZBH3110230), living cultures JZB3110229, JZB3110230.

Notes – *Fusarium planum* was recently identified from symptomatic tissues of maize ear rot from Guangdong province, China and it was confirmed that this species can cause maize stalk rot (Han et al. 2023). Based on the combined sequences of ITS, tef and rpb2 sequence data, two isolates (JZB3110229 and JZB3110230) clustered with the reference strains of *F. planum* (LC15876: ex-type, LC18411, LC18578) with 100% ML and 1.00 BYPP supports. Morphologically, our isolates differ from the ex-type of *F. planum*, by having a larger size of sporodochial conidia (Han et al. 2023). Based on the pathogenicity test result, this species does not produce any symptoms on detached sweet cherry shoots. So far, *F. planum* has not been reported from *Prunus avium* worldwide, therefore here we report a novel host association of *F. planum* on *Prunus avium* in China.

Fusarium annulatum Bugnic. (1952) Fig. 23

Index Fungorum number: IF509381

Associated with *Prunus avium* branch with die-back symptoms. Sexual morph: not observed. Asexual morph: *Phialides* 10–31.3 × 2.4–3.7 μm (n = 20). *Abundant microcondia* forming on CLA, fusiformis or oblong oval, 5.0–8.7 × 1.9–3.6 μm (av. = 6.7 × 2.6 μm, n = 40). *Aerial macroconidia*, 1(–2)–4 septate, falciform, little curved, 1-septate conidia 17.1–27.7 × 3.1–4.4 μm (av. = 22.1 × 3.5 μm, n = 12); 3-septate conidia 33.7–46.8 × 3.4–5.3 μm (av. = 39.3× 4.3 μm, n = 11); 4-septate conidia 44–55 × 3.9–4.8 μm (av. = 49 × 4.4 μm, n = 8). *Chlamydospore* globose to obovoid, 8.8–15.6 × 6.6–12.9 μm (av. = 12.3 ×8.6 μm, n = 6), terminal or intercalary.

Cultural characteristics – Colonies on PDA growing in the dark with an average radial growth rate of 13–17 mm/d and reaching 57–69 mm diameter at 25 °C for 4 days.

Material examined – China, Beijing, from the *Prunus avium* branch with die-back symptoms, March 2021, P. Chen (dried cultures JZBH3110234–JZBH3110241), living cultures JZB3110234–JZB3110241. Shandong Province, from the *Prunus avium* branch with die-back symptoms, March 2021, P. Chen (dried cultures JZBH3110231–JZBH3110233), living cultures JZB3110231–JZB3110233.

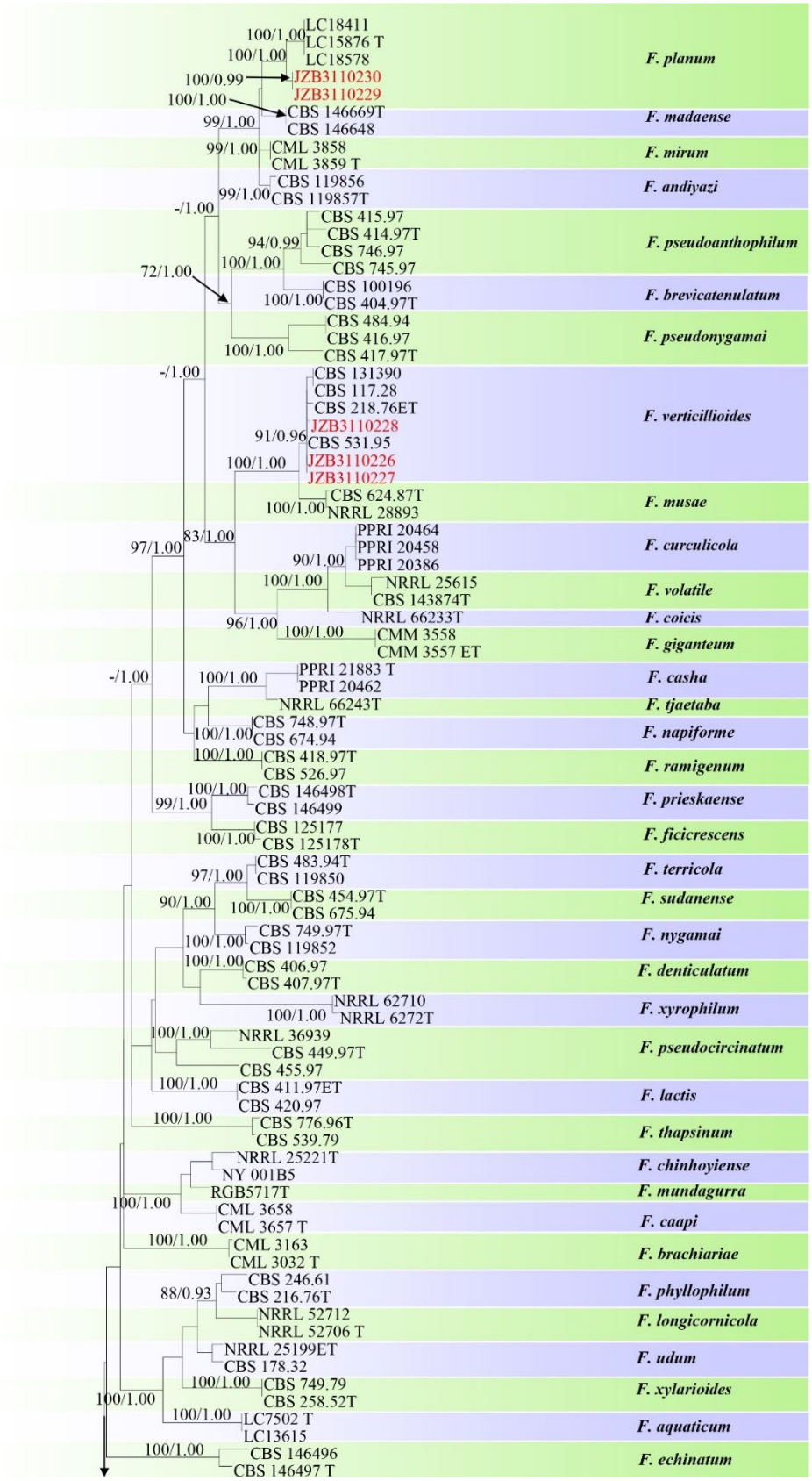

Figure 21 – Phylogenetic tree generated by maximum likelihood analysis of combined TEF and rpb2 sequence data of species belonging to *Fusarium fujikuroi* species complex (FFSC). The tree was rooted with *F. nirenbergiae* (CBS 744.97). RAxML bootstrap support values ≥ 60% and (BT) Bayesian posterior probabilities ≥ 0.90 (PP) are shown respectively near the nodes. The scale bar indicates 0.009 changes. The ex-type strains are marked in bold and the isolate numbers from the current study are in red. The maximum likelihood alignment matrix has 660 distinct alignment

patterns with 13.17% of undetermined characters or gaps. Estimated base frequencies were as follows: A = 0.255988, C = 0.261858, G = 0.244615, T = 0.237539. substitution rates AC = 1.152795, AG = 4.869703, AT = 1.218621, CG = 0.726940, CT = 9.030367, GT = 1.000000; gamma distribution shape parameter α= 0.863895.

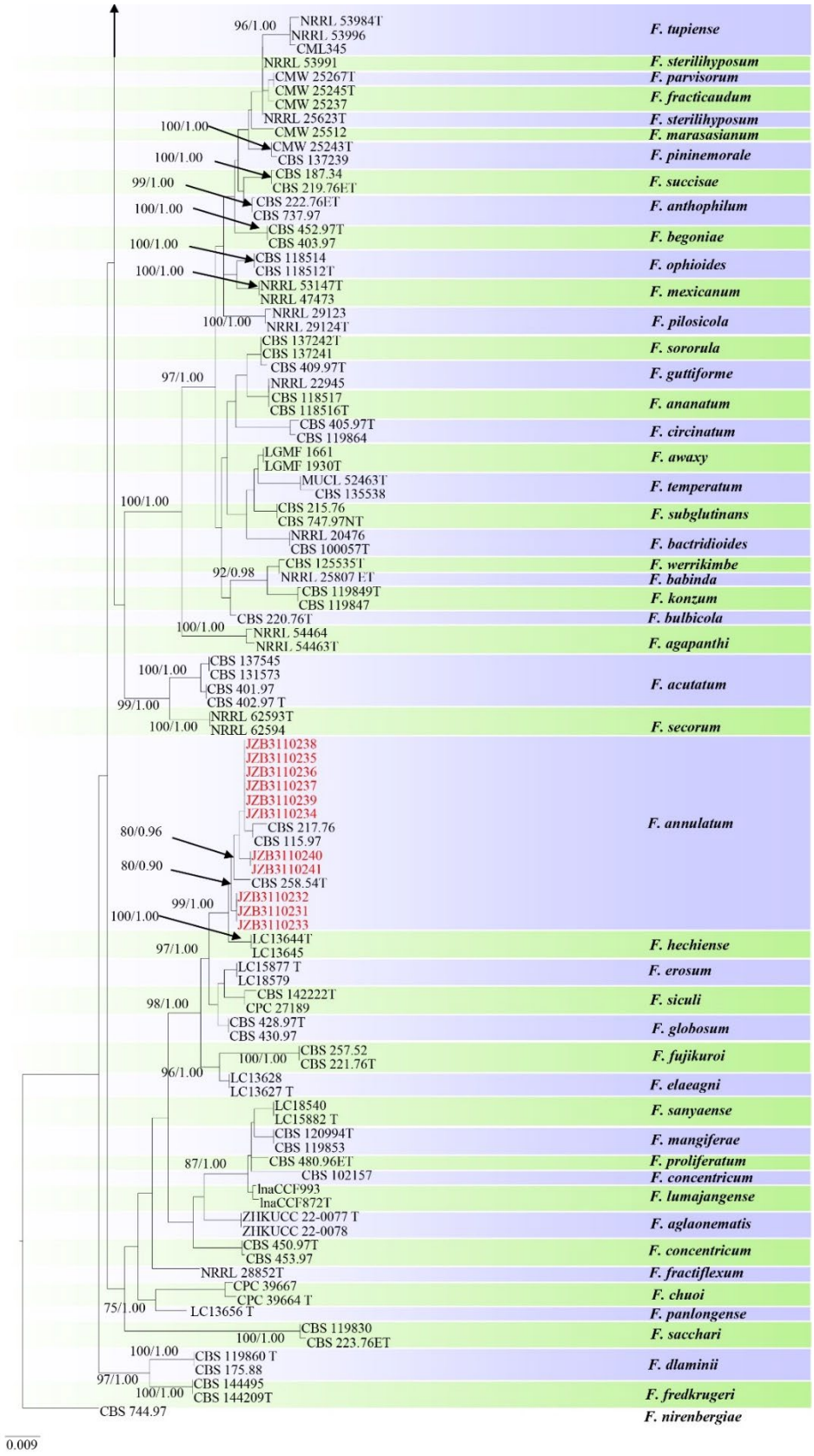

Figure 21 – Continued.

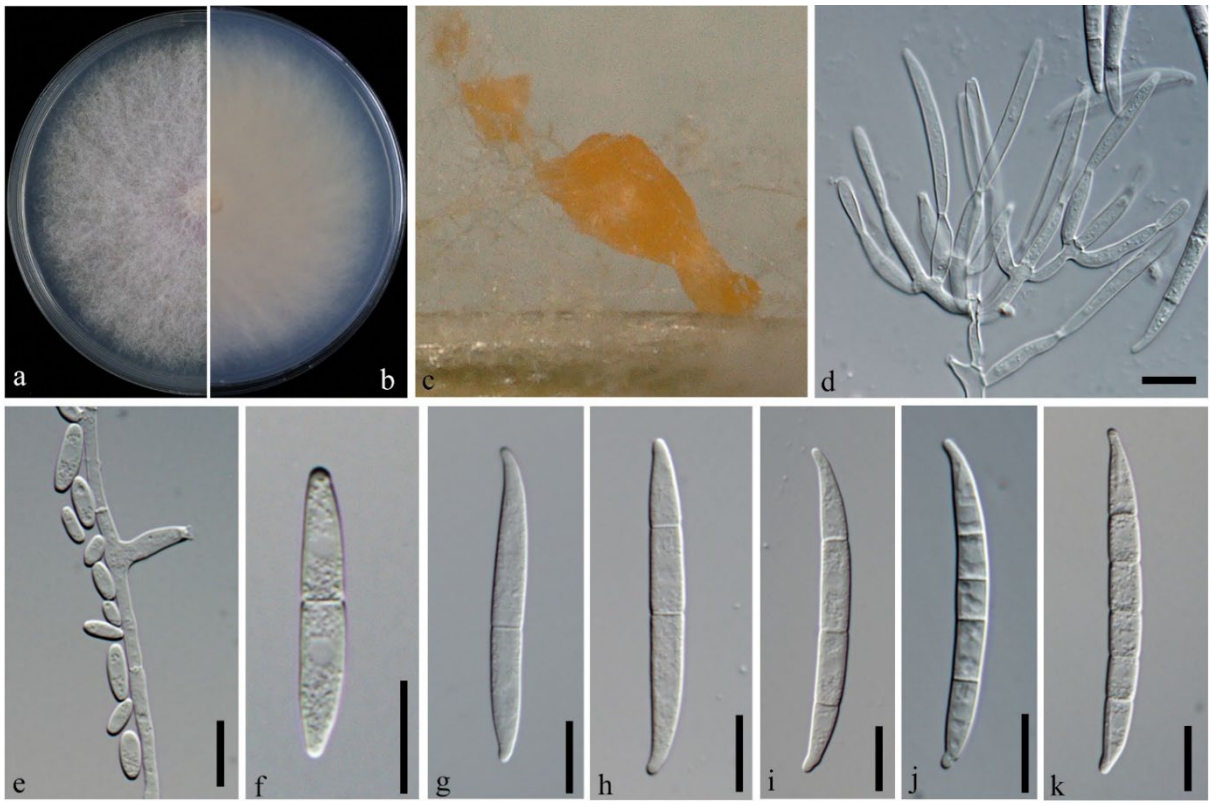

Figure 22 – *Fusarium planum* (JZB3110229). a Upper view. b Reverse view of the colony in PDA after 7 d at 25 °C in the dark. c Sporodochia formed on the surface of carnation leaves. d Conidiogenous cells, sporodochial conidiophores and phialides. e Aerial phialides and microconidia. f–k Macroconidia. Scale bars: d–k = 10 μm.

Notes – *Fusarium annulatum* was initially described from *Oryza sativa* (Bugnicourt 1952, Han et al. 2023, USDA host-fungal database 2024; https://fungi.ars.usda.gov/). Based on the analysis of combined RPB2 and tef1-α sequence data, eleven isolates of *Fusarium* were clade with reference strain of *Fusarium annulatum* (NRRL 22944) with 100% ML and 0.90 BYPP values. Morphologically, these isolates showed similar characteristics to the reference strain of *F. annulatum* (NRRL 22944) with minor size differences. So far, this species has not been reported from *Prunus avium* worldwide. Therefore, here we report the novel host association of *Fusarium annulatum* on *Prunus avium* in the world.

Fusarium verticillioides (Sacc.) Nirenberg (1976) Fig. 24

Index Fungorum number: IF314223

Pathogenic on *Prunus avium*. Sexual morph: not observed. Asexual morph: on PDA, *Conidiophores* in the aerial mycelium with branched, terminal and lateral monophialides. *Phialides* subulate to subcylindrical, 0-1 septate, 20–40 × 2.5–3.7 μm, apex 1.2–1.7 μm (n = 8). *Microconidia* hyaline, generally aseptate, ellipsoidal, subclavate, smooth and thin-walled, granular, 5.5–12.4 × 2.5–4.7 μm (av. 8.1 × 3.5 μm, n = 40). *Sporodochia* orange, formed abundantly on carnation leaves. *Macroconidia* on sporodochia, falcate, hyaline, 1–6 septate: 1-septate conidia 20.9–23.2 × 3.4–4.4 μm (av. 22.1 × 3.9 μm, n = 2); 2-septate conidia 28.9 × 3.2 μm; 3-septate conidia 43.1–60.1 × 4.3–5.2 μm (av. 51.7 × 4.7 μm, n = 8); 4-septate conidia 49.3–71.7 × 3.7–4.9 μm (av. 61 × 4.4 μm, n = 16); 5-septate conidia 54.2–78.3 × 3.9–5.6 μm (av. 65.5 × 4.8 μm); 6-septate conidia 70.8 × 5.2 (n = 1). *Chlamydospores* not observed.

Cultural characteristics – Colonies on PDA reaching 53–56 mm diam. in 4 d at 25 °C (growth rate: 12–13 mm/d). Colony surface felty, aerial mycelium moderate, white to purple, with white margins. Reverse pink near the margin, dark purple in the centre.

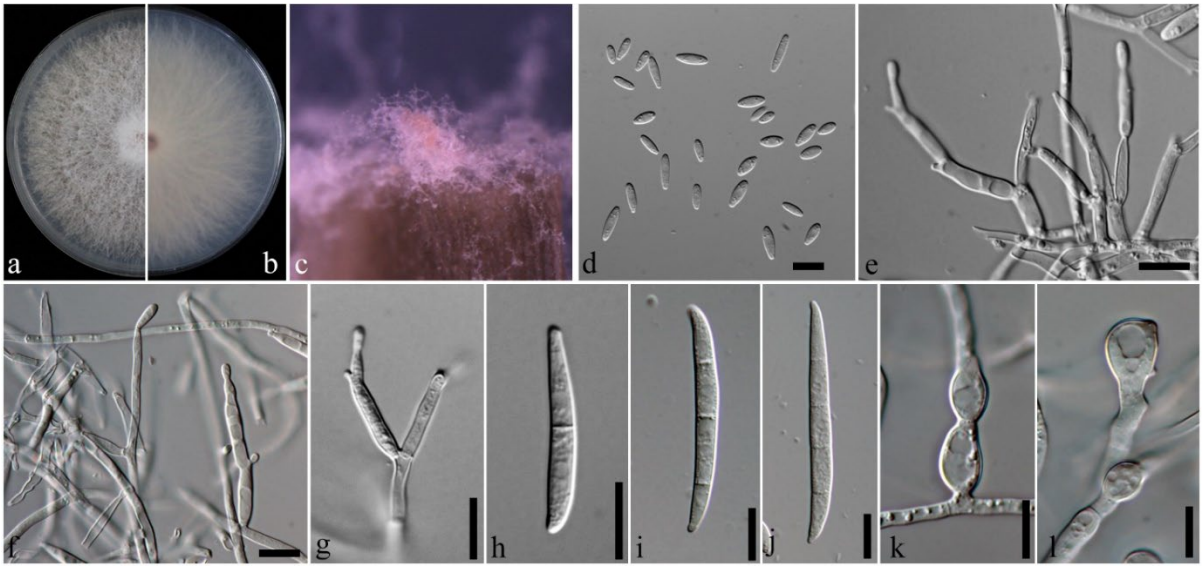

Figure 23 – *Fusarium annulatum* (JZB3110231). a Upper view. b Reverse view of the colony in PDA after 7 d at 25 °C in the dark. c Sporodochium formed on the surface of carnation leaves. d Microconidia. e–g Aerial conidiophores and phialides. h–k Macroconidia. l–m Chlamydospore. Scale bars: d–m = 10 μm.

Material examined – China, Liaoning Province, from the *Prunus avium* branch with die-back symptoms (*Rosaceae*), 24 March 2021, P. Chen, (dried cultures JZBH3110226–JZBH3110228), living cultures JZB3110226–JZB3110228.

Notes – *Fusarium verticillioides* is classified into the *Fusarium fujikuroi* species complex (FFSC). *Fusarium verticillioides* is recognized as an important pathogen on economically important crops, including cereal crops. It is also reported that these species are known to cause rice bakanae disease, maize ear rot (Qiu et al. 2015, 2020), soybean root rot (Pedrozo et al. 2017), leaf spots (pineapple) and fruit rots (banana, pineapple, tomato) (Abd Murad et al. 2016, Hirata et al. 2001, Salem et al. 2020). Further, this species has been reported as an endophyte from cherry trees (*Prunus avium*) in Iran (Abdollahi Aghdam & Fotouhifar 2017). In this study, based on the phylogenetic analysis of the combined rpb2 and tef sequences, three *Fusarium* isolates cluster with *F. verticillioides* strain CBS 734.97 with high statistical support (100% ML/1.00 BYPP). All isolates showed a similar morphology with *Fusarium verticillioides* in colony and conidia characters, though having a faster growth rate than *Fusarium verticillioides* (ATCC 38932) and (ATCC 38933) (5–6 mm/d) (Hirata et al. 2001). This species has not been reported on sweet cherries in China; therefore, we report a new geographical report of *F. verticillioides* on *Prunus avium* in China.

Fusarium citri M.M. Wang, Qian Chen & L. Cai (2019) Fig. 26

Index Fungorum number: IF829534

Pathogenic on *Prunus avium*. Sexual morph: not observed. Asexual morph: *Sporodochia* greyish orange, nearly spherical or irregular, forming abundantly on carnation leaves. *Sporodochial macroconidia* falcate, straight to slightly curved, with a blunt to hooked apical cell and a poorly developed, foot-shaped basal cell, (1–)2–5 septate conidia, hyaline. 1–2-septate conidia: 12.9–20.5 × 3.4–5.7 μm (av. ± SD: 17.4 ± 2.2 × 4.6 ± 0.6 μm, n = 12); 3-septate conidia: 17.4–28 × 3.7–6.5 μm (av.± SD: 22.4 ± 2.7 × 5.3 ± 0.6 μm, n = 40); 4-septate conidia: 26.1–29.3 × 5.3–6.4 μm (av. 28.1 ± 1.1× 5.8 ± 0.4 μm, n = 5); 5-septate conidia: 27.9–34.3 × 5.3–7.0 μm (av. ± SD: 30.9 ± 2.4 × 6.3 ± 0.5 μm, n = 7). *Chlamydospores* and microconidia were not observed.

Cultural characteristics – Colonies on PDA growing in the dark with an average radial growth rate of 18 mm/d and reaching 66–70 mm diam. after 4 d at 25 °C (filling the Petri dish after 7d). Colony white to pale yellow, reverse grass yellow, aerial mycelia slightly dense, colony margin entire white.

Material examined – China, Beijing City, Tongzhou District, from the diseased twigs of *Prunus avium*, April 2022, S. X. Ji & P. Chen, (dried cultures JZBH3110253–JZBH3110255), living cultures JZB3110253–JZB3110255.

Notes – Initially, *Fusarium citri* was described from the leaf of *Citrus reticulata* in China. Currently, *Fusarium citri* has been reported from *Amygdalus triloba*, *Capsicum* sp., *Chenopodium quinoa*, *Citrus reticulata*, *Diplotaxis tenuifolia*, *Lactuca sativa*, *Medicago sativa* and *Triticum* species (USDA host-fungus database 2024; https://fungi.ars.usda.gov/). Recently, Zhou et al. (2022) have reported that *Fusarium citri* is causing leaf spot disease on *Prunus avium* in China. Based on ITS, tef and rpb2 sequence analysis, three isolates recovered from diseased twigs of *Prunus avium* are classified with the reference strains of *Fusarium citri* with high statistical support (Fig. 25). So far, this species has not been reported from *Prunus avium* in the world. Therefore, we report a novel host association of *F. citri* on *Prunus avium* in China. Based on pathogenicity test results, this species developed symptoms on detached green shoots of *P. avium*.

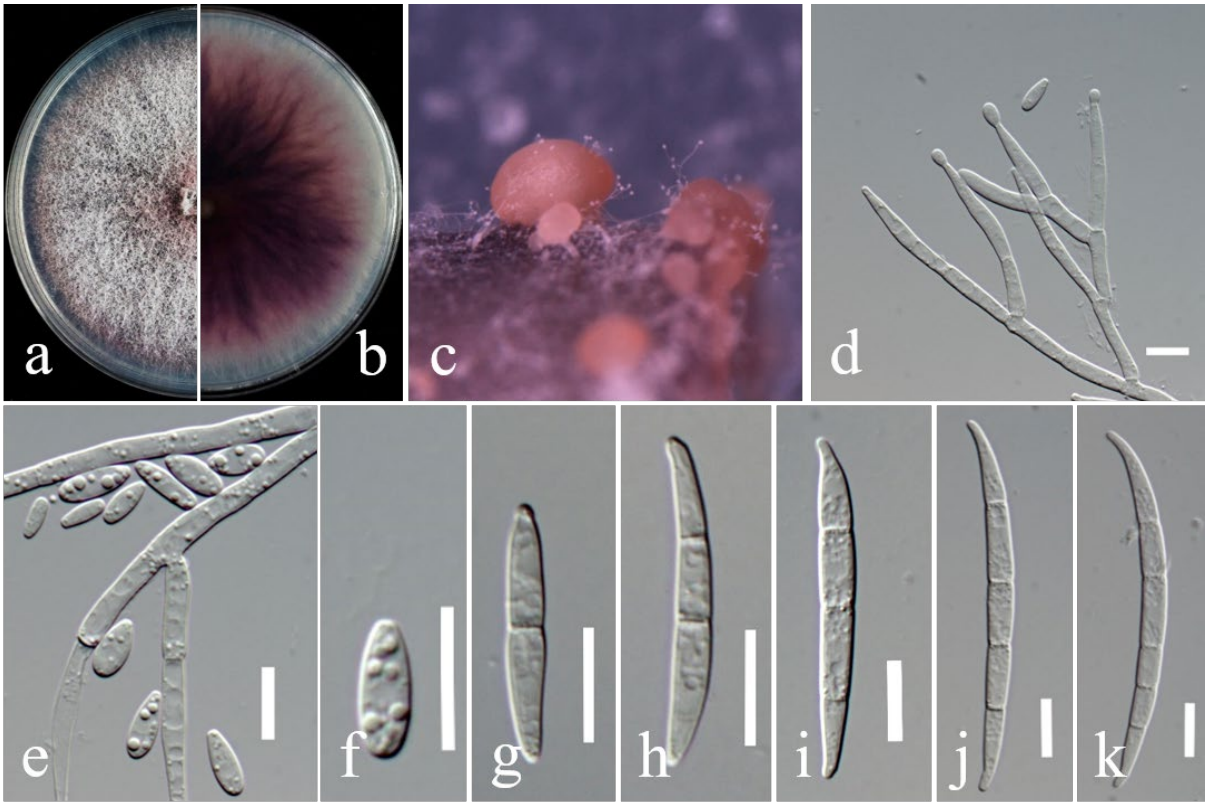

Figure 24 – *Fusarium verticillioides* (JZB3110226). a Upper view. b Reverse view of the colony in PDA after 7 d at 25 °C in the dark. C Sporodochia formed on the surface of carnation leaves. d Conidiogenous cells, aerial conidiophores and microconidia. e–f Microconidia. g–k Macroconidia. Scale bars: d–k = 10 µm.

Fusarium compactum (Wollenw.) Raillo (1950) Fig. 27

Index Fungorum number: IF297537

Pathogenic on *Prunus avium*. Sexual morph: not observed. Asexual morph: *Sporodochia* irregular, pink orange. *Sporodochial phialides* subulate to subcylindrical, 10.4–18.8 × 2.9–3.8 µm (av. ± SD: 13.5 ± 2.4 × 3.5 ± 0.3 µm, n = 13). *Macroconidia* falcate, slightly curved, with a tapered to elongated apex and a poorly or well-developed and foot-shaped basal cell, (2–)5–6-septate, predominantly 5-septate, hyaline, smooth-walled. 2-septate conidia: 35.7 × 4.8 µm (n = 1); 3-septate conidia: 28.9–30.9 × 3.0–4.4 µm (av. ± SD: 30.2 ± 0.9 × 3.5 ± 0.7 µm, n = 3); 4-septate conidia 61.9 × 4.0 µm (n = 1), 5-septate conidia 48.7–65.7 × 4.4–5.7 µm (av. ± SD: 57.8 ± 4.5 × 4.9 ± 0.4 µm, n

= 40); 6-septate conidia 56.9–66.1 × 4.4–5.1 µm (av. ± S D: 62 ± 3.5 × 4.7 ± 0.3 µm, n = 4). *Chlamydospores* and microconidia were not observed.

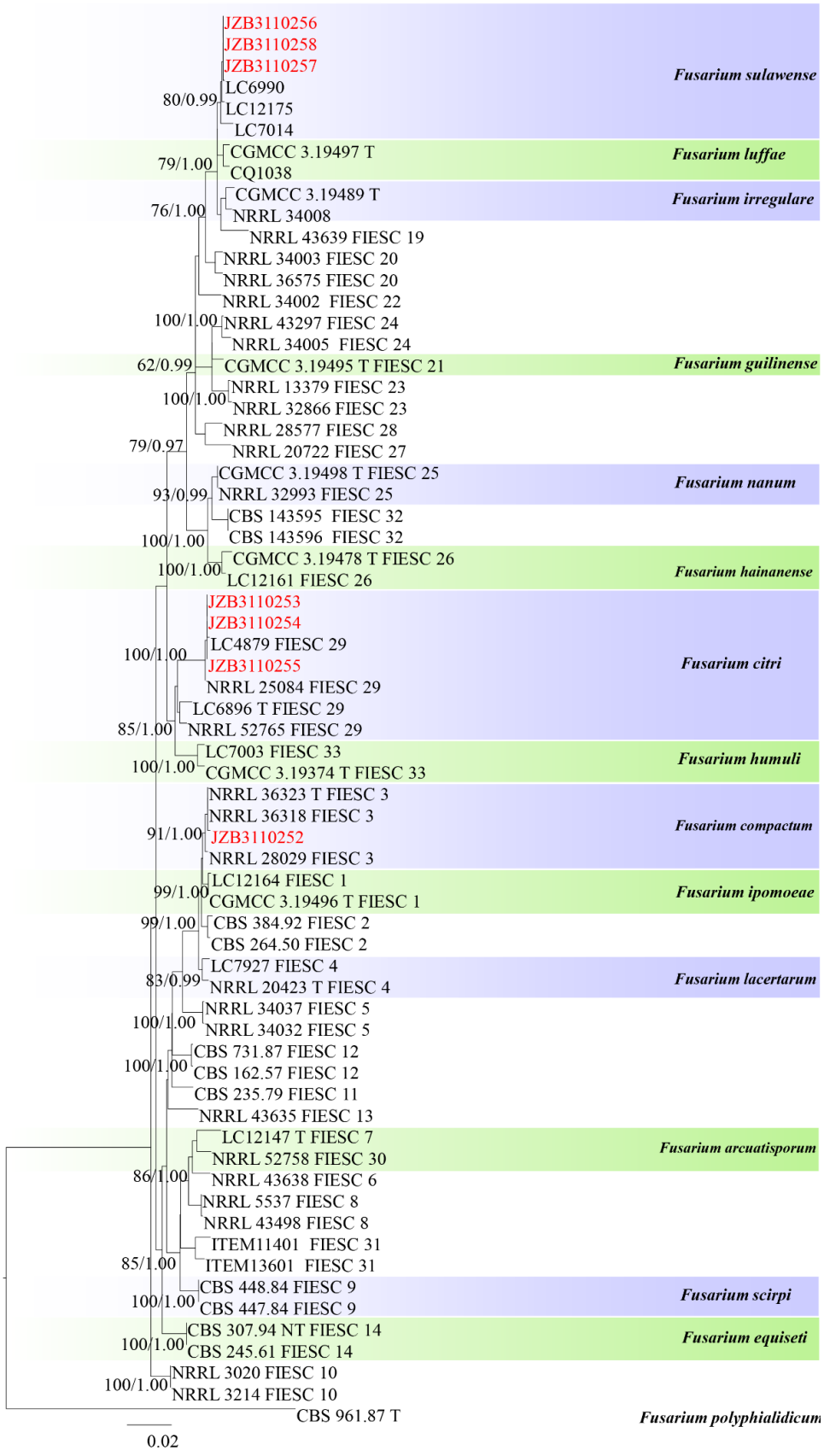

Figure 25 – Phylogenetic tree generated by maximum likelihood analysis of combined ITS, TEF and rpb2 sequence data of species belonging to *Fusarium incarnatum-equiseti* species complex (FIESC).

The tree was rooted with *F. polyphialidicum* (CBS 961.87, FCSC). RAxML bootstrap support values (BT) ≥ 60% and Bayesian posterior probabilities (PP) ≥ 0.90 are shown respectively near the nodes. The scale bar indicates 0.02 changes. The ex-type strains are in bold and isolates from the current study are in red. The maximum likelihood alignment matrix had 477 distinct alignment patterns, with 5.58% of undetermined characters or gaps. Estimated base frequencies were as follows; A = 0.262769, C = 0.264487, G = 0.241220, T = 0.231523; substitution rates AC = 1.088978, AG = 2.832881, AT = 1.344447, CG = 0.664138, CT = 8.466029, GT = 1.000000; gamma distribution shape parameter α = 0.726717.

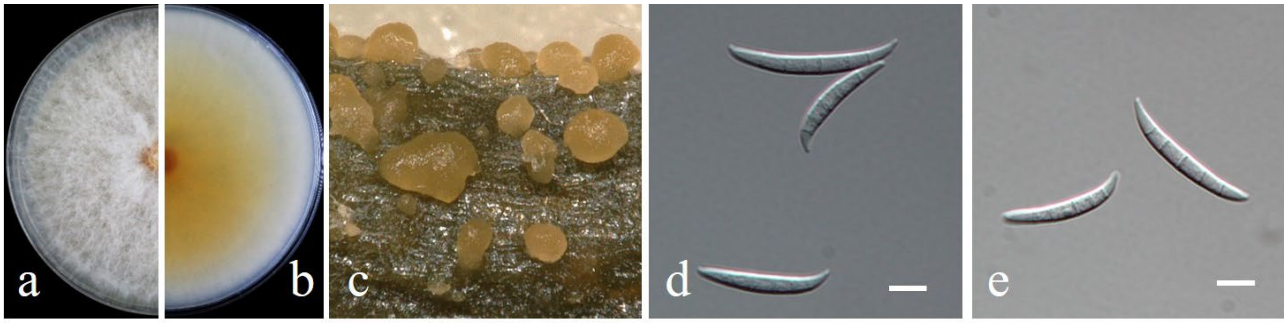

Figure 26 – *Fusarium citri* (JZB3110254). a Upper view. b Reverse view of the colony in PDA after 7 d at 25 °C in the dark. c Sporodochia on carnation leaves. d, e Macroconidia. Scale bars: c–d = 10 μm.

Cultural characteristics – Colonies on PDA reaching 47–60 mm (av. 54 mm, 13.5 mm/d) after 4 d at 25 ℃. White, reverse pale yellow with white margin. Cottony, mycelium abundant.

Material examined – China, Beijing, from the *Prunus avium* branch with die-back symptoms, August 2022, S. X. Ji & P. Chen (dried culture JZBH3110252), living culture JZB3110252.

Notes – *Fusarium compactum* has been reported from several host plants in the world (USDA host-fungus database 2023; https://fungi.ars.usda.gov/). Zhou et al. (2022) have reported that *Fusarium compactum* is causing leaf spot disease on *Prunus avium* in China. In this study, we have identified an isolate (JZBH3110252) recovered from a branch of *Prunus avium* with die-back symptoms, and it is classified with the reference strains of *Fusarium compactum* in ITS, tef and rpb2 sequence phylogeny. In this study, we introduce a new collection of *F. compactum* causing trunk disease on *Prunus avium* in China.

Fusarium sulawesiense Maryani, Sand.-Den., L. Lombard, Kema & Crous [as 'sulawense'] (2019) Fig. 28

Index Fungorum number: IF830777

Associated with diseased twigs of *Prunus avium*. Sexual morph: not observed. Asexual morph: *Sporodochia* forming on carnation leaves, orange, irregular. *Aerial monophialides* subulate to subcylindrical, smooth- and thin-walled, 15.7–31.6 × 2.2–3.9 μm. *Macroconidia*, aseptate (12.4× 3.5 μm, n = 1) or (1–)3–6(–7)-septate, hyaline, falcate, curved or slightly curved, with a pointed apical cell, and a papillate, non-foot-shaped basal cell. 1-septate conidia: 19.3–23.9 × 3.9–4.9 μm (av. ± SD: 18.5 ± 42.3×4.4 ± 0.5 μm, n = 2); 3-septate conidia: 21.3–34.8 × 3.5–5.3 μm (av. ± SD: 29.2 ± 3.5×4.4 ± 0.5, n = 18); 4-septate conidia: 29.1–36.8 × 4.0–6.2 μm (av. ± SD: 34.1 ± 2.5 × 5.0 ± 0.7 μm, n = 10); 5-septate conidia: 29.3–47.4 ×4.0–6.5 μm (av. ± SD: 37.1 ± 3.8 × 5 ± 0.6 μm, n = 40); 6-septate conidia: 37.4–49.2 × 4.6–6.2 (av. ± SD: 43.4 ± 4.8 × 5.5 ± 0.7μm, n = 4). *Chlamydospores* and microconidia not observed.

Culture characteristics – Colonies on PDA reaching 60–70 mm (average: 66 mm, 16.3 mm/d) after 4 d at 25 ℃. White, cottony, aerial mycelium dense, reverse pale orange with white margin.

Material examined – China, Beijing City, Tongzhou District, from the diseased twig of *Prunus avium*, July 2022, S. X. Ji & P. Chen, (dried cultures JZB3110256–JZB3110258), living cultures JZB3110256–JZB3110258.

Notes – *Fusarium sulawesiense was* initially described from the diseased pseudo-stem of *Musa acuminata* in Indonesia (Maryani et al. 2019a). This species belongs to the *Fusarium incarnatum-equiseti* species complex (Maryani et al. 2019a). This species previously has been reported from several host plants in China, including *Capsicum* sp., *Carica papaya*, *Citrus reticulata*, *Colocasia esculenta*, *Ipomoea aquatica*, *Musa nana*, *Oryza sativa* and *Syngonium auritum* (USDA host-fungus database 2024; https://fungi.ars.usda.gov/). We recovered three isolates from a diseased twig of *Prunus avium* and all isolates classified with the reference strains of *F. sulawesiense* in ITS, tef and RPB2 sequence phylogeny (Fig. 25). So far, this species has not been reported from *Prunus avium* worldwide, therefore here we report the first host association of *F. sulawesiense* on *Prunus avium* in the world.

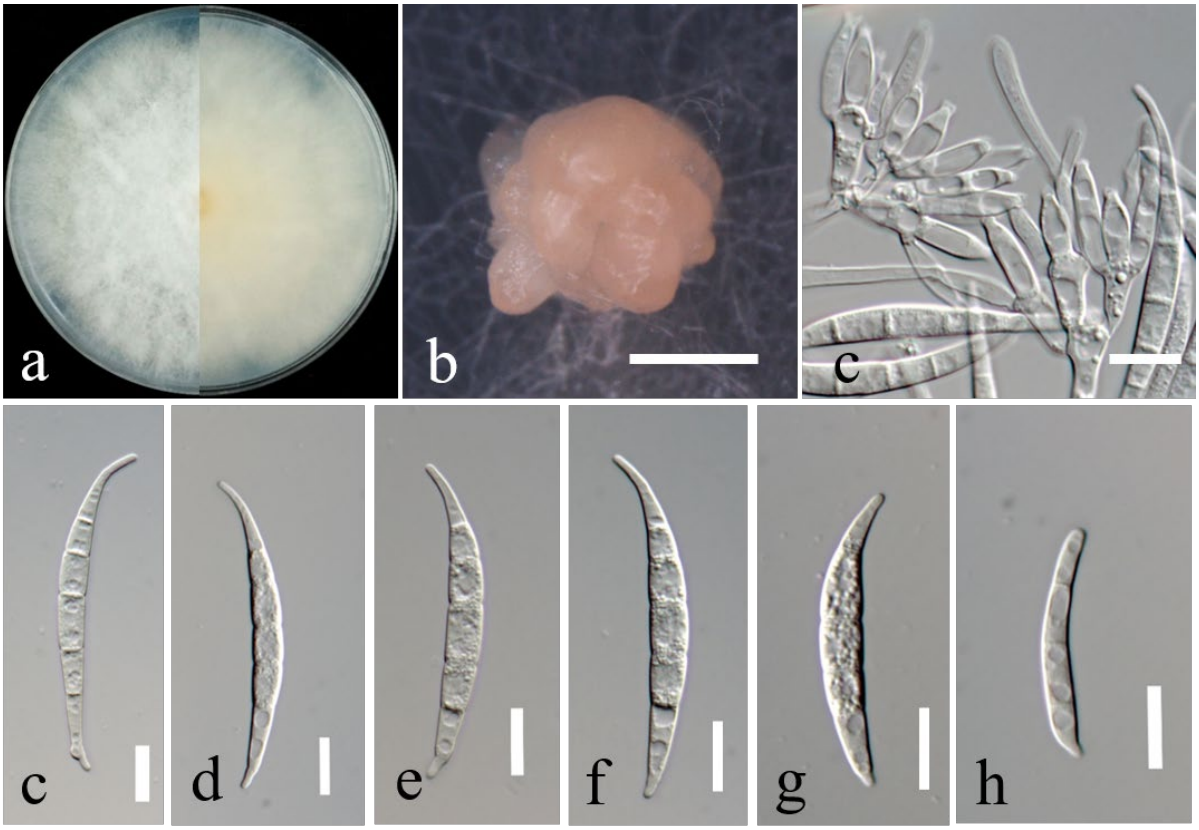

Figure 27 – *Fusarium compactum* (JZB3110252). a Upper and reverse view of the colony in PDA after 7 d at 25 °C in the dark. b Sporodochium. c Sporodochial conidiophores and phialides. c–h Macroconidia. Scale bars: b = 50 µm, c–h = 10 µm.

Fusarium lateritium Nees. (1816) Fig. 30

Index Fungorum number: IF225937

Associated with diseased twigs of *Prunus avium.* Sexual morph: not observed. Asexual morph: *Sporodochia* forming on carnation leaves, hyaline or orange, globules or irregular. *Macroconidia* falcate, 3–6-septa, hyaline. 3-septa conidia: 33 × 4.4 µm. 4-septa conidia: 38.2–57.3 × 3.9–5.4 µm (av. ± SD: 47.1 ± 4.5 × 4.6 ± 0.4 µm, n = 40); 5-septa conidia: 3.4–61.8 × 3.2–4.9 µm (av. ± SD: 55.3 ± 4.9× 4.5 ± 0.3 µm, n = 40). 6-septa conidia: 56.8–58.2 × 4.5–5 µm (av. ± SD: 57.5 ± 0.7 × 4.8 ± 0.2 µm, n = 2). *Chlamydospores* and microconidia were not observed.

Culture characteristics – Colony on PDA reaching 51 mm after 6 days at 25 °C. White, cottony, reverse pale orange, with a white margin.

Material examined – China, Shandong Province, from the diseased twig of *Prunus avium*, July 2021, S. X. Ji & P. Chen, (dried cultures JZBH3110343-JZBH3110348, JZBH3110350-JZBH3110352, JZBH3110354, JZBH3110357-JZBH3110359), living cultures (JZB3110343-JZB3110348, JZB3110350-JZB3110352, JZB3110354, JZB3110357-JZB3110359).

Notes – *Fusarium lateritium* belongs to *F. lateritium* species complex (FLSC) however comprehensive multi-locus phylogenetic studies have not been performed for the FLSC (Cavalcanti et al. 2020). In this study, we have obtained 13 isolates that were clade in *F. lateritium* species complex. According to the multi-loci phylogeny, our isolates perform separate sister clade related to Lateritium clade IIA, Lateritium clade IIB, *F. stilboides* and *F. cassia* (Fig. 29). Morphological characteristics of our isolates showed more similarity to the species in Lateritium clades, and therefore we keep our isolates as *Fusarium lateritium* (Geiser et al. 2005). Further studies are needed for the more precise identification of these species belonging to which Lateritium clade. Isolates in Lateritium clade are widely known as wound pathogens of woody hosts, causing a wide variety of diseases. Most of these associated with coffee wilt, and isolates were from coffee, either from berries, bark or vascular tissue (Geiser et al. 2005). In this study, we report a species in *F. lateritium* clade for the first time associated with *Prunus avium* in the world.

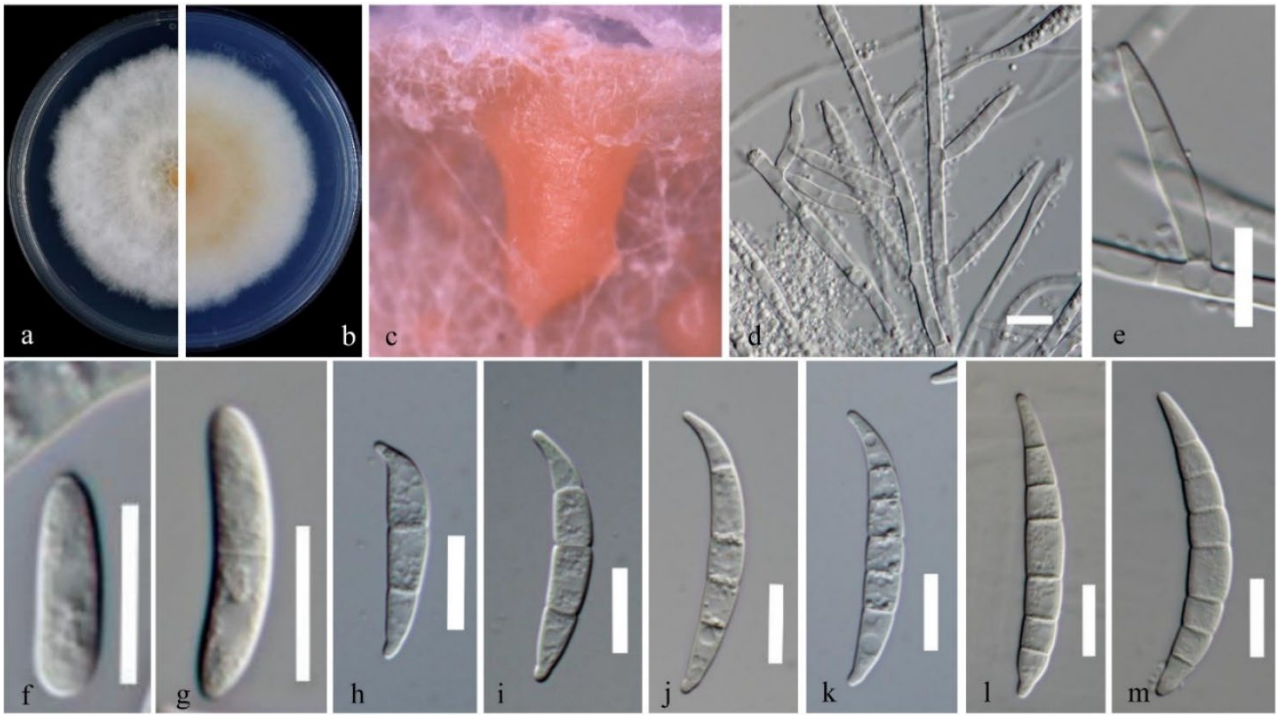

Figure 28 – *Fusarium sulawesiense* (JZB3110256). a, b Upper and reverse view of the colony in PDA after 7 d at 25 °C in the dark. c Sporodochium. d, e Sporodochial conidiophores and phialides. f–m Macroconidia. Scale bars: 10 μm.

***Fusarium* sp.** Fig. 32

Pathogenic on *Prunus avium*. Sexual morph: not observed. Asexual morph: *Sporodochia* not observed on the cultures. *Microconidia* hyaline, generally aseptate, ellipsoidal, subclavate, smooth and thin-walled, granular, 6.29–11.99 × 2.37–4.66 μm (avg. = 8.93 × 3.32 μm, n = 40). *Chlamydospores* and Macroconidia not observed.

Cultural characteristics – Colonies on PDA reaching 90mm after 3 d at 25 °C. White to light pink, cottony, aerial mycelium dense, reverse pink with white margin.

Material examined – China, Shandong Province, from the diseased twig of *Prunus avium*, July 2021, S. X. Ji & P. Chen, (dried cultures JZBH3110360-JZBH3110363), living cultures (JZB3110360-JZB3110363).

Notes – In this study, we have isolated four strains that clade within the *Fusarium oxysporum* species complex (Fig. 31). However, with the currently available sequence data we are unable to confirm them to a species level. In the phylogenetic tree of tef1-α and RPB2 sequence data, our isolates have formed a clade with isolates of *F. odoratissimum, F. phialophorum* and *F. purpurascens.*

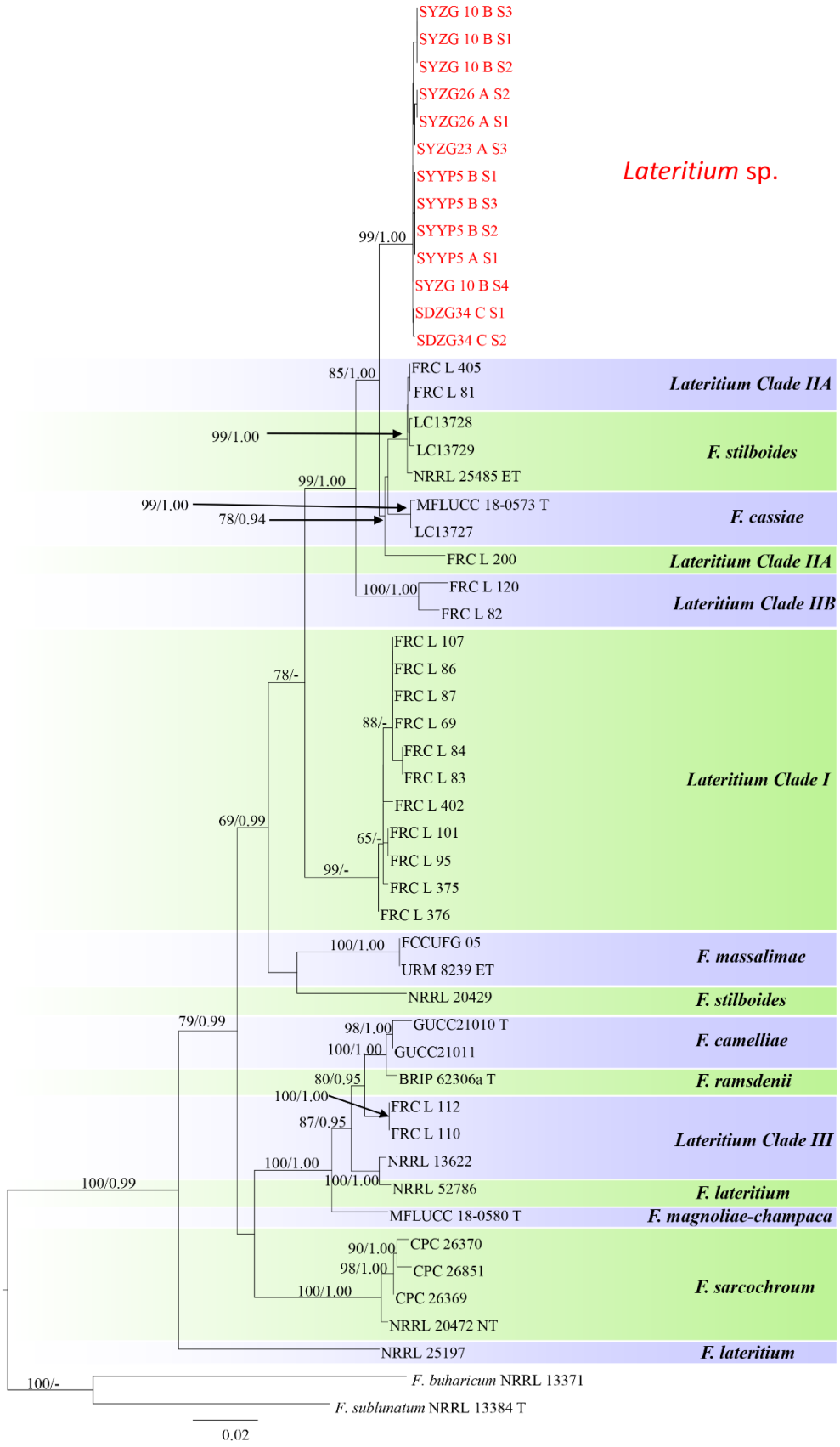

Figure 29 – Phylogenetic tree generated by maximum likelihood analysis of combined TEF and rpb2 sequence data of species belonging to *Fusarium lateritum* species complex. The tree was rooted with *F. buharicum* (NRRL 13371) and *F. sublunatum* (NRRL 13384 T). RAxML bootstrap support values (BT) ≥ 60% and Bayesian posterior probabilities (PP) ≥ 0.90 are shown respectively near the nodes.

The scale bar indicates 0.02 changes. The ex-type strains are marked in bold and the isolate numbers from the current study are in red. Maximum Likelihood alignment matrix had 444 distinct alignment patterns, with 30.50 % of undetermined characters or gaps. Estimated base frequencies were as follows; A = 0.250680, C = 0.272396, G = 0.245624, T = 0.231299; substitution rates AC = 1.633659, AG = 7.046929, AT = 2.459783, CG = 1.060685, CT = 14.972139, GT = 1.000000; gamma distribution shape parameter α = 0.776892.

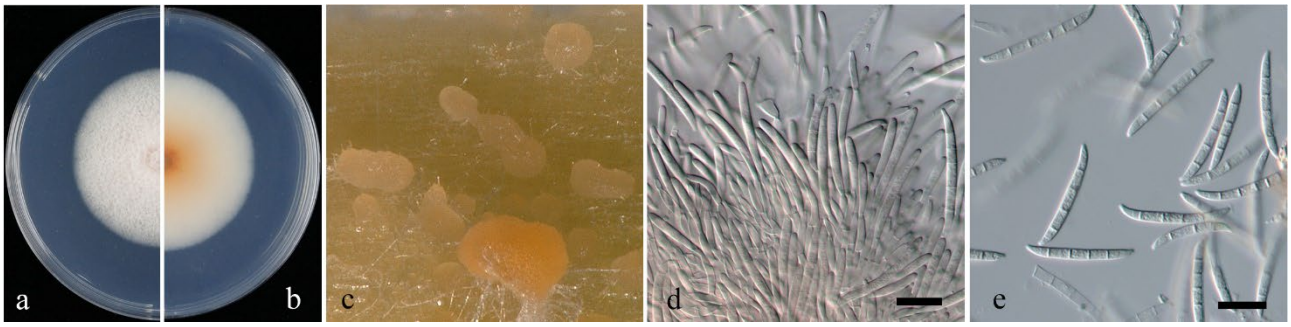

Figure 30 – *Fusarium lateritium* (JZB JZB3110343). a, b Upper and reverse view of the colony in PDA after 7 d at 25 °C in the dark. c Sporodochia. d Sporodochial conidiophores and phialides. e Macroconidia. Scale bars: d, e = 20 µm.

These species were previously described from infected pseudostem of *Musa*, Indonesia by Maryani et al. (2019b) and characterized as a fungal pathogen that poses a global threat to banana production, causing fusarium wilting disease (Maryani et al. 2019b). However, Bedoya et al. (2021) have stated that the introduction of these species and the taxonomic changes stated by Maryani et al. (2019b) are premature. Bedoya et al. (2021) attempted to replicate their phylogenetic analysis and failed to recover a clade corresponding to their lineage 1 as in Maryani et al. (2019b) and Bedoya et al. (2021) have observed that the members of species *F. odoratissimum* and *F. purpurascens* are clade together with *F. tardichlamydosporum* and *F. phialophorum*. We also observe a similar pattern in our phylogenetic analysis and therefore at the moment we wish to keep our isolates recovered from *Prunus avium* in China as *Fusarium* sp. into the *Fusarium oxysporum* species complex. Further, the taxonomic resolve of the *Fusarium oxysporum* species complex is recommended.

Neocosmospora E.F. Sm.,

Neocosmospora was introduced by Smith (1899) to accommodate *N. vasinfecta* as the type species. *Neocosmospora* includes the synonymous genera *Euricoa*, *Hyaloflorea*, and *Haematonectria* (Sandoval-Denis et al. 2019). Later, *Neocosmospora* was reconsidered as an independent genus through phylogenetic analysis (Lombard et al. 2015, Sandoval-Denis et al. 2019), and supported by recent research (Crous et al. 2021, 2022, Perera et al. 2023). Species in *Neocosmospora* are reported as saprobes, plant pathogens and isolated from a wide range of habitats, including soil, nematodes, and plant materials (Sandoval-Denis et al. 2019, Crous et al. 2021, Perera et al. 2023). Currently, more than 100 species have been accepted to *Neocosmospora* and they are mainly distributed in tropical and subtropical regions (Sandoval-Denis et al. 2019, Crous et al. 2021, 2022, Perera et al. 2023, Zeng & Zhuang 2023).

Neocosmospora falciformis (Carrión) L. Lombard & Crous (2015) Fig. 34

Index Fungorum number: IF810958

Pathogenic on *Prunus avium*. Sexual morph: not observed. Asexual morph: *Microconidia* fusiform, 6.5–17.3 × 3.3–5.9 µm (av. = 11.0 × 4.3 µm, n = 40); *Macroconidia* nearly elliptical to falcate, 0–3 septa; 0-septa conidia: 15.7–16.7 × 4.6–5.0 µm (n = 2); *1-septa conidia*: 13.5–27.7 × 3.9–6.6 µm (av. = 20.8×5.1 µm, n = 40); *2-septa conidia*: 24.1–32.3 × 4.5–6.6 µm (av. = 28.3×5.7 µm, n = 22); *3-septa conidia*: 25.6–40.8 × 4.7–7.2 µm (av. = 32.7 × 5.7 µm, n = 40). *Chlamydospores*

globose to subglobose, 8.6–21.9 × 7.8–9.8 µm (av. = 13.0 × 8.6, n = 8). *Sporodochia* and *conidiophore* not observed.

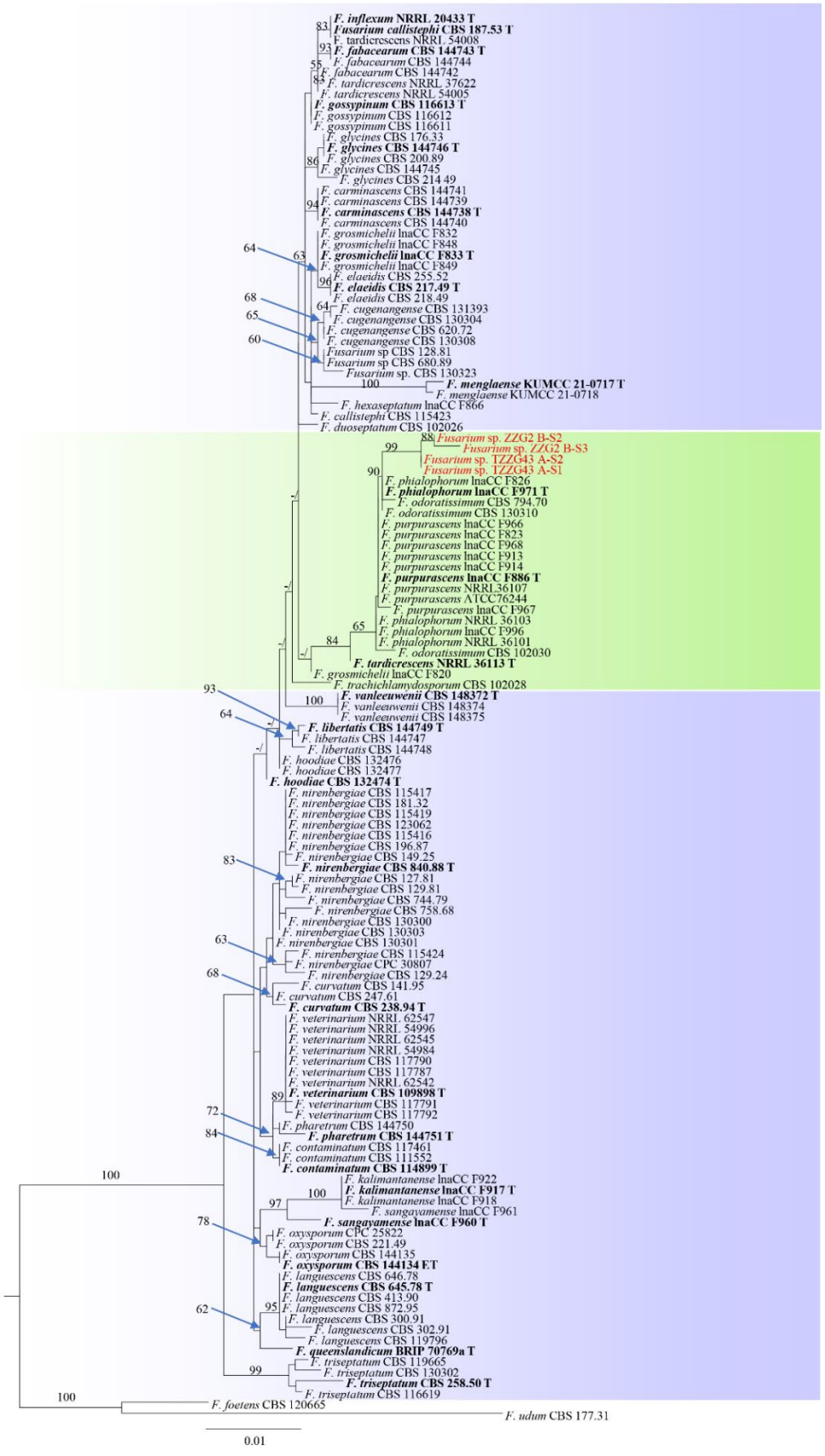

Figure 31 – Phylogenetic tree generated by maximum likelihood analysis of combined TEF and rpb2 sequence data of species belonging to *Fusarium oxysporum* species complex. The tree was rooted

with *F. foetens* (CBS 120665) and *F. udum* (CBS 177.31). RAxML bootstrap support values (BT) ≥ 60% are shown respectively near the nodes. The scale bar indicates 0.01 changes. The ex-type strains are marked in bold and the isolate numbers from the current study are in red. Maximum Likelihood alignment matrix had 444 distinct alignment patterns, with 30.50% of undetermined characters or gaps. Estimated base frequencies were as follows; A = 0.250680, C = 0.272396, G = 0.245624, T = 0.231299; substitution rates AC = 1.633659, AG = 7.046929, AT = 2.459783, CG = 1.060685, CT = 14.972139, GT = 1.000000; gamma distribution shape parameter α = 0.776892

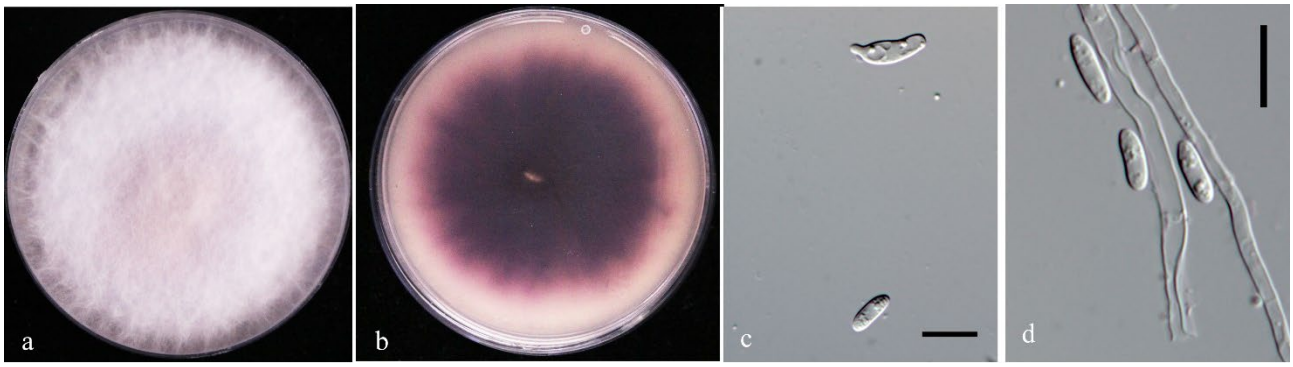

Figure 32 – *Fusarium* sp. (JZB3110362). a Upper view. b reverse view of the colony in PDA after 7 d at 25 °C in the dark. c–d Microconidia. Scale bars: c–d = 10 µm.

Cultural characteristics – Colony on PDA reaching 49.5–58 mm in 7 d at 25°C, with an average growth rate of 7 mm/d. Surface white, reverse dark brown in the centre and brown to orange-yellow in the margin, medium aerial mycelia.

Material examined – China, Beijing, from the *Prunus avium* branch with die-back symptoms (*Rosaceae*), March 2021, P. Chen (dried cultures JZBH3110250, JZBH3110251), living cultures JZB3110250, JZB3110251.

Notes – *Neocosmospora falciformis* has a wide host range and is known to cause root and stem rot in papaya (*Carica papaya*) (Vega-Gutiérrez et al. 2019), crown rot and root rot of pistachio (*Pistacia vera*) (Crespo et al. 2019), wilt and root rot of Muskmelon (*Cucumis melo*) (González et al. 2020) and guava decline (Veloso et al. 2021). We have recovered two isolates of *Neocosmospora* and based on morpho-molecular data they have been identified as *N. falciformis.* This species has not been reported on *Prunus avium* worldwide, therefore here we report the novel host association of *N. falciformis* on *Prunus avium* in the world.

Neocosmospora solani (Mart.) L. Lombard & Crous (2015) Fig. 36

Index Fungorum number: IF810964

Pathogenic on *Prunus avium*. Sexual morph: not observed. Asexual morph: *Conidiophores* unbranched or branched several times, bearing terminal and lateral, single monophialides; phialides subcylindrical, subulate to acicular. *Macroconidia* fusiform to falcate, straight or gently dorsiventrally curved, (0–) 3–5 septate, 36.9–49.9×4.8–6.7 µm (av. 44.8×5.5 µm, n = 40).

Cultural characteristics – Colonies on PDA growing in the dark with an average radial growth rate of 10–11 mm/d and reaching 76–85 mm diam. in 7 d at 25 °C, surface white to pale gray, reverse pale brown in the centre, white at in the margin, abundant aerial mycelia.

Material examined – China, Beijing, from the *Prunus avium* branch with die-back symptoms (*Rosaceae*), March 2021, P. Chen (dried cultures JZB3110245, JZB3110246, JZB3110248, JZB3110249), living cultures JZB3110245, JZB3110246, JZB3110248, JZB3110249.

Notes – In this study, we have recovered four isolates of *N. solani* that are associated with *Prunus avium* branches with die-back symptoms. Phylogenetically these isolates clade together with other reference isolates of *N. solani*, with 81 ML/1.00 BIPP statistical support. *Neocosmospora solani* (as *F. solani*) was reported to be pathogenic on many woody hosts. This species was recorded as the

causal agent of stem canker on walnuts (*Juglans regia*) in Turkey (Polat et al. 2020) and stem rot, crown rot and root rot disease on Pistachio in California, the USA (Crespo et al. 2019). However, *N. solani* has not been reported on *Prunus avium* worldwide, therefore here we report the first host association of *N. solani* on *Prunus avium* in the world.

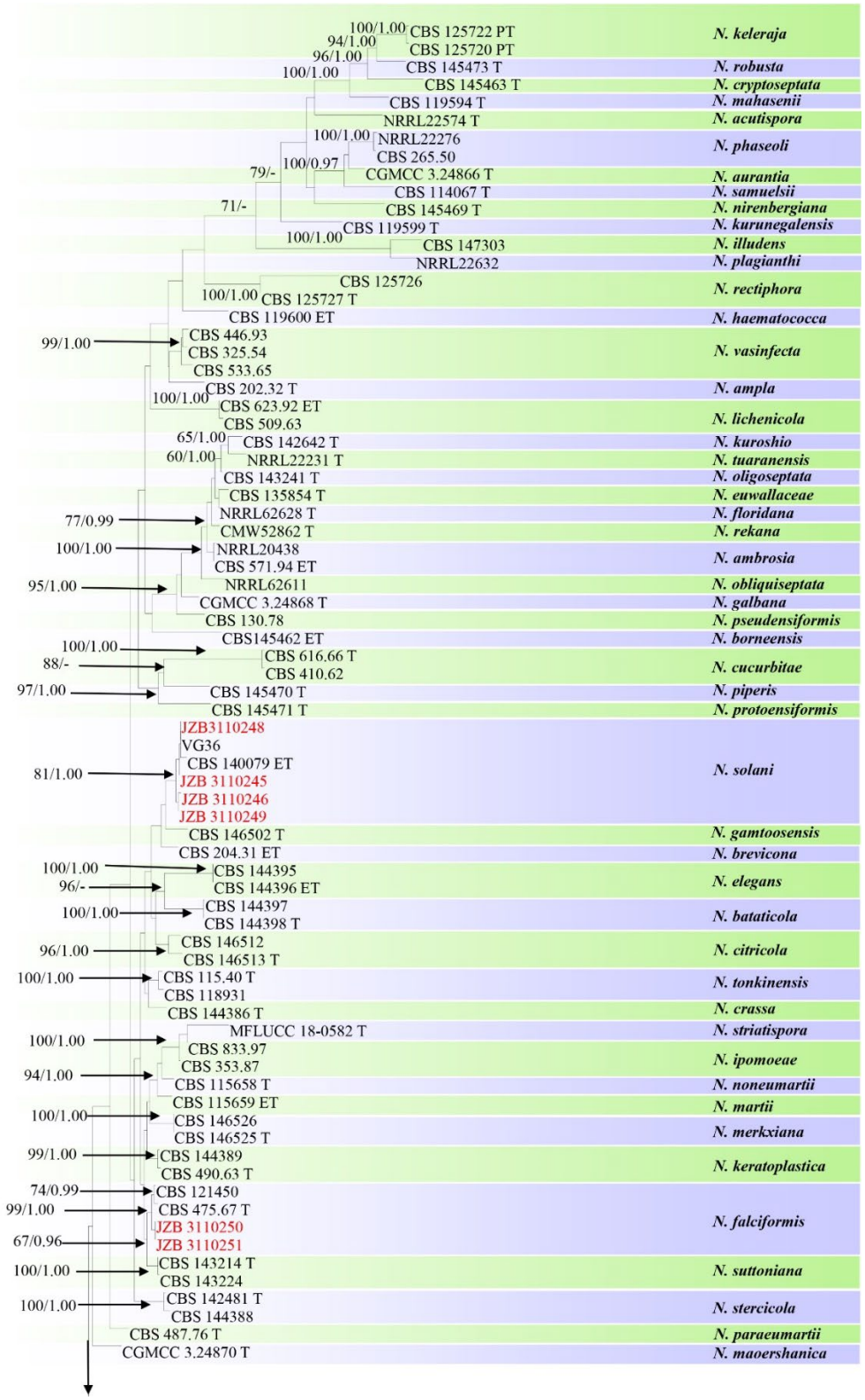

Figure 33 – Phylogenetic tree generated by maximum likelihood analysis of combined ITS, rpb2 and TEF sequence data of species belonging to *Neocosmospora*. The tree was rooted with *Geejayessia atrofusca* (NRRL 22316) and *G. cicatricum* (CBS 125552). RAxML bootstrap support values (BT)

≥ 60% and Bayesian posterior probabilities (PP) ≥ 0.90 are shown respectively near the nodes. The scale bar indicates 0.05 changes. The ex-type strains are marked in bold and the isolate numbers from the current study are in red. The maximum likelihood alignment matrix has 1045 distinct alignment patterns with 8.38% of undetermined characters or gaps. Estimated base frequencies were as follows: A = 0.236442, C = 0.293052, G = 0.249106, T = 0.221400. substitution rates AC = 1.869665, AG = 6.312238, AT = 2.703942, CG = 1.188786, CT = 12.517040, GT = 1.000000; gamma distribution shape parameter α = 0.685562.

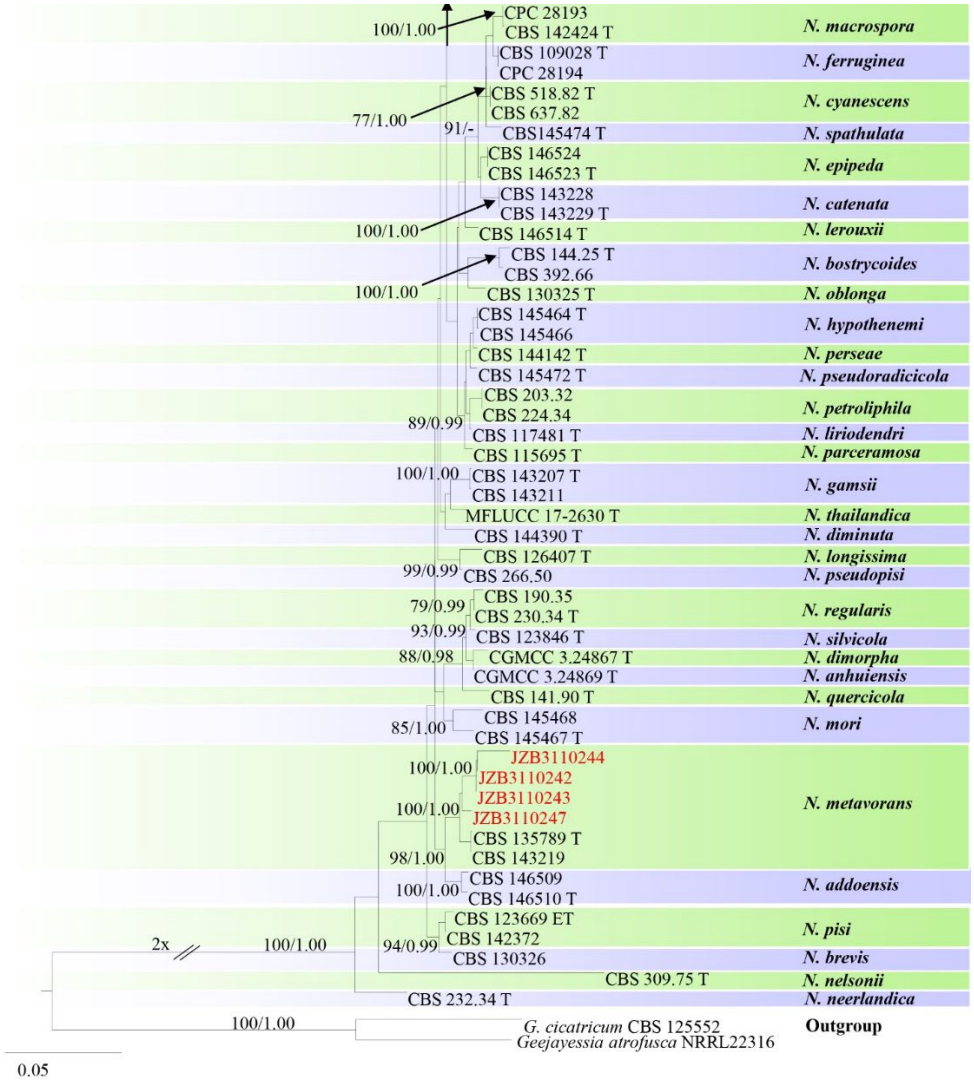

Figure 33 – Continued.

Pathogenicity assay

Colletotrichum godetiae (JZB330337), *C. fioriniae* (JZB330346), *Fusarium proliferatum* (FFSC) (JZB3110231), *Fusarium planum* (FFSC) (JZB3110229), *F. verticillioides* (FFSC) (JZB3110228), *Fusarium lateritium* (FLSC) (SYZG10-B-S2), *F. compactum* (FIESC) (JZB3110252), *F. sulawaense* (FIESC) (JZB3110256), *F. citri* (FIESC) (JZB3110255), *Fusarium* sp. (FOSC) (TZZG43-A-S2), *Neocosmospora solani* (JZB3110249), *N. metavorans* (JZB3110247) and *N. falciformis* (JZB3110250) were subjected to detached shoot inoculation assay on a cultivar of *Prunus avium* cv 'Brooks' or 'Tieton' (Tables 3, 4). Overall, the observed necrosis symptoms on the shoot tissues appeared brown, and the lesion extended into the inner wood, leading to the cell death of the inoculated shoots with time. No symptoms were observed on the shoots that were maintained as controls. Re-isolation from lesions confirmed the inoculated fungus based on cultural and

morphological characteristics such as colony characters and conidial characters. Further, it was confirmed by sequencing the ITS region for the re-isolated fungus.

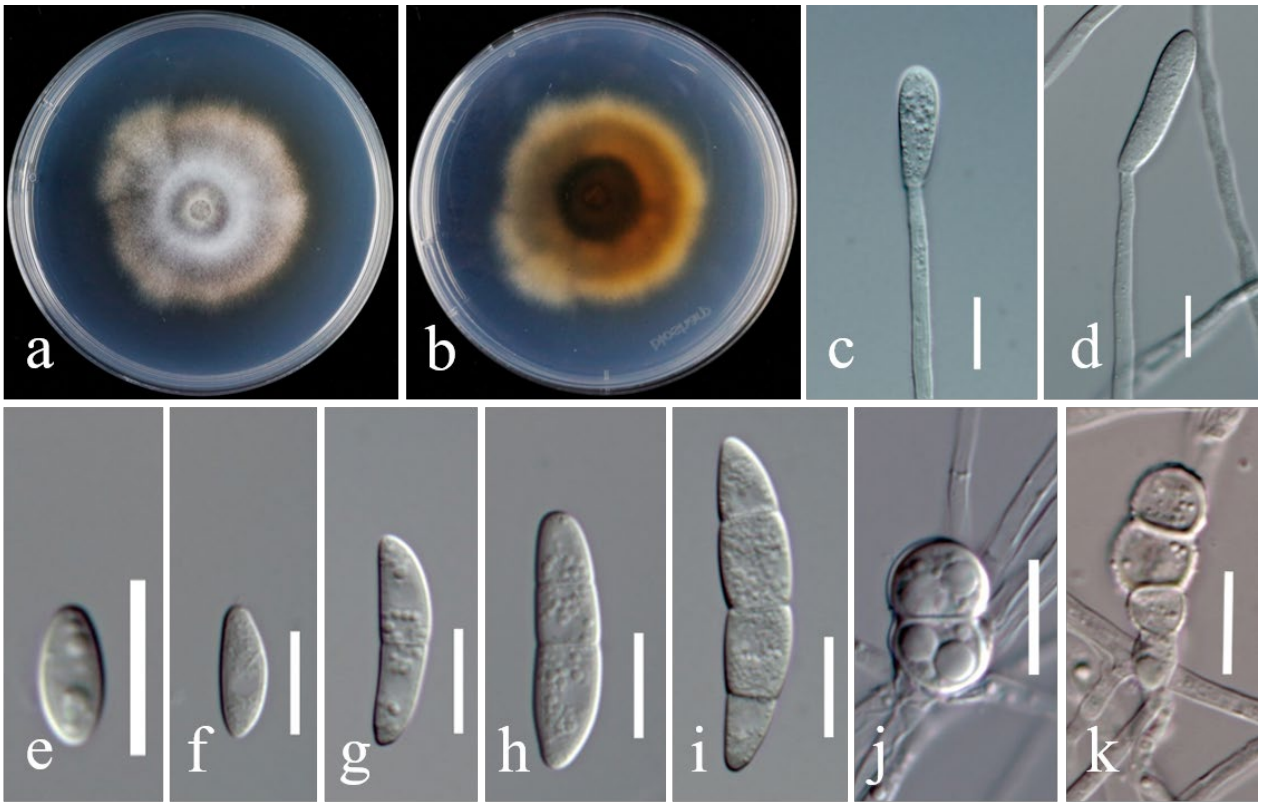

Figure 34 – *Neocosmospora falciformis* (JZB3110250). a Upper view. b reverse view of the colony in PDA after 7 d at 25 °C in the dark. c–d Aerial monophialides. e Microconidia. f–i Macroconidia. j–k Chlamydospores. Scale bars: c–k = 10 µm.

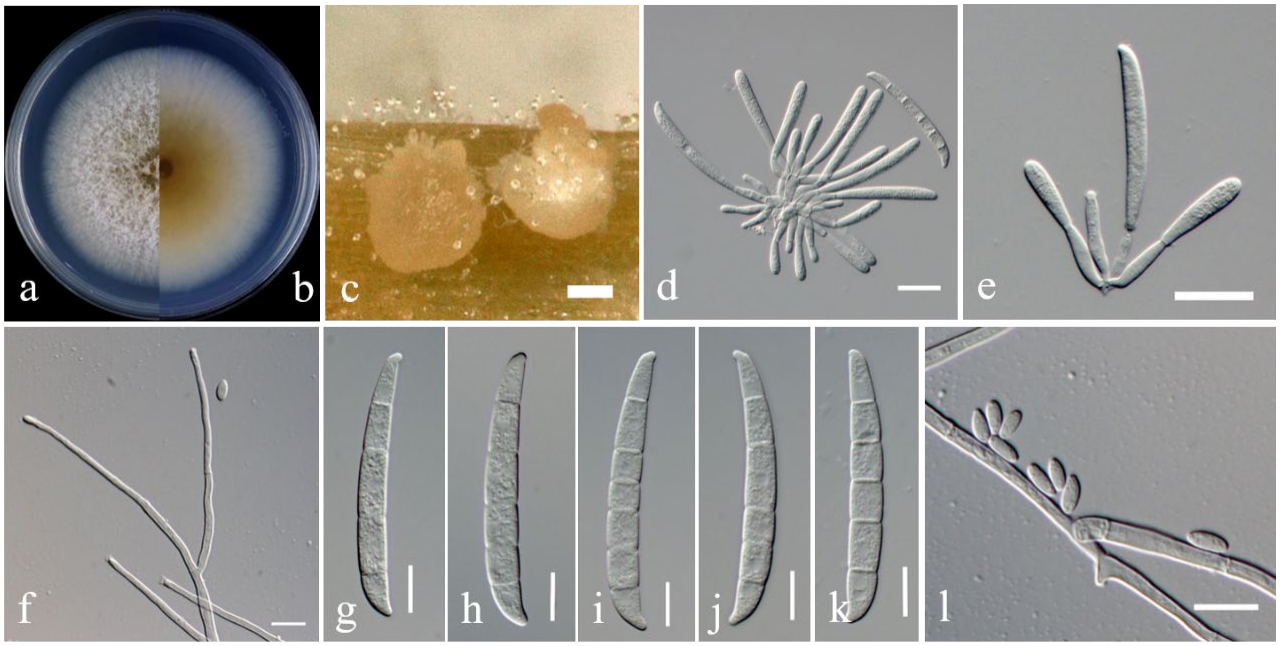

Figure 35 – *Neocosmospora metavorans* (JZB3110243). a Upper view. b Reverse view of the colony in PDA after 7 d at 25 °C in the dark. c Sporodochia formed on the surface of carnation leaves. d–e Conidiogenous cells, sporodochial conidiophores and phialides. f Aerial conidiophores. g–k Macroconidia. l Microconidia. Scale bars: c = 100 µm, d–e = 20 µm, f–l = 10 µm.

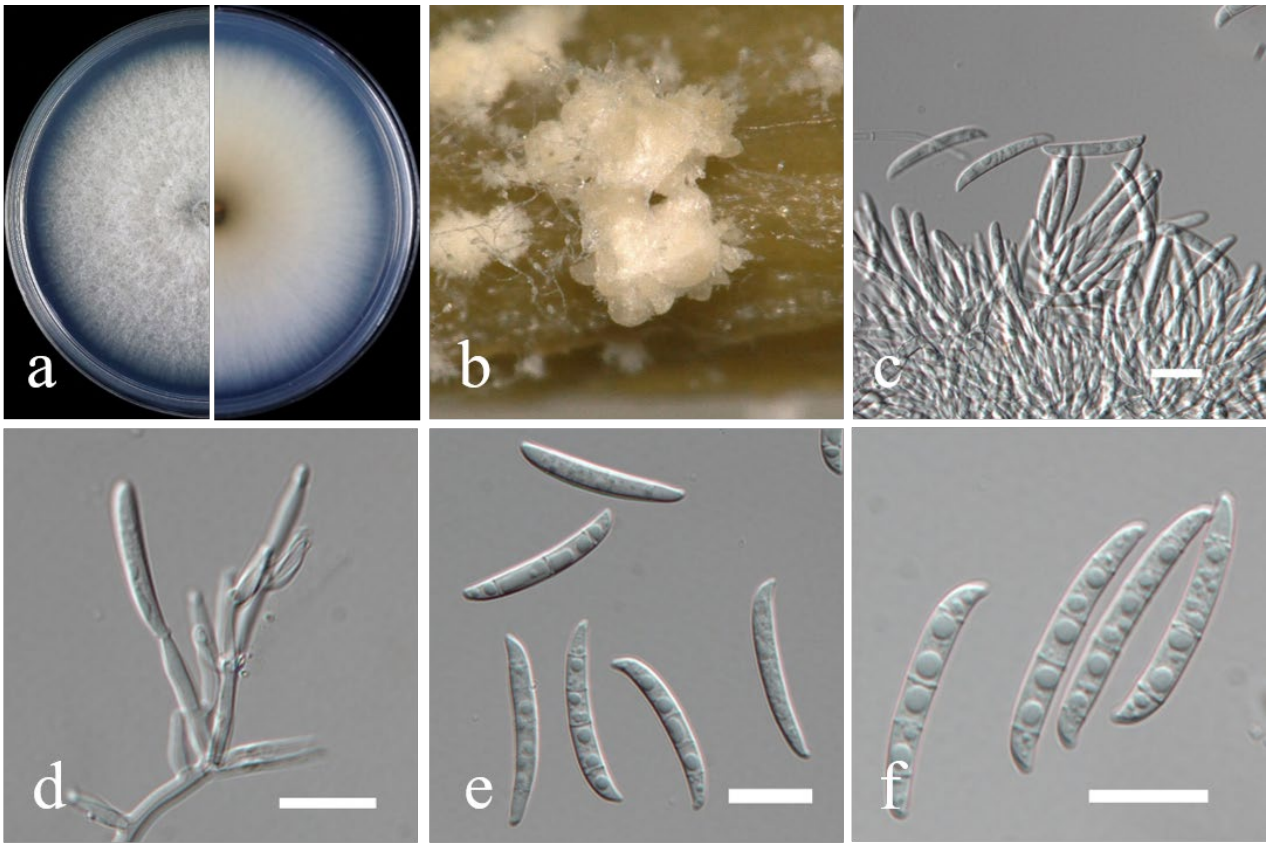

Figure 36 – *Neocosmospora solani* (JZB3110249). a Upper and reverse view of the colony in PDA after 7 d at 25 °C in the dark. B Sporodochia formed on the surface of carnation leaves. c–d Sporodochial conidiophores and phialides. e–f Macroconidia. Scale bars: c–f = 20 µm.

Pathogenicity of *Colletotrichum* species on 1-year-old Cherry shoots

Colletotrichum godetiae and *C. fioriniae* developed disease symptoms three days after inoculation. The average lesion length recorded was 1.11 cm for C. *godetiae* and 0.69 cm for *C. fioriniae*, with a significant difference ($p < 0.05$). The average length of lesions was significantly larger than the control and the disease incidence rates were 90% for C. *godetiae* and 60% for *C. fioriniae*. In comparison, the control group (inoculated with only PDA plugs) did not show any disease development (Table 3, Fig. 37). The statistical analysis further confirmed the significant differences in the lesion length between the control group and the green shoots inoculated with the *Colletotrichum* species (Table 3).

Table 3 Pathogenicity assay of representative of *Colletotrichum* species on 1-year-old Cherry shoots.

	Average Lesion Length (cm)	**Standard Deviation (SD)**	**Significance (p = 0.05) ***	**Incidence rate (%)**
Control	0.51	0.03	a	0
Colletotrichum godetiae JZB330337	1.11	0.36	b	90
Colletotrichum fioriniae JZB330346	0.69	0.18	b	60

* SD: Standard Deviation**,** *a, b: Isolates that do not share the same letter are significantly different. JZB: Culture collection of Beijing Academy of Agriculture and Forestry Sciences.

Pathogenicity of *Fusarium* and *Neocosmospora* species on 1-year-old Cherry shoots

Representative isolates of eight *Fusarium* species and three *Neocosmospora* species were also subjected to test the pathogenicity on 1-year-old cherry shoots. The disease symptoms start to develop

two days after inoculation on shoots inoculated with *Fusarium proliferatum*, *F. verticillioides*, *F. lateritium*, *F. compactum*, *Fusarium* sp., *Neocosmospora solani*, *N. metavorans* and *N. falciformis*. When comparing the lesion development, *Neocosmospora* species showed the longest lesion development than *Fusarium* isolates. Among the isolates of *Fusarium* and *Neocosmospora*, *Neocosmospora metavorans* produced the longest lesion length (1.43 cm), five days after inoculation (Table 4, Fig. 38). However, we observe that the average lesion length recorded for *F. citri* (JZB3110255), *Fusarium planum* (JZB3110229) and *F. sulawaense* (JZB3110256) is not significantly different ($p < 0.05$) to the control.

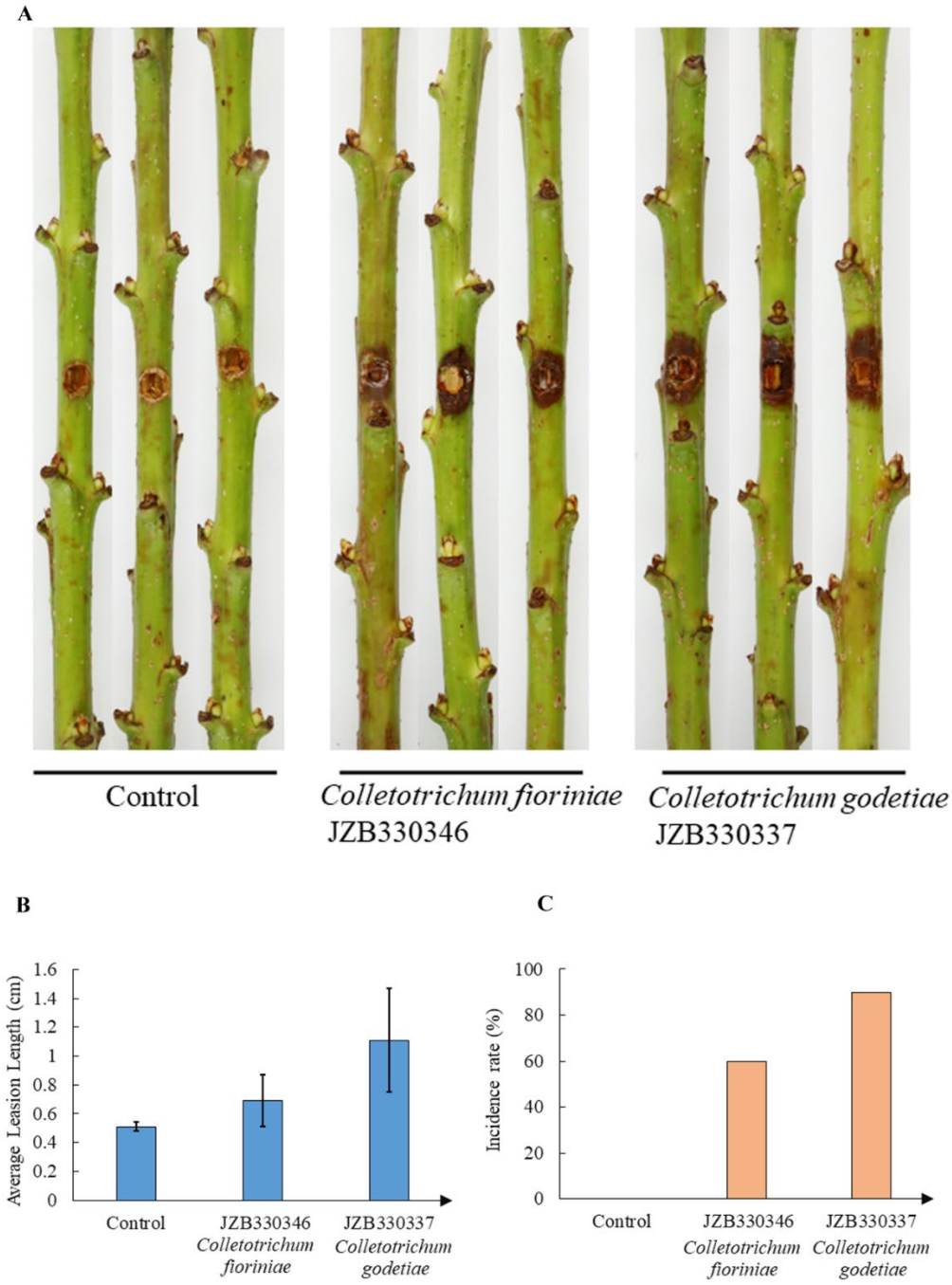

Figure 37 – The pathogenicity of *Colletotrichum godetiae* (JZB330337) and *C. fioriniae* (JZB330346) on shoots of sweet cherry cultivar 'Tieton. A. The representative symptoms on one-

year-old, detached branches (7dpi). B. The average length of shoot lesion. C. The disease incidence rates under different treatments. The bar indicates the standard error ($p<0.05$).

Table 4 Pathogenicity assay of representative of *Fusarium* and *Neocosmospora* species on 1-year-old Cherry shoots.

No.	Fungal species	Average Lesion Length (cm)	SD	Significance ($p<0.05$) *	Incidence rate (%)
1	Control (ck)	0.57	0.09	f	0
2	*Fusarium annulatum* JZB3110231 (SDZG3-B-S1)	0.88	0.18	e	86.7
3	*F. planum* JZB3110229 (TZZG22-C-S1)	0.59	0.07	f	0
4	*F. verticillioides* JZB3110228 (LNZG4-A-S3)	1.17	0.13	b	100
5	*F. lateritium* JZB3110346 (SYZG10-B-S2)	0.92	0.15	de	93.3
6	*F. compactum* JZB3110252 (TZZG45-A-S1)	0.99	0.28	cde	80
7	*F. sulawaense* JZB3110256 (TZZG49-A-S2)	0.57	0.11	f	6.6
8	*F. citri* JZB3110255 (TZZG49-A-S1)	0.69	0.18	f	6.6
9	*Fusarium* sp. JZB3110363 (TZZG43-A-S2)	0.84	0.15	e	66.7
10	*Neocosmospora solani* JZB3110249 (T7-6)	1.05	0.32	bcd	93.3
11	*N. metavorans* JZB3110247 (T6-2)	1.43	0.35	a	100
12	*N. falciformis* JZB3110250 (ZZG2-A-S2)	1.09	0.13	bc	100

* Standard Deviation, ck: Control treatment, *a-f: Isolates that do not share the same letter are significantly different. JZB: Culture collection of Beijing Academy of Agriculture and Forestry Sciences.

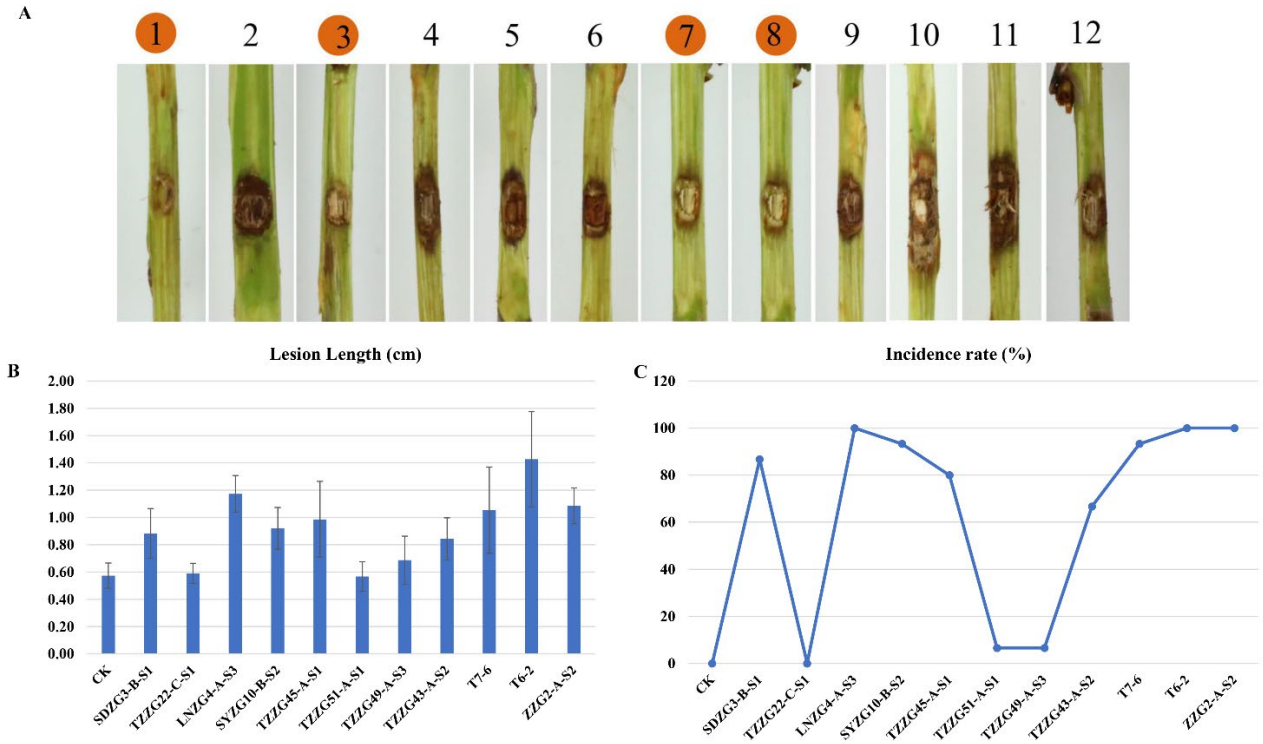

Figure 38 – The pathogenicity of *Fusarium* and *Neocosmospora* on shoots of sweet cherry cultivar 'Tieton'. A The representative symptoms on one-year-old, detached branches (10dpi). B The average length of shoot lesion. C Line graph of the disease incidence rates under different treatments. The bar indicated the standard error ($p < 0.05$).

DISCUSSION

Herein we provide the first comprehensive study on fungal species exhibiting associated and/or pathogenic lifestyles on sweet cherries in China. Sweet cherries have been cultivated worldwide due to their aromatic and tasty fruits (Chen et al. 2023). With the annual expansion of the total land area under cultivation, the yield is not rising corresponding to the area, because cherry plants are subjected to numerous abiotic and/or biotic factors (Wani et al. 2014, Uyemoto et al. 2018, Chen et al. 2023). Among various diseases, trunk disease has received less attention even though it affects the lifespan of perennial plants.

Based on morpho-molecular data, we provide illustrations and descriptions of 26 fungal species belonging to ten genera, and nine families in seven orders. These fungi are scattered in three classes: Dothideomycetes, Leotiomycetes, and Sordariomycetes. Most fungal isolates recovered in this study belonged to *Alternaria* (47 isolates), by following *Fusarium* (41 isolates), *Cladosporium* (35 isolates), *Nothophoma* (25 isolates) and *Colletotrichum* (22 isolates). In total, we obtained 193 fungal isolates and due to the high number of isolates, we could not perform the pathogenicity experiments for all the isolates. Therefore, we selected 13 fungal isolates belonging to three genera (*Colletotrichum*, *Fusarium* and *Neocosmospora*) to test their pathogenicity on detached sweet cherry shoots (Figs 37, 38).

Based on pathogenicity test results, we identified ten fungal species (*Colletotrichum godetiae*, *C. fioriniae*, *Fusarium annulatum*, *F. verticillioides*, *F. compactum*, *F. citri*, *Fusarium* sp., *Neocosmospora solani* and *N. metavorans*) capable of causing symptoms on healthy sweet cherry shoots (Tables 3, 4, Figs 37, 38). *Neocosmospora metavorans* formed the highest lesions (Fig. 38). However, three *Fusarium* species (*Fusarium planum*, *F. sulawesiense* and *F. lateritium*), did not produce any symptoms during the trial. We believe they do not induce disease in sweet cherries; rather, they may act as secondary invaders/saprobes on necrotic tissues or endophytes seen in sweet cherry trunks. Further research is needed to determine the precise role and lifestyle of these species in the sweet cherry mycobiome.

In total, we collected eight *Fusarium* species from diseased sweet cherry branches in China. Previously, *F. ventricosa* and *F. oxysporum* species were reported to cause root rot on sweet cherries in China and British Columbia, respectively (Chen et al. 2016, Úrbez-Torres et al. 2016). Zhou et al. (2022) have identified *F. luffae*, *F. lateritium*, *F. compactum*, *F. nygamai*, *F. citri*, *F. ipomoeae* and *F. curvatum* cause sweet cherry leaf spot disease in China and all these species have proven to be pathogenic on cherry leaves whereas *F. compactum*, *F. luffae* and *F. ipomoeae* showed relatively high virulence (Zhou et al. 2022).

This study isolated three species of *Neocosmospora.* Zheng et al. (2022) identified *Neocosmospora* strains ('as *F. solani*') known to cause Fusarium wilt in sweet cherries in China. Up until now, we haven't found any other *Neocosmospora* species reported from *Prunus avium* in the world. Therefore, this study provides novel host association reports of *N. metavorans* and *N. falciformis* on sweet cherries. However, it is important to know the role of *Neocosmospora* species on sweet cherries and it is recommended to study *Necosmospora* and *Prunus avium* patho-system further.

Two *Colletotrichum* species were identified and proven to be pathogenic on detached cherry shoots here. *Colletotrichum* species are known as one of the top 10 fungal genera of economic and scientific importance (Dean et al. 2012, Peng et al. 2022, Zhou et al. 2023a). *Colletotrichum* spp. infect leaves and cherry fruits at various phases of growth, however, they are rarely associated with cherry trunk diseases. Fifteen *Colletotrichum* species (*C. aenigma*, *C. acutatum*, *C. conoides*, *C. dematium, C. fructicola*, *C. gloeosporioides*, *C. hebeiense*, *C. incanum*, *C. karsti*, *C. liaoningense*, *C. plurivorum*, *C. pseudotheobromicola*, *C. siamense*, *C. sojae*, *C. temperatum*, and *C. truncatum*) have

been reported to cause cherry leaf spot disease worldwide (Børve et al. 2010, Chethana et al. 2019, Peng et al. 2022, Zhou et al. 2023a). *Colletotrichum godetiae* has been identified as the causative agent of sweet cherry anthracnose in Guizhou, China (Peng et al. 2022) and *C. theobromicola* reported causing necrotic and sunken spots on Barbados cherries in Brazil (Bragança et al. 2014). *Colletotrichum acutatum* was found to overwinter on the sweet cherry buds and shoots (Børve & Stensvand 2006, Stensvand et al. 2017). We observed that different *Colletotrichum* species were recovered from the same cherry orchard (e.g. *Colletotrichum* species identified from Guizhou province). This may suggest that the pathogen population that is responsible for sweet cherry trunk diseases are complex. We have recovered *C. godetiae* and *C. fioriniae* in Guizhou from diseased sweet cherry branches. However, according to the pathogenicity assay, they showed different disease developments. Therefore, the characterization and test pathogenic potential of different fungal species in the same genus is also important for the identification of accurate pathogens and the implementation of disease control measures.

Based on morphology and multi-loci phylogenetic sequence data, 16 fungal species were identified to be associated with sweet cherry trunk diseases; *Botryosphaeria dothidea*, *Cladosporium anthropophilum*, *C. cladosporioides*, *C. perangustum*, *C. ramotenellum*, *C. sphaerospermum*, *C. tenuissimum*, *Nothophoma pruni*, *N. quercina*, *Alternaria alternata*, *Monilinia fructicola*, *Cytospora leucostoma*, *Clonostachys farinose*, *Fusarium planum*, *F. sulawesiense* and *F. lateritium*.

Botryosphaeria dothidea is an abundant pathogen in many parts of the world (Marsberg et al. 2017, Abeywickrama et al. 2023), while this species has been reported from many fruit crops in China including sweet cherries as well. Pathogenic fungi in *Botryosphaeriaceae* colonize the xylem tissues and can block the vessels and eventually cause death (Wang et al. 2024). During the colonization, they produce phytotoxic compounds and circulate through the xylem sap. This may induce the disease symptoms in the canopy, including leaf wilt and chlorosis (Wang et al. 2024). *Botryospheria dothidea* has been reported to be causing Gummosis disease in sweet cherries in China (Zhang et al. 2019). In addition, this species has also been reported to cause the stem canker of *Prunus serrulata* (*Rosaceae*; Japanese Cherry) in China (Yan et al. 2016). However, we were not able to find any other common Botryospheriaceous canker and die-back pathogens such as *Diplodia* spp., *Dothiorella* spp., or *Neofusicoccum* spp., during our survey (Lawrence et al. 2017, Valencia et al. 2019, Díaz et al. 2022).

Alternaria alternata, Nothophoma pruni and *N. quercina* also have been previously reported to cause cherry leaf spot disease in China (Chethana et al. 2019). *Alternaria* species are common and frequently isolated from various plants as both endophytes and pathogens. However, it is not very clear the role of *Alternaria* species; especially *A. alternata* on a crop, therefore it is necessary for plant pathologists to know whether a given strain of *A. alternata* indicates a threat to the crop health or simply the presence of an endophyte. *Nothophoma* is a species-rich genus in *Didymellaceae* and many species are mainly reported as plant pathogens or saprobes from different plant species worldwide (Chen et al. 2015, Chethana et al. 2019). In this study, two *Nothophoma* species (*Nothophoma pruni*, *N. quercina*) have been identified from diseased sweet cherry branches collected from Beijing and Shandong province. Initially, these two species were identified as saprobe from leaf spots of *Prunus avium* in Beijing in 2017. We have to test and confirm the ability to cause trunk diseases of isolated *Alternaria* and *Nothophoma* strains on *Prunus avium* in China.

We recovered seven *Monilinia* isolates and based on morphology and multi-loci phylogeny, we identified them as *M. fructicola.* Brown rot (Monilinia Rot, blossom blight) is one of the most economically important and destructive diseases in stone fruits, and *Monilinia fructicola* is known as one of the main organisms among three related pathogens (others; *Monilinia fructigena* and *M. laxa*) (Martini & Mari 2014, Baltazar et al. 2023). *Monilinia* species causing brown rot are difficult to distinguish from each other, therefore combination of morpho-cultural characters with molecular detection is recommended. In China, *Monilinia fructicola* have been reported from several stone fruits, including sweet cherry, Chinese dwarf cherry (*Cerasus humilis*), Chinese sour cherry (*Cerasus pseudocerasus*), Peach (*Prunus persica*), Plum (*Prunus salicina*) and Common apricot (*Prunus armeniaca*) (Yin et al. 2013, 2017). However, most of the studies of Brown rot disease in China

mainly focused on peaches. Only a few studies have been focused on other stone fruits. According to the EPPO global database, since 2021 this pathogen has been categorized as a quarantine pest in China (https://gd.eppo.int/taxon/MONIFC/categorization).

Species in *Cladosporium*, are most found as saprobes and are also pathogenic to both humans and plants (Yang et al. 2023). Cladosporium rot of cherries is a very common disease in many cherry-growing regions, especially in post-harvest conditions. Few species of *Cladosporium* (*Cladosporium anthropophilum, C. cladosporioides*, *C. herbarum, C. macrocarpum C. malorum C. ramotenellum,* and *C. tenuissimum*) have been reported to be associated with Cherries in worldwide (USDA host-fungus database 2024; https://fungi.ars.usda.gov/). In this study we reported novel host associations of two *Cladosporium* species; named *C. perangustum*, *C. sphaerospermum*, from sweet cherries in China. However, their pathogenicity on cherry trunks needs to be evaluated with plant assays in future.

CONCLUSION

Plants including woody fruit crops are constantly exposed to many biotic factors including fungal pathogens. These existing and emerging phytopathogens have seriously threatened global crop production and food security. We report novel host and geographical associations of several fungi on sweet cherries and this may indicate that over the course, pathogens are on the move and colonize new hosts in the agricultural ecosystems, thus changing the plant disease landscape globally. Therefore, the early detection and identification of pathogens is of utmost importance to reduce the associated agricultural losses. This study presents a compilation of microfungi exhibiting pathogenic lifestyle or associated with sweet cherry trunk diseases in China and it shows *Prunus avium* could be host to a wide range of fungi species. Further, a list of the most important pathogens has been identified in this study. The impact of these pathogens needs to be taken into consideration, especially dense cultivations of large areas with monocultures.

ACKNOWLEDGEMENTS

The authors would like to express their gratitude to the cherry orchard owners, growers and farmers for their help during the sample collection. The authors would like to acknowledge the financial support from the Beijing Academy of Agriculture and Forestry Sciences (KJCX20210403, KJCX20240326), Beijing Municipal Science and Technology Project (Z231100003723001), and International Science and Technology Cooperation Platform (2024-03). KD Hyde and F. Al-Otibi extend their appreciation to the Researchers Supporting Project (number- RSP2025R114), King Saud University, Riyadh, Saudi Arabia. This research work was financially supported by the grant received from the Beijing Natural Science Foundation-International Scientist Project (No. 1S24085) for Pranami D. Abeywickrama.

CONFLICT OF INTEREST

The authors declare that they have no conflict of interest. The author list includes members of the Editorial Board of Mycosphere. They were not involved in the journal's review process, or any kind of decisions related to this manuscript.

REFERENCES

Abate D, Pastore C, Gerin D, De Miccolis Angelini RM et al. 2018 – Characterization of *Monilinia* spp. populations on stone fruit in south Italy. Plant Disease, 102, 1708–1717.

Abd Murad NB, Mohamed Nor NMI, Shohaimi S, Mohd Zainudin NAI. 2017 – Genetic diversity and pathogenicity of *Fusarium* species associated with fruit rot disease in banana across Peninsular Malaysia. Journal of applied microbiology, 123, 1533–1546.

Abdollahi Aghdam S, Fotouhifar KB. 2017 – Identification of some endophytic fungi of cherry trees (*Prunus avium*) in Iran. Iranian Journal of Plant Protection Science 48, 43–57.

Abdollahzadeh J, Groenewald JZ, Coetzee MPA, Wingfield MJ et al. 2020 – Evolution of lifestyles in Capnodiales. Studies in Mycology 95, 381–414.
Abeywickrama PD, Qian N, Jayawardena RS, Li Y et al. 2023 – Endophytic fungi in green manure crops; friends or foe? Mycosphere 14, 1–106.
Abeywickrama PD, Zhang W, Li X, Jayawardena RS et al. 2021 – *Campylocarpon fasciculare* (Nectriaceae, Sordariomycetes); Novel Emergence of Black-Foot Causing Pathogen on Young Grapevines in China. Pathogens, 10, 1555.
Alves A, Crous PW, Correia A, Phillips AJL. 2008 – Morphological and molecular data reveal cryptic species in *Lasiodiplodia theobromae*. Fungal Diversity 28, 1–13.
Armand A, Hyde KD, Huanraluek N, Wang Y, Jayawardena RS. 2023 – Identification and characterization of *Colletotrichum* species associated with durian fruit in northern Thailand. Mycosphere 14, 107–129.
Baltazar E, Rodrigues S, Ares A, Camelo A et al. 2023 – Morphological, molecular and genomic identification and characterization of *Monilinia fructicola* in *Prunus persica* from Portugal. Agronomy 13, 1493.
Batista E, Lopes A, Alves A. 2021 – What do we know about Botryosphaeriaceae? an overview of a worldwide cured dataset. Forests 12, 313.
Bedoya ET, Bebber DP, Studholme DJ. 2021– Taxonomic revision of the banana Fusarium Wilt TR4 pathogen is premature. Phytopathology 111, 2141–2145.
Bensch K, Braun U, Groenewald JZ, Crous PW. 2012 – The genus *Cladosporium*. Studies in Mycology, 72, 1–401.
Bensch K, Groenewald JZ, Braun U, Dijksterhuis J et al. 2015 – Common but different: The expanding realm of *Cladosporium*. Studies in Mycology 82, 23–74.
Bensch K, Groenewald JZ, Dijksterhuis J, Starink-Willemse M et al. 2010 – Species and ecological diversity within the *Cladosporium cladosporioides* complex (Davidiellaceae, Capnodiales). Studies in Mycology 67, 1–94.
Bensch K, Groenewald JZ, Meijer M, Dijksterhuis J et al. 2018 – *Cladosporium* species in indoor environments. Studies in Mycology 89, 177–301.
Berbee ML, Pirseyedi M, Hubbard S. 1999 – *Cochliobolus* phylogenetics and the origin of known, highly virulent pathogens, inferred from ITS and glyceraldehyde-3-phosphate dehydrogenase gene sequences. Mycologia 91, 964–977.
Bhunjun CS, Phillips AJL, Jayawardena RS, Promputtha I, Hyde KD. 2021a – Importance of molecular data to identify fungal plant pathogens and guidelines for pathogenicity testing based on Koch's postulates. Pathogens, 10, 1096.
Bhunjun CS, Phukhamsakda C, Jayawardena RS, Jeewon R. et al. 2021b – Investigating species boundaries in *Colletotrichum*. Fungal Diversity 107, 107–127.
Blando F, Oomah BD. 2019 – Sweet and sour cherries: Origin, distribution, nutritional composition and health benefits. Trends in Food Science & Technology 86, 517–529.
Børve J, Djønne RT, Stensvand A. 2010 – *Colletotrichum acutatum* occurs asymptomatically on sweet cherry leaves. European Journal of Plant Pathology 127, 325–332.
Børve J, Stensvand A. 2006 – *Colletotrichum acutatum* overwinters on sweet cherry buds. Plant Disease 90, 1452–1456.
Bragança CAD, Nogueira Junior AF, Rogério F, Massola Jr. NS. 2014 – First report of anthracnose caused by *Colletotrichum theobromicola* on Barbados Cherry (*Malpighia emarginata*) in Brazil. Plant Disease 98, 1272–1272.
Bugnicourt F. 1952 – Une espèce fusarienne nouvelle, parasite du riz. Revue Génerale de Botanique. 59: 13–18.
Capella-Gutiérrez S, Silla-Martínez JM, Gabaldón T. 2009 – trimAl: a tool for automated alignment trimming in large-scale phylogenetic analyses. Bioinformatics 25, 1972–1973.
Cannon PF, Damm U, Johnston PR, Weir BS. 2012 – *Colletotrichum* current status and future directions. Studies in Mycology 73, 181–213.

Carbone I, Kohn LM. 1999 – A method for designing primer sets for speciation studies in filamentous ascomycetes. Mycologia 91, 553–556.
Cavalcanti AD, da Silva Santos AC, de Oliveira Ferro L, Bezerra JDP et al. 2020 – *Fusarium massalimae* sp. nov. (*F. lateritium* species complex) occurs endophytically in leaves of *Handroanthus chrysotrichus*. Mycological Progress 19, 1133–1142.
Chen QF, Liang YX, Zhang HJ, Wu HY et al. 2016 – Identification and biological characteristics research of the pathogen from cherry tree root-rot. Journal of Shanxi Agricultural University (Natural Science Edition) 36, 15–19.
Chen Q, Hou LW, Duan WJ, Crous PW et al. 2017 – Didymellaceae revisited. Studies in Mycology, 87, 105–159.
Chen Q, Jiang JR, Zhang GZ, Cai L. 2015 – Resolving the *Phoma enigma*. Studies in Mycology, 82, 137–217.
Chen P, Abeywickrama PD, Ji S, Zhou Y. 2023 – Molecular identification and pathogenicity of *Diaporthe eres* and *D. hongkongensis* (Diaporthales, Ascomycota) associated with Cherry trunk diseases in China. Microorganisms, 11, 2400.
Chethana KWT, Jayawardene RS, Zhang W, Zhou YY et al. 2019 – Molecular characterization and pathogenicity of fungal taxa associated with cherry leaf spot disease. Mycosphere 10, 490–530.
Cho SE, Oh JY, Lee DH. 2023 – The complete mitochondrial genome of *Cladosporium anthropophilum* (Cladosporiaceae, Dothideomycetes). Mitochondrial DNA Part B 8, 164–166.
Cloete M, Fourie PH, Damm U, Crous PW, Mostert L. 2011 – Fungi associated with die-back symptoms of apple and pear trees, a possible inoculum source of grapevine trunk disease pathogens. Phytopathologia Mediterranea 50, S176–S190.
Corda ACI. 1831 – Die Pilze Deutschlands. In: Sturm J (ed) Deutschlands Flora in Abbildungen nach der Natur mit Beschreibungen. Sturm, Nürnberg vol. 3, Abt. 12, 33–64, tab, 21–32.
Corda ACJ 1839 – Icones fungorum hucusque cognitorum, Prague: Prague.
Crespo M, Lawrence DP, Nouri MT, Doll DA et al. 2019 – Characterization of *Fusarium* and *Neocosmospora* species associated with crown rot and stem canker of pistachio rootstocks in California. Plant disease, 103, 1931–1939.
Crous PW, Lombard L, Sandoval-Denis M, Seifert KA, et al. 2021 – *Fusarium*: more than a node or a foot-shaped basal cell. Studies in mycology 98, 100116.
Crous PW, Sandoval-Denis M, Costa MM, Groenewald JZ et al. 2022 – *Fusarium* and allied fusarioid taxa (FUSA). 1. Fungal Systematics and Evolution 9, 161–200.
Crous PW, Slippers B, Wingfield MJ, Rheeder J et al. 2006 – Phylogenetic lineages in the Botryosphaeriaceae. Studies in Mycology 55, 235–253.
Damm U, Cannon PF, Woudenberg JHC, Johnston PR et al. 2012a – The *Colletotrichum boninense* species complex. Studies in Mycology 73, 1–36.
Damm U, Cannon PF, Woudenberg JHC, Crous PW. 2012b – The *Colletotrichum acutatum* species complex. Studies in mycology 73, 37–113.
Damm U, Mostert L, Crous PW, Fourie PH. 2008 – Novel *Phaeoacremonium* species associated with necrotic wood of *Prunus* trees. Persoonia 20, 87–102.
Dean R, Van Kan JA, Pretorius ZA, Hammond-Kosack KE et al. 2012 – The top 10 fungal pathogens in molecular plant pathology. Molecular Plant Pathology 13, 414–430.
Díaz GA, Valdez A, Halleen F, Ferrada E et al. 2022 – Characterization and pathogenicity of *Diplodia, Lasiodiplodia*, and *Neofusicoccum* species causing Botryosphaeria canker and dieback of apple trees in central Chile. Plant Disease, 106, 925–937.
Dong W, Hyde KD, Jeewon R, Liao CF et al. 2023 – Mycosphere notes 449–468: saprobic and endophytic fungi in China, Thailand, and Uzbekistan. Mycosphere 14, 2208–2262.
Ebrahim W, Özkaya FC, Ebada SS. 2020 – Antifungal metabolites from endophytic fungus *Fusarium verticillioides* strain WF18. South African journal of botany 133, 40–44.
Ehrenberg CG 1818 – Sylvae Mycologicae Berolinenses. Formis Theophili Bruschcke, Berlin, Germany.

Ekanayaka AH, Hyde KD, Gentekaki E, McKenzie EHC et al. 2019 – Preliminary classification of Leotiomycetes. Mycosphere 10, 310–489.
Eriksson OE, Winka K. 1997 – Supraordinal taxa of Ascomycota. Myconet 1, 1–16.
EPPO 2023 – EPPO Global Database. https://gd.eppo.int (Accessed on 11. 09. 2023)
Fan XL, Bezerra JDP, Tian CM, Crous PW. 2020 – *Cytospora* (Diaporthales) in China. Persoonia 45, 1–45.
FAO. 2023 – https://www.fao.org/faostat/en/#home (Accessed on 7. 08. 2023)
Fries E. 1821 – Systema mycologicum 1. Mauritius, Gryphiswaldae.
Geng Y, Wang JG, Zhang JL, Chen G et al. 2022 – First report of *Cladosporium tenuissimum* causing leaf spot of *Arachis hypogaea* in China. Plant Disease 106, 2754.
Glass NL, Donaldson GC. 1995 – Development of primer sets designed for use with the PCR to amplify conserved genes from filamentous ascomycetes. Applied and Environmental Microbiology 61, 132–1330.
Geiser DM, Lewis Ivey ML, Hakiza G, Juba JH et al. 2005 – *Gibberella xylarioides* (anamorph: *Fusarium xylarioides*), a causative agent of coffee wilt disease in Africa, is a previously unrecognized member of the *G. fujikuroi* species complex. Mycologia 97, 191–201.
Gomes IR, Silva JL, Costa TE, Pinto PS et al. 2023 – First report of *Cladosporium tenuissimum* causing spot diseases on leaves and fruits of cucurbits in Brazil. Plant Disease 107, 2540.
González V, García-Martínez S, Flores-León A, Ruiz JJ et al. 2020 – *Neocosmospora keratoplastica*, a relevant human fusarial pathogen is found to be associated with wilt and root rot of muskmelon and watermelon crops in Spain: Epidemiological and molecular evidences. European journal of plant pathology 156, 1189–1196.
Guarnaccia V, Kraus C, Markakis E, Alves A. 2022 – Fungal trunk diseases of fruit trees in Europe: pathogens, spread and future directions. Phytopathologia Mediterranea 61, 563–599.
Hall TA. 1999 – BioEdit: a user-friendly biological sequence alignment editor and analysis program for Windows 95/98/NT. In Nucleic acids symposium series 41, 95–98.
Han SL, Wang MM, Ma ZY, Raza M et al. 2023 – *Fusarium* diversity associated with diseased cereals in China, with an updated phylogenomic assessment of the genus. Studies in Mycology 104, 87–148.
Hassan O, Lim YS, Chang T. 2021 – Phylogenetic and Morphological Characterization of *Cladosporium perangustum* Associated with Flyspeck on Shine Muscat Grapes in South Korea, Mycobiology 49, 183–187.
Hrustić J, Mihajlović M, Grahovac M, Delibašić G et al. 2012 – Genus *Monilinia* on pome and stone fruit species. Pesticidi I Fitomedicina, 27, 283–297.
Hirata T, Kimishima E, Aoki T, Nirenberg HI et al. 2001 – Morphological and molecular characterization of *Fusarium verticillioides* from rotten banana imported into Japan. Mycoscience 42, 155–166.
Hongsanan S, Hyde KD, Phookamsak R, Wanasinghe DN et al. 2020a – Refined families of Dothideomycetes: Dothideomycetidae and Pleosporomycetidae. Mycosphere 11, 1553–2107.
Hongsanan S, Hyde KD, Phookamsak R, Wanasinghe DN et al. 2020b – Refined families of Dothideomycetes: Orders and families incertae sedis in Dothideomycetes. Fungal Diversity 105, 17–318.
Huang F, Chen GQ, Hou X, Fu YS et al. 2013 – *Colletotrichum* species associated with cultivated citrus in China. Fungal Divers 61, 61–74.
Hu J. 2023 – First Report of *Cladosporium ramotenellum* causing sooty spot on postharvest clementines in the United States. Plant Disease. Doi 10.1094/PDIS-02-23-0210-PDN
Hyde KD, Cai L, McKenzie EHC, Yang YL et al. 2009a – *Colletotrichum*: a catalogue of confusion. Fungal Diversity 39, 1–17.
Hyde KD, Cai L, Cannon PF, Crouch JA et al. 2009b – *Colletotrichum* – names in current use. Fungal Diversity 39, 147–182.
Hyde KD, Chaiwan N, Norphanphoun C, Boonmee S et al. 2018 – Mycosphere notes 169–224. Mycosphere 9, 271–430.

Hyde KD, Dong Y, Phookamsak R, Jeewon R et al. 2020a – Fungal diversity notes 1151–1276: taxonomic and phylogenetic contributions on genera and species of fungal taxa. Fungal Diversity 100, 5–277.
Hyde KD, Norphanphoun C, Maharachchikumbura SSN, Bhat DJ et al 2020b – Refined families of Sordariomycetes. Mycosphere 11, 305–1059.
Hyde KD, Amuhenage TB, Apurillo CCS, Asghari R et al. 2023 – Fungalpedia, an illustrated compendium for the fungi and fungus-like taxa. Mycosphere 14, 1835–1959.
Hyde KD, Noorabadi MT, Thiyagaraja V, He MQ et al. 2024 – The 2024 Outline of Fungi and fungus-like taxa. Mycosphere 15(1), 5146–6239.
Index Fungorum. 2025 – Available from: https://www.indexfungorum.org/names/Names.asp (Accessed on January 10, 2025).
Iqbal S, Abbas A, Mubeen I, Sathish M et al. 2022 – Taxonomy, distribution, epidemiology, disease cycle and management of brown rot disease of peach (*Monilinia* spp.). Notulae Botanicae Horti Agrobotanici Cluj-Napoca 50, 12630.
Jayawardena RS, Hyde KD, Damm U, Cai L et al. 2016 – Notes on currently accepted species of *Colletotrichum*. Mycosphere 7, 1192–1260.
Jayawardena RS, Hyde KD, Chethana KWT, Daranagama DA et al. 2018 – Mycosphere Notes 102–168: Saprotrophic fungi on *Vitis* in China, Italy, Russia and Thailand. Mycosphere 9, 1–114.
Jayawardena RS, Hyde KD, Jeewon R, Ghobad-Nejhad M et al. 2019a – One stop shop II: taxonomic update with molecular phylogeny for important phytopathogenic genera: 26–50. Fungal Diversity 94: 41−129.
Jayawardena RS, Hyde KD, McKenzie EHC, Jeewon R et al. 2019b – One stop shop III: taxonomic update with molecular phylogeny for important phytopathogenic genera: 51–75. Fungal Diversity 98: 77−160.
Jayawardena RS, Bhunjun CS, Hyde KD, Gentekaki E, Itthayakorn P. 2021 – *Colletotrichum*: lifestyles, biology, morpho-species, species complexes and accepted species. Mycosphere 12, 519–669.
Jayawardena RS, Hyde KD, Wang S, Sun YR et al. 2022 – Fungal diversity notes 1512–1610: taxonomic and phylogenetic contributions on genera and species of fungal taxa. Fungal Diversity 117, 1–272.
Lawrence DP, Hand FP, Gubler WD, Trouillas FP. 2017 – Botryosphaeriaceae species associated with dieback and canker disease of bay laurel in northern California with the description of *Dothiorella californica* sp. nov. Fungal biology 121, 347–360.
Lee DJ, Lee JS, Lee HB, Choi Y. 2019 – Four endophytic ascomycetes new to Korea: *Cladosporium anthropophilum*, *C. pseudocladosporioides*, *Daldinia eschscholtzii*, and *Nigrospora chinensis*. Korean Journal of Mycology 47, 187–97.
Li C, Cao P, Du C, Xu X et al. 2021 – First report of leaf spot caused by *Cladosporium tenuissimum* on panicle hydrangea (*Hydrangea paniculata*) in China. Plant Disease, 105, 2240.
Li JF, Jiang HB, Jeewon R, Hongsanan S et al. 2023 – *Alternaria*: update on species limits, evolution, multi-locus phylogeny, and classification. Studies in Fungi 8: 1.
Li WJ, McKenzie EHC, Liu JK, Bhat JD et al. 2020 – Taxonomy and phylogeny of hyaline-spored coelomycetes. Fungal Diversity 100, 279–801.
Link HF. 1809 – Observationes in ordines plantarum naturals, Dissetatio I. Mag. Ges. Naturf. Freunde. Berlin 3: 3–42.
Link HF. 1816 – Observationes in ordines plantarum naturales. Dissertatio II, sistens nuperas de Mucedinum et Gastromycorum ordinibus observationes. Der Gesellschaft naturforschender Freunde zu Berlin Magazin für die neuesten Entdeckungen in der gesammten Naturkunde 7: 25–45
Liu YJ, Whelen S, Hall BD. 1999 – Phylogenetic relationships among ascomycetes: evidence from an RNA polymerse II subunit. Molecular Biology and Evolution 16, 1799–1808.

Liu Y, Shi Y, Zhuo D, Yang T et al. 2023 – Characterization of *Colletotrichum* causing anthracnose on rubber trees in Yunnan: Two new records and two new species from China. Plant Disease 107, 3037–3050.
Lombard L, Van der Merwe NA, Groenewald JZ, Crous PW. 2015 – Generic concepts in Nectriaceae. Studies in Mycology, 80, 189–245.
Lu LM, Cheng BP, Pu ZX, Hu XR et al. 2015 – First report of *Cladosporium perangustum* causing leaf spot of *Myrica rubra* in China. Plant Disease 99, 1283–1283.
Manawasinghe IS, Calabon MS, Jones EBG, Zhang YX et al. 2022 – Mycosphere notes 345–386. Mycosphere 13, 454–557.
Manawasinghe IS, Phillips AJL, Hyde KD, Chethana KWT et al. 2016 – Mycosphere Essays 14: Assessing the aggressiveness of plant pathogenic Botryosphaeriaceae. Mycosphere 7, 883–892.
Mapook A, Hyde KD, Hassan K. Kemkuignou BM et al. 2022 – Ten decadal advances in fungal biology leading towards human well-being. Fungal Diversity 116, 547–614.
Marsberg A, Kemler M, Jami F, Nagel JH. 2017 – *Botryosphaeria dothidea*: a latent pathogen of global importance to woody plant health. Molecular plant pathology 18, 477–488.
Marin-Felix Y, Groenewald JZ, Cai L, Chen Q et al. 2017 – Genera of phytopathogenic fungi: GOPHY 1, Studies in Mycology 86, 99–216.
Martini C. 2012 – PhD thesis: Phenotype and genotype characterization of *Monilinia* spp. isolates and preformed antifungal compounds in peach peel fruit at different developmental stages.
Martini C, Mari M 2014 – *Monilinia fructicola*, *Monilinia laxa* (Monilinia rot, brown rot). In Postharvest decay, Academic Press 233–265.
Maryani N, Sandoval-Denis M, Lombard L, Crous PW et al. 2019a – hitch-hiking with pathogenic *Fusarium* strains causing Panama disease in small-holder banana plots in Indonesia. Persoonia 43, 48–69.
Maryani N, Lombard L, Poerba YS, Subandiyah S et al. 2019b – Phylogeny and genetic diversity of the banana Fusarium wilt pathogen *Fusarium oxysporum* f. sp. *cubense* in the Indonesian centre of origin. Studies in Mycology 92, 155–194.
Miller MA, Pfeiffer W, Schwartz T. 2010 – "Creating the CIPRES Science Gateway for inference of large phylogenetic trees" in Proceedings of the Gateway Computing Environments Workshop (GCE), 14 Nov. 2010, New Orleans, LA, 1–8.
Moretti AN. 2009 – Taxonomy of *Fusarium* genus, a continuous fight between lumpers and splitters, Zbornik Matice Srpske Za Prirodne Nauke, (117), 7–13.
Moyo P, Damm U, Mostert L, Halleen F. 2018 – *Eutypa*, *Eutypella*, and *Cryptovalsa* species (Diatrypaceae) associated with *Prunus* species in South Africa. Plant disease 102, 1402–1409.
Murciano C, Orihuel-Iranzo B, Oliver-Chirito JJ. 2021 – Pathogen identification and control of sooty spot caused by *Cladosporium ramotenellum*, appearing on fresh easy peeler mandarins from Perú. Journal of Plant Science and Phytopathology 5, 044–052.
Nannfeldt JA. 1932 – Studien uber die Morphologic und Systematik der nichtlichenisierten nonoperculaten Discomyceten. Nova acta Regiae Societatis Scientiarum Upsaliensis 48, 1–368.
Nees VE 1816 – Das System der Pilze und Schwämme. Wurzburg, Germany, 329 pp.
Norphanphoun C, Doilom M, Daranagama DA, Phookamsak R et al. 2017 – Revisiting the genus *Cytospora* and allied species. Mycosphere 8, 51–97.
Nylander JAA. 2004 – MrModeltest v2. Program distributed by the author. Evolutionary Biology Centre, Uppsala University.
O'Donnell K, Cigelnik E 1997 – Two divergent intragenomic rDNA ITS2 types within a monophyletic lineage of the fungus *Fusarium* are nonorthologous. Molecular Phylogenetics and Evolution 7, 103–116.
O'Donnell K, Kistler H, Cigelnik E, Ploetz RC. 1998 – Multiple evolutionary origins of the fungus causing panama disease of banana: concordant evidence from nuclear and mitochondrial gene genealogies. Proceedings of the National Academy of Sciences of the United States of America 95, 2044–2049.

Oliveira RR, Aguiar RL, Tessmann DJ, Nunes WMC. 2014 – First report of leaf spot caused by *Cladosporium perangustum* on *Syagrus oleracea* in Brazil. Plant disease 98, 280.
Pan M, Zhu H, Tian C, Fan X. 2021 – Assessment of *Cytospora* isolates from conifer cankers in China, with the descriptions of four new *Cytospora* species. Frontiers in Plant Science, 12, 636460.
Pedrozo R, Little CR. 2017 – *Fusarium verticillioides* inoculum potential influences soybean seed quality. European Journal of Plant Pathology 148, 749–754.
Peng XJ, Wang QC, Zhang SK, Guo K, Zhou XD. 2023 – *Colletotrichum* species associated with Camellia anthracnose in China. Mycosphere 14, 130–157.
Peng K, Zeng X, Jiang S, Zhao Z et al. 2022 – Characterization and fungicide sensitivity of *Colletotrichum godetiae* causing sweet cherry fruit anthracnose in Guizhou, China. Frontiers in Microbiology 13, 923181.
Perera RH, Hyde KD, Jones EBG, Maharachchikumbura SSN et al. 2023 – Profile of Bionectriaceae, Calcarisporiaceae, Hypocreaceae, Nectriaceae, Tilachlidiaceae, Ijuhyaceae fam. nov., Stromatonectriaceae fam. nov. and Xanthonectriaceae fam. nov. Fungal Diversity 118, 95–271.
Phillips AJ, Alves A, Abdollahzadeh J, Slippers B et al. 2013 – The Botryosphaeriaceae: genera and species known from culture. Studies in Mycology 76, 51–167.
Phillips AJL, Hyde KD, Alves A, Liu JK. 2019 – Families in Botryosphaeriales: A phylogenetic, morphological and evolutionary perspective. Fungal Diversity 94, 1–22.
Pem D, Hyde KD, McKenzie EHC, Hongsanan S et al. 2024 – A comprehensive overview of genera in Dothideomycetes. Mycosphere 15(1), 2175–4568.
Polat Z, Gültekin MA, Palacıoğlu G, Bayraktar H. 2020 – First report of *Neocosmospora solani* causing stem canker on Juglans regia in Turkey. Journal of Plant Pathology 102, 1289–1289.
Qiu J, Lu Y, He D, Lee Y. 2020 – *Fusarium fujikuroi* species complex associated with rice, maize, and soybean from Jiangsu province, China: phylogenetic, pathogenic, and toxigenic analysis. Plant Disease 104, 2193–2201.
Qiu J, Xu J, Dong F, Yin X, Shi J. 2015 – Isolation and characterization of *Fusarium verticillioides* from maize in eastern China. European Journal of Plant Pathology 142, 791–800.
Rayner RW. 1970 – A mycological colour chart. A mycological colour chart.
Rehner SA, Samuels GJ. 1994 – Taxonomy and phylogeny of *Gliocladium* analysed from nuclear large subunit ribosomal DNA sequences. Mycological Research 98, 625–634.
Ronquist FM, Teslenko P, van der Mark DL, Ayres A. 2012 – MRBAYES 3.2: Efficient Bayesian phylogenetic inference and model selection across a large model space. Systematic Biology 61, 539–542.
Rossman AY, Samuels GJ, Rogerson CT, Lowen R. 1999 – Genera of Bionectriaceae, Hypocreaceae and Nectriaceae (Hypocreales, Ascomycetes) (No. 42). Centraalbureau voor Schimmelcultures (CBS).
Salem NM, Almomany AM, Tahat MM, Aldakil H. 2020 – First report of *Fusarium verticillioides* causing banana fruit rot in Jordan. Plant Disease 104, 3255.
Smith EF. 1899 – Wilt disease of cotton, watermelon and cowpea. United States Department of Agriculture Bulletin 17, 1–53.
Sandoval-Denis M, Gené J, Sutton DA, Wiederhold NP et al. 2016 – New species of *Cladosporium* associated with human and animal infections. Persoonia 36, 281–98.
Sandoval-Denis M, Lombard L, Crous PW. 2019 – Back to the roots: a reappraisal of *Neocosmospora*. Persoonia 43, 90–185.
Sandoval-Denis M, Sutton DA, Martin-Vicente A, Cano-Lira JF et al. 2015 – *Cladosporium* species recovered from clinical samples in the United States. Journal of Clinical Microbiology 53, 2990–3000.
Senanayake IC, Jeewon R, Chomnunti P, Wanasinghe DN et al. 2018 – Taxonomic circumscription of Diaporthales based on multigene phylogeny and morphology. Fungal Diversity 93, 241–443.

Senanayake IC, Rathnayaka AR, Marasinghe DS, Calabon MS. 2020 – Morphological approaches in studying fungi: Collection, examination, isolation, sporulation and preservation. Mycosphere 11, 2678–2754.
Senanayake IC, Rossi W, Leonardi M, Weir A et al. 2023 – Fungal diversity notes 1611–1716: taxonomic and phylogenetic contributions on fungal genera and species emphasis in south China. Fungal Diversity 122, 161–403.
Slippers B, Wingfield MJ. 2007 – Botryosphaeriaceae as endophytes and latent pathogens of woody plants: Diversity, ecology and impact. Fungal Biology Reviews 21, 90–106.
Soltaninejad N, Mohammadi H, Massumi H. 2017 – Isolation, identification and pathogenicity of Botryosphaeriaceae and *Phaeoacremonium* species associated with decline of *Prunus* species in Iran. Journal of Plant Pathology, 571–581.
Song Y, Hu S, de Hoog GS, Liu X et al. 2023 – Medical *Fusarium*: novel species, or uncertain identification? Mycosphere 14, 2263–2283.
Species Fungorum 2025 – https://www.speciesfungorum.org/ (Accessed on 08.02.2025).
Srivastava KK, Kumar D, Barman P. 2019 – Sweet cherry cultivars influencing the growth and productivity under HDP. Journal of Horticultural Sciences, 14, 43–47.
Stensvand A, Børve J, Talgø V. 2017 – Overwintering diseased plant parts and newly infected flowers and fruit as sources of inoculum for *Colletotrichum acutatum* in Sour Cherry. Plant Disease 101, 1207–1213.
Sung GH, Sung JM, Hywel-Jones NL, Spatafora JW. 2007 – A multi-gene phylogeny of Clavicipitaceae (Ascomycota, Fungi): identification of localized incongruence using a combinational bootstrap approach. Molecular Phylogenetics and Evolution 44, 1204–1223.
Sutton BC. 1980 – The Coelomycetes. Fungi Imperfecti with Pycnidia, Acervuli and Stromata. Commonwealth Mycological Institute, Kew, Surrey, England, 1–696.
Sutton BC. 1992 – The genus *Glomerella* and its anamorph *Colletotrichum*. In: *Colletotrichum*: Biology, Pathology and Control (Bailey JA, Jeger MJ eds). CABI, Wallingford, UK: 1–26.
Talhinhas P, Baroncelli R. 2021 – *Colletotrichum* species and complexes: geographic distribution, host range and conservation status. Fungal Diversity 110, 109–198.
Talhinhas P, Baroncelli R. 2023 – Hosts of *Colletotrichum*. Mycosphere 14, 158–261.
Than PP, Jeewon R, Hyde KD, Pongsupasamit S et al. 2008 – Characterization and pathogenicity of *Colletotrichum* species associated with anthracnose on chilli (*Capsicum* spp.) in Thailand. Plant Pathology 57, 562–572.
Thambugala KM, Wanasinghe DN, Phillips AJL, Camporesi E et al. 2017 – Mycosphere notes 1-50: Grass (Poaceae) inhabiting Dothideomycetes. Mycosphere 8(4), 697–796.
Templeton MD, Rikkerink EHA, Solon SL, Crowhurst RN. 1992 – Cloning and molecular characterization of the glyceraldehyde-3-phosphate dehydrogenase-encoding gene and cDNA from the plant pathogenic fungus *Glomerella cingulata*. Gene 122, 225–230.
Tibpromma S, Mortimer PE, Karunarathna SC, Zhan F et al. 2019 – Morphology and multi-gene phylogeny reveal *Pestalotiopsis pinicola* sp. nov. and a new host record of *Cladosporium anthropophilum* from edible pine (*Pinus armandii*) seeds in Yunnan Province, China. Pathogens 8, 285.
Torbati M, Arzanlou M, Sandoval-Denis M, Crous PW. 2019 – Multigene phylogeny reveals new fungicolous species in the *Fusarium tricinctum* species complex and novel hosts in the genus *Fusarium* from Iran. Mycological Progress 18, 119–133.
Tulasne L, Tulasne C 1865 – Selecta Fungorum Carpologia: Nectriei-Phacidiei-Pezizei, 3.
Úrbez-Torres JR, Boulé J, Haag P, Hampson C, O'Gorman DT. 2016 – First report of root and crown rot caused by *Fusarium oxysporum* on sweet cherry (*Prunus avium*) in British Columbia. Plant Disease 100, 855.
USDA host-fungal database 2024 – https://fungi.ars.usda.gov/ (Accessed on 12.02.2024).
Uyemoto JK, Ogawa JM, Jaffee BA. 2018 – Common Names of Plant Diseases: Diseases of Sweet Cherry (*Prunus avium* L.) and Sour Cherry (*P. cerasus* L.). The American Phytopathological Society. USA

Valencia AL, Gil PM, Latorre BA, Rosales IM. 2019 – Characterization and pathogenicity of Botryosphaeriaceae species obtained from avocado trees with branch canker and dieback and from avocado fruit with stem end rot in Chile. Plant Disease 103, 996–1005.
Valenzuela-Lopez N, Cano-Lira JF, Guarro J, Sutton DA. 2018 – Coelomycetous Dothideomycetes with emphasis on the families Cucurbitariaceae and Didymellaceae. Studies in mycology 90, 1–69.
Vega-Gutiérrez TA, López-Orona CA, López-Urquídez GA, Velarde-Félix S et al. 2019 – Foot rot and wilt in tomato caused by *Fusarium falciforme* (FSSC 3+ 4) in Mexico. Plant disease 103, 157.
Veloso JS, Câmara MP, Souza RM. 2021 – Guava decline: updating its etiology from '*Fusarium solani*' to *Neocosmospora falciformis*. European Journal of Plant Pathology 159, 455–460.
Vilanova L, Valero-Jiménez CA, van Kan JA. 2021– Deciphering the *Monilinia fructicola* genome to discover effector genes possibly involved in virulence. Genes 12, 568.
Vilgalys R, Hester M. 1990 – Rapid genetic identification and mapping of enzymatically amplified ribosomal DNA from several *Cryptococcus* species. Journal of Bacteriology 172, 4238–4246.
Wang SY, Wang Y, Li Y. 2022 – *Cladosporium* spp. (Cladosporiaceae) isolated from *Eucommia ulmoides* in China. MycoKeys 91, 151–168.
Wang X, Zhang W, Peng J, Manawasinghe IS et al. 2024 – Lifestyle changes in Botryosphaeriaceae as evidenced by ancestral genome expansion and horizontal gene transfer. Fungal Diversity 125, 221–241.
Wani AA, Singh P, Gul K, Wani MH. 2014 – Sweet cherry (*Prunus avium*): Critical factors affecting the composition and shelf life. Food packaging and Shelf life 1, 86–99.
White TJ, Bruns T, Lee S, Taylor J. 1990 – Amplification and direct sequencing of fungal ribosomal RNA genes for phylogenetics. In: Innis MA, Gelfand DH, Sninsky JJ, White TJ (eds.) PCR protocols: a guide to methods and applications. Academic Press, San Diego, 315–322.
Wijayawardene NN, Hyde KD, Al-Ani LKT, Tedersoo L, et al. 2020 – Outline of Fungi and fungus-like taxa. Mycosphere Online: Journal of Fungal Biology 11, 1060–1456.
Wijayawardene NN, Hyde KD, Dai DQ, Sánchez-García M et al. 2022a – Outline of Fungi and fungus-like taxa – 2021. Mycosphere 13, 53–453
Wijayawardene NN, Phillips AJL, Pereira DS, Dai DQ et al. 2022b – Forecasting the number of species of asexually reproducing fungi (Ascomycota and Basidiomycota). Fungal Diversity 114, 463–490.
Wollenweber HW, Reinking OA. 1935 – Die Fusarien, ihre Beschreibung, Schadwirkung und Bekampfung. Verlag Paul Parey, Berlin.
Woudenberg JHC, Aveskamp MM, de Gruyter J, Spiers AG et al. 2009 – Multiple *Didymella* teleomorphs are linked to the *Phoma clematidina* morphotype. Persoonia 22, 56–62.
Wu NA, Dissanayake AJ, Manawasinghe IS, Rathnayaka AR. 2021 – https://botryosphaeriales.org/, an online platform for up-to-date classification and account of taxa of Botryosphaeriales. Database baab061.
Xiao Y, Xie Y, Su Q, Huo G. 2023 – First report of brown spot of dekopon fruit caused by *Cladosporium tenuissimum* in China. Plant Disease 107, 559.
Yan JY, Xie Y, Zhang W, Wang Y et al. 2013 – Species of Botryosphaeriaceae involved in grapevine dieback in China. Fungal Diversity 61, 221–236.
Yan YC, Zhang ZX, Song YJ, Deng DF. 2016 – First report of *Prunus serrulata* stem canker caused by *Botryosphaeria dothidea* in China. Plant Disease 100, 858–858.
Yang Y, Luo W, Zhang W, Mridha MAU et al. 2023 – *Cladosporium* species associated with fruit trees in Guizhou province, China. Journal of Fungi 9, 250.
Yin LF, Cai ML, Du SF, Luo CX. 2017 – Identification of two *Monilia* species from apricot in China. Journal of integrative agriculture 16, 2496–2503.
Yin LF, Chen SN, Yuan NN, Zhai LX et al. 2013 – First report of peach brown rot caused by *Monilinia fructicola* in Central and Western China. Plant Disease 97, 1255–1255.

Zalar P, de Hoog GS, Schroers HJ, Crous PW. 2007 – Phylogeny and ecology of the ubiquitous saprobe *Cladosporium sphaerospermum*, with descriptions of seven new species from hypersaline environments. Studies in Mycology 58, 157–183.

Zeng ZQ, Zhuang WY. 2023 – New Species of *Neocosmospora* (Ascomycota) from China as evidenced by morphological and molecular data. Life, 13, 1515

Zhang X, Wang J, Zhang K, Yan G et al. 2017 – Sweet cherry growing in China. In VIII International Cherry Symposium 1235. pp. 133–140.

Zhang H, Zeng Y, Wei TP, Jiang YL, Zeng XY 2023a – Endophytic *Fusarium* and allied fungi from *Rosa roxburghii* in China. Mycosphere 14, 2092–2207.

Zhang LZ, Zhang Q, Yang P, Niu Y et al. 2019 – First report of gummosis disease of sweet cherry caused by *Botryosphaeria dothidea* in China. Plant disease 103, 3283–3283.

Zhang M, He W, Wu JR, Zhang Y. 2016 – Two new species of *Spencermartinsia* (Botryosphaeriaceae, Botryosphaeriales) from China. Mycosphere 7, 942–949.

Zhang Q, Nizamani MM, Feng Y, Yang YQ et al. 2023b – Genome-scale and multi-gene phylogenetic analyses of *Colletotrichum* spp. host preference and associated with medicinal plants. Mycosphere 14, 1–106.

Zhang W, Groenewald JZ, Lombard L, Schumacher RK et al. 2021 – Evaluating species in Botryosphaeriales. Persoonia 46, 63–115.

Zhang YX, Chen JW, Manawasinghe IS, Lin YH, Jayawardena RS et al. 2023c – Identification and characterization of *Colletotrichum* species associated with ornamental plants in Southern China. Mycosphere 14, 262–302.

Zhao L, Groenewald JZ, Hernández-Restrepo M, Schroers HJ et al. 2023 – Revising *Clonostachys* and allied genera in Bionectriaceae. Studies in Mycology 1051, 204–265.

Zhou Y, Zhang W, Li Y, Ji S et al. 2023a – Identification and characterization of *Colletotrichum* species associated with cherry leaf spot disease in China. Plant Disease 107, 500–513.

Zhou Y, Zhang W, Li X, Ji S et al. 2022 – *Fusarium* species associated with Cherry Leaf Spot in China. Plants 2022, 11, 2760.

Zhou Y, Zhang W, Li X, Jia J et al. 2021 – Identification of *Botryosphaeria dothidea* associated with cherry leaf spot disease. Acta Phytopathologica Sinica 51, 636–640 (in Chinese).

Zhou Y, Zhang W, Wu LN, Zhang J et al. 2023b – Diversity of fungal communities associated with grapevine trunk diseases in China. Mycosphere 14, 1340–1435.